Calcium signalling in immune cells

A thesis submitted for the degree of Doctor of Philosophy

by

Siaw-Wei Ng

New College

Department of Physiology, Anatomy & Genetics

University Of Oxford

Hilary 2011

Siaw-Wei Ng
New College
Hilary 2011

Calcium signalling in immune cells

Abstract

Inappropriate stimulation of mast cells can trigger allergies including asthma, allergic rhinitis and eczema which, combined, affect almost 30% of the population in western societies. Mast cell activation begins with aggregation of IgE receptors in response to antigen. This then triggers a series of reactions resulting in the tyrosine phosphorylation of Syk kinase, PKC activation and ultimately both degranulation and secretion of leukotrienes and cytokines. CRAC channels are expressed on mast cells, and are essential for IgE-mediated mast cell activation.

Previous work in our laboratory has shown that local Ca^{2+} influx through CRAC channels activates Ca^{2+}-dependent phopholipase A_2, ERK and 5-lipoxygenase, resulting in LTC_4 secretion from mast cells. Therefore, I have investigated how Ca^{2+} microdomains through CRAC channels are detected and how they trigger cellular responses. I find that phosphorylation of Syk following antigen stimulation is enhanced by Ca^{2+} influx through CRAC channels. I also show synergy between CRAC channels and antigen in activating Syk. These findings reveal a novel positive feedback step in mast cell activation, where local Ca^{2+} entry through CRAC channels activates Syk which, in turn, supports CRAC channels.

Earlier work from our group has demonstrated that in RBL cells, Ca^{2+} influx through CRAC channels induces expression of the gene *c-fos*, an important regulator of pro-inflammatory gene expression. I have discovered that local Ca^{2+} entry is sensed by the non-receptor tyrosine kinase Syk, which accumulates at the cell periphery. Syk then signals to the nucleus through recruitment of the transcription factor STAT5. The results therefore identify Syk as a new link in excitation-transcription coupling, converting local Ca^{2+} influx into expression of genes that are essential for immune cell activation.

Activation of G protein-coupled cysteinyl leukotriene type I receptors by the pro-inflammatory molecule LTC_4 is tightly linked to immune cell function and the receptor is an established therapeutic target for allergies including asthma. Desensitization of cysteinyl leukotriene type I receptors arises following protein kinase C-dependent phosphorylation of three serine residues in the receptor C-terminus. Here I show that abolishing leukotriene receptor desensitization suppresses agonist-driven gene expression. Physiological concentrations of LTC_4 led to repetitive cytoplasmic Ca^{2+} oscillations, which were accompanied by the opening of store-operated CRAC channels in the plasma membrane. Ca^{2+} microdomains near the open channels were relayed to the nucleus to increase expression of the transcription factor *c-fos*. In the absence of receptor desensitization, agonist-driven gene expression was suppressed. Mechanistically, stimulation of non-desensitizing receptors evoked prolonged Ca^{2+} release, which led to accelerated Ca^{2+}-dependent inactivation of CRAC channels and a subsequent loss of excitation-transcription coupling. Rather than serving to turn off a biological response, the experiments show that reversible receptor desensitization is an 'on'switch', sustaining long-term signalling in the immune system.

Acknowledgements

It is a pleasure to thank those who made this thesis possible. First and foremost, I owe my deepest gratitude to my supervisor, Professor Anant Parekh, who has supported me throughout my thesis with his patience and scientific knowledge. Without his wise guidance and inspiration, this thesis would not have been possible.

I would also like to extend my gratitude and thanks to these inviduals who have assisted me and they are: Malcolm Begg and David House for being my industrial supervisors; and Dr William Poole, my college tutor for graduates. I would also like to acknowledge my funding sources, GSK and BBSRC for awarding me the Dorothy Hodgkin Postgraduate Award without which I would not be able to carry out my research and producing this thesis. The study is also supported by the MRC programme grant. Throughout my three years of study at the University of Oxford for my DPhil, New College has without a doubt provided me with a very condusive research environment. The Department of Physiology, Anatomy & Genetics, in particular, has provided all the support and equipment that I needed to carry out my research work and the writing up of this thesis.

My colleagues at the department have also helped and assisted me in my work in various ways and I would like to thank all these individuals too. They are Joseph Di Capite, Charmain Nelson, Daniel Bakowski, Karthika Singaravelu, Sophie Douglas and Pulak Kar.

I would like to thank my beloved family for their spiritual support and encouragement throughout my entire life. I am immensely indebted to my parents for their constant love and support. Besides, I wish to express my since thanks to my partner, Seow-Meng Goh for his unprecedented support through my DPhil.

Last but not least, I would like to express my appreciation to all my lovely friends for cheering me up and the moral support they provided.

Statement of Originality

The experiments presented in this thesis are my own original work except for the patch clamp data in Fig. 3-4, 3-5, 5-5 and 5-6, which were performed with Dr Bakowski. I am also grateful to Ms Charmaine Nelson for the imaging experiment in Fig. 4.5 and Dr Di Capite for the imaging experiment in Fig. 3-6*B*.

Publications

1. Sustained activation of the tyrosine kinase Syk by antigen in mast cells requires local Ca^{2+} influx through Ca^{2+} release-activated Ca^{2+} channels. Ng SW, di Capite J, Singaravelu K, Parekh AB. J Biol Chem. 2008 Nov 14; 283(46):31348-55. Epub 2008 Sep 19.
2. Coupling of Ca^{2+} microdomains to spatially and temporally distinct cellular responses by the tyrosine kinase Syk. Ng SW, Nelson C, and Parekh AB. J Biol Chem. 2009 Sep 11:284(37):24767-72. Epub 2009 Jul 7.
3. Cysteinyl leukotriene type I receptor desensitization sustains Ca^{2+}-dependent gene expression. Ng SW, Bakowski D, Mehta R, Nelson C, and Parekh AB. Submitted

Contents

Chapter 1 Introduction ***1***

1.1 Mast Cell 2

1.2 CRAC Channel 6

1.2.1 CRAC Channels are selective for Ca^{2+} 9

1.2.2 Pharmacology of CRAC channels 10

1.2.3 Single CRAC channel conductance 11

1.2.4 Ca^{2+} microdomains near CRAC channels 12

1.2.5 Mitochondria: a link in the endoplasmic reticulum-CRAC channel axis 12

1.3 CRAC channels in mast cells 16

1.3.1 Local Ca^{2+} influx in mast cells: cracking the Ca^{2+} paradox 17

1.3.2 Ca^{2+} microdomains and the MEK/ ERK pathway in mast cells 17

1.3.3 How is local Ca^{2+} detected? 18

1.3.4 Ca^{2+} microdomains and LTC_4 secretion in mast cells 18

1.3.5 Synergy between CRAC channels and protein kinase C generates short-term potentiation in mast cells 20

1.3.6 Graded versus all-or none responses in mast cells 21

1.4 Aims of this thesis 26

Chapter 2 Materials & Methods ***27***

2.1 Materials 28

2.2 Cell Culture 28

2.3 Cell stimulation 29

2.4 Ca^{2+} Imaging 29

2.5 Patch Clamp Recordings 29

2.6 Preparation of Cell Lysates 30

2.7 Western Blotting 31

2.8 Transfection and RNAi.....32

2.9 Reverse Transcriptase-PCR 32

2.10 Immunofluorescence 33

2.11 Statistical Analysis 34

Chapter 3 Sustained Activation of the Tyrosine Kinase Syk By Antigen Requires Local Ca^{2+} influx through CRAC channels..... 35

3.1 Introduction.....36

3.2 Results 38

3.2.1 Antigen-evoked responses depend on functional Syk 38

3.2.2 Ca^{2+} influx enhances Syk activity..... 38

3.2.3 Local Ca^{2+} influx maintains Syk activity 42

3.2.4 The Ca^{2+} influx pathway sustaining Syk activity is the store-operated CRAC channel 44

3.2.5 RNAi knockdown of Orai1 reduces antigen-dependent Syk activation..... 49

3.2.6 Synergy between CRAC channels and FcεRI receptors in phosphorylating Syk..... 51

3.3 Discussion.....53

Chapter 4 Local Ca^{2+} influx through CRAC channels activates c-fos gene expression through Syk and STAT5 55

4.1 Introduction.....56

4.2 Results 58

4.2.1 Local Ca^{2+} influx through CRAC channels induces c-fos mRNA gene expression..... 58

4.2.2 Effects of changing the size of the Ca^{2+} microdomain on c-fos expression 60

4.2.3 The fast Ca^{2+} chelator BAPTA inhibits thapsigargin-induced c-fos expression 63

4.2.4 Syk couples CRAC channel activity to gene expression 65

4.2.5 Syk recruits the transcription factor STAT5 68

4.2.6 RNAi knockdown of Syk reduces ERK phosphorylation 72

4.3 Discussion.....74

Chapter 5 Cysteinyl leukotriene type I receptor desensitization sustains Ca^{2+}-dependent gene expression 76

5.1 Introduction.....77

5.2 Results 79

5.2.1 CysLT1 receptor activation and thapsigargin induce similar c-fos expression despite different extents of I_{CRAC} activation..... 79

5.2.2 There is no synergistic effect between cytoplasmic Ca^{2+} and protein kinase C..... 83

5.2.3 Interference with protein kinase C activity impairs agonist-but not thapsigargin-evoked c-fos expression..... 85

5.2.4 CysLT1 receptor-driven gene expression can be rescued by preventing a bulk cytoplasmic Ca^{2+} rise 88

5.2.5 Ca^{2+}-dependent slow inactivation underlies the suppression of c-fos expression to non-desensitizing cysLT1 receptors..... 92

5.2.6 c-fos expression has high sensitivity to Ca^{2+} influx and is a high gain system 96

5.3 Discussion.....99

Chapter 6 General Discussion 100

6.1 General discussion 101

Chapter 7 References..... 106

7.1 References 107

List of Figures

Figure 1-1. Signalling pathways after FcεRI aggregation by antigen. 5

Figure 1-2. Mechanism for CRAC channel activation and structure of CRAC channel subunit, Orai1 and STIM1.. 8

Figure 1-3. Coupling between STIM1 and Orai1 within ER-PM junctions..... 9

Figure 1-4. CRAC channel has a very high selectivity for Ca^{2+} over Na^{+}. 10

Figure 1-5. Simplified model of regulation of Ca^{2+} by MCU. 14

Figure 1-6. The formation of LTA_4 from arachidonic acid via the 5-lipoxygenase pathway and the conversion of LTA_4 to LTC_4 and LTB_4..... 20

Figure 1-7. Paracrine signalling of LTC_4 in mast cells.. 26

Figure 2-1. Structure of Synta Compound. 28

Figure 3-1. IgE-mediated mast cell activation. 37

Figure 3-2. Activity of the tyrosine kinase Syk is required for, and sustained by, Ca^{2+} influx in response to FCεRI receptor activation. 40

Figure 3-3. Local Ca^{2+} influx activates Syk. 43

Figure 3-4. Pharmacological block of CRAC channels reduced antigen-evoked Syk phosphorylation.. 46

Figure 3-5. The Synta compound does not impair other plasma membrane ion transporters..... 47

Figure 3-6. Knocking down expression of Orai1 suppressed antigen-evoked Ca^{2+} influx and subsequent Syk phosphorylation. 50

Figure 3-7. Antigen and CRAC channels interact synergistically to sustain Syk phosphorylation.. 52

Figure 4-1. Local Ca^{2+} entry activates c-*fos* expression. 59

Figure 4-2. Changes in local Ca^{2+} influx impact upon c-*fos* expression.. 61

Figure 4-3. Thapsigargin-evoked c-*fos* expression is blocked by cytoplasmic BAPTA but not EGTA. 64

Figure 4-4. Syk is involved in excitation-transcription coupling.. 67

Figure 4-5. Syk recruits the transcription factor STAT5..... 70

Figure 4-6. Syk knockdown reduces ERK activation..... 73

Figure 4-7. Parallel processing of the Ca^{2+} microdomain by Syk. 75

Figure 5-1. CysLT1 receptor activation and thapsigargin induce similar c-fos expression despite different extents of I_{CRAC} activation..... 82

Figure 5-2. No synergistic effect between cytoplasmic Ca^{2+} and protein kinase C occurs. 84

Figure 5-3. Interference with protein kinase C activity impairs agonist-but not thapsigargin-evoked c-fos expression..... 86

Figure 5-4. CysLT1 receptor-driven gene expression can be rescued by preventing a bulk cytoplasmic Ca^{2+} rise.. 90

Figure 5-5. Ca^{2+}-dependent slow inactivation underlies the suppression of c-fos expression to non-desensitizing CysLT1 receptors. 95

Figure 5-6. c-fos expression has high sensitivity to Ca^{2+} influx and is a high gain system. 97

List of Tables

Table 1-1. ***Biophysical properties of CRAC channels*** **..... 8**

Table 2-1. ***siRNA sequences*** **..... 32**

Table 2-2. ***PCR primer sequences, optimal amplification cycles, and product sizes*** **..... 33**

Abbreviations

2-APB	2-Aminoethoxy Diphenyl Borate
5-LO	5-Lipoxygenase
AA	Arachidonic Acid
ATP	Adenosine Triphosphate
BAPTA	1,2-bis(2-aminophenoxy)ethane-*N*,*N*,*N*',*N*'-tetraacetic acid
Ca^{2+}	Calcium
$cPLA_2$	Ca^{2+}-Dependent Phospholipase A_2
CRAC	Calcium Release-Activated Calcium
Cs	Cesium
CysLT	Cysteinyl Leukotriene
DAG	Diacylglycerol
EGTA	Ethylene Glycol Tetraacetic Acid
ER	Endoplasmic Reticulum
ERK	Extracellular Signal-Regulated Kinase
eYFP	Enhanced Yellow Fluorescent Protein
Gd^{3+}	Gadolinium Ion
GFP	Green Fluorescent Protein
IgE	Immunoglobulin E
IL-4	Interleukin-4
$InsP_3$	Inositol 1,4,5-Trisphosphate
La^{3+}	Lanthanum Ion
LTC_4	Leukotriene C_4
MEK	Mitogen-Activated Protein Kinase/ERK kinase
PBS	Phosphate-Buffered Saline
PLC	Phospholipase C
PKC	Protein Kinase C
PMA	Phorbol 12-Myristate 13-Acetate
R	Receptor
RBL-1	Rat Basophilic Leukaemia-1
RNAi	RNA interference
STIM	Stromal Interaction Molecule
STAT	Signal Transducers And Activators Of Transcription
Syk	Spleen Tyrosine Kinase
TBS	Tris-Buffered Saline
TEA	Tetraethylammonium Chloride
Thap	Thapsigargin
TNF-α	Tumour Necrosis Factor-α

Chapter 1 Introduction

1.1 Mast Cell

Mast cells are immune cells that were first discovered by Paul Ehrlich in 1878 in human connective tissue on the basis of the metachromatic staining properties of their proteoglycan and protease-rich cytoplasmic granules (1). Besides the metachromatic granules, other cytoplasmic organelles of mature mast cells include numerous mitochondria, rough endoplasmic reticulum and free ribosomes. Mast cells arise from pluripotential haematopoietic cells in the bone marrow (2-4), circulate in the blood as precursors and subsequently migrate to tissues, where they gain their mature morphology under microenvironmental factors (5). Mast cells are widely distributed in tissues throughout the body, particularly in association with structures such as blood and nerves and in close contact with the external environment such as skin, airways, and the gastrointestinal tract (6). Under physiological conditions, mast cells are involved in the regulation of a wide range of activities including epithelial functions (secretion and epithelial permeability), smooth muscle activities (peristalsis and bronchoconstriction), endothelial functions (blood flow, coagulation and vascular permeability), immune responses (recruitment and activation of neutrophils, eosinophils and lymphocytes), neuronal aspects (neuro-immune interactions, peristalsis and pain) and other tissue functions (wound healing and fibrosis) (7-15). Mast cells have been implicated in the pathogenesis of several inflammatory conditions such as allergic diseases (asthma, allergic rhinitis and eczema), autoimmune disorders (multiple sclerosis, rheumatoid arthritis), immunodeficiency, inflammatory bowel disease and psoriasis (16). Recent studies have shown that mast cells play a key role in both innate and adaptive immune responses against pathogens (17).

Mast cell activation is a biphasic process (6). The initial, rapid response occurs within seconds to minutes of stimulation and includes degranulation and release of preformed inflammatory mediators such as histamine and adenosine triphosphate (ATP), and *de novo* synthesis and secretion of pro-inflammatory lipid mediators (leukotrienes, prostaglandin and platelet activating factor) (12). In the late phase reaction which occurs several hours later, mast cells synthesize and release further pro-inflammatory mediators, including chemokines and cytokines such as tumour necrosis factor–alpha (TNF-α), interleukin-2 (IL-2) and IL-4 (16,18).

Mast cell activation is mediated by either FcεRI-dependent or FcεRI-independent receptor cross-linking. FcεRI receptors are multimeric cell surface receptors that bind the Fc fragment of IgE with high affinity (19). The receptor exists as a tetramer ($\alpha\beta\gamma_2$), composed of one unique α-chain noncovalently attached to one β- and one pair of disulfide-bonded γ-chains in rodents. In humans, the receptor can be expressed as two different isoforms, tetramer ($\alpha\beta\gamma_2$) or a trimer ($\alpha\gamma_2$). The α chain belongs to the immunoglobulin superfamily and is required for the binding of IgE molecule whereas the β and γ-chains are involved in signal transduction through this receptor. The β and γ-chains each have an immunoreceptor tyrosine-based activation motif (ITAM), which is tyrosine phosphorylated by the receptor associated tyrosine kinase, Lyn, after antigen cross-linking of receptor-bound IgE molecules. The phosphorylation results in the association of the β- and γ-chains with intracellular signalling molecules through their SRC homology 2 (SH2) domains. Lyn is recruited to the phosphorylated β-chains whereas the phosphorylated ITAM regions of the γ chain serve as docking sites for spleen tyrosine kinase (Syk).

Activation of Syk is crucial for FcεRI mediated mast cell activation as shown in Figure 1-1. Syk is responsible for phosphorylating key tyrosine residues on an

adaptor molecule called Linker for Activation of T cells (LAT), which is essential to mast cell function. Tyrosine phosphorylated LAT interacts with other downstream signalling molecules that are responsible for Ca^{2+} influx which results in degranulation (20). LAT is required for tyrosine phosphorylation of phospholipase C (PLC)-γ1 and 2. Phosphorylated PLC-γ hydrolyses the minor membrane phospholipids phosphatidylinositol 4,5-biphosphate ($PI(4,5)P_2$) to generate the second messengers, diacylglycerol (DAG) and inositol-1,4,5-trisphosphate ($InsP_3$). DAG activates protein kinase C (PKC) and $InsP_3$ initiates Ca^{2+} release via intracellular receptors ($InsP_3R$) on endoplasmic reticulum (ER), generating complex cytoplasmic Ca^{2+} concentration signals. In the absence of LAT, signalling downstream of the FcεRI is impaired, with the principal defects localized to phosphorylation of lymphocyte cytosolic protein 2 (SLP-76), PLC-γ1, PLC-γ2 and cytoplasmic Ca^{2+} signals (21).

In addition to this Lyn-Syk-LAT pathway, there is another complementary signalling pathway initiated by Src-family kinase Fyn, which phosphorylates the adaptor protein Gab2 (Grb2-associated binder-2). Gab2 is essential for FcεRI-mediated activation of PI-3 kinase (phosphatidylinositol 3-kinase), which generates phosphatidylinositol-3,4,5-triphosphate, $PtdIns(3,4,5)P_3$ (PIP_3) (22). In the absence of Gab2, mast cell degranulation and cytokine production are impaired (22). Lyn-deficiency enhanced Fyn-dependent signals and degranulation, but inhibited the Ca^{2+} response (23). Fyn-deficiency impaired degranulation, whereas Lyn-mediated signalling and Ca^{2+} was normal (24). Thus, FcεRI-dependent mast cell degranulation involves cross-talk between Fyn and Lyn kinases and contributes to the induction of cytokines. These two distinct complexes regulate Ca^{2+} (primarily through LAT) and PKC (primarily through Gab2).

IgE-mediated mast cell activation evokes a biphasic increase in intracellular Ca^{2+}. The rapid initial transient rise is caused by $InsP_3$-dependent Ca^{2+} release from the intracellular Ca^{2+} stores and is followed by a more sustained rise that is due to Ca^{2+} entry into the cell. Ca^{2+} influx is required for the mast cell degranulation (25). In mast cells, the main mechanism for the entry of extracellular Ca^{2+} across the plasma membrane is store-operated Ca^{2+} entry, mediated by the Ca^{2+} release-activated Ca^{2+} (CRAC) channels (26). These channels were first discovered in mast cells almost 20 years ago (26). Store-operated channels (SOC) are plasma-membrane Ca^{2+}-permeable channels that open following depletion of Ca^{2+} within the endoplasmic reticulum, which occurs following $InsP_3$-dependent Ca^{2+} release. To date, the best characterised SOC channel in non excitable cells is the CRAC channel (27).

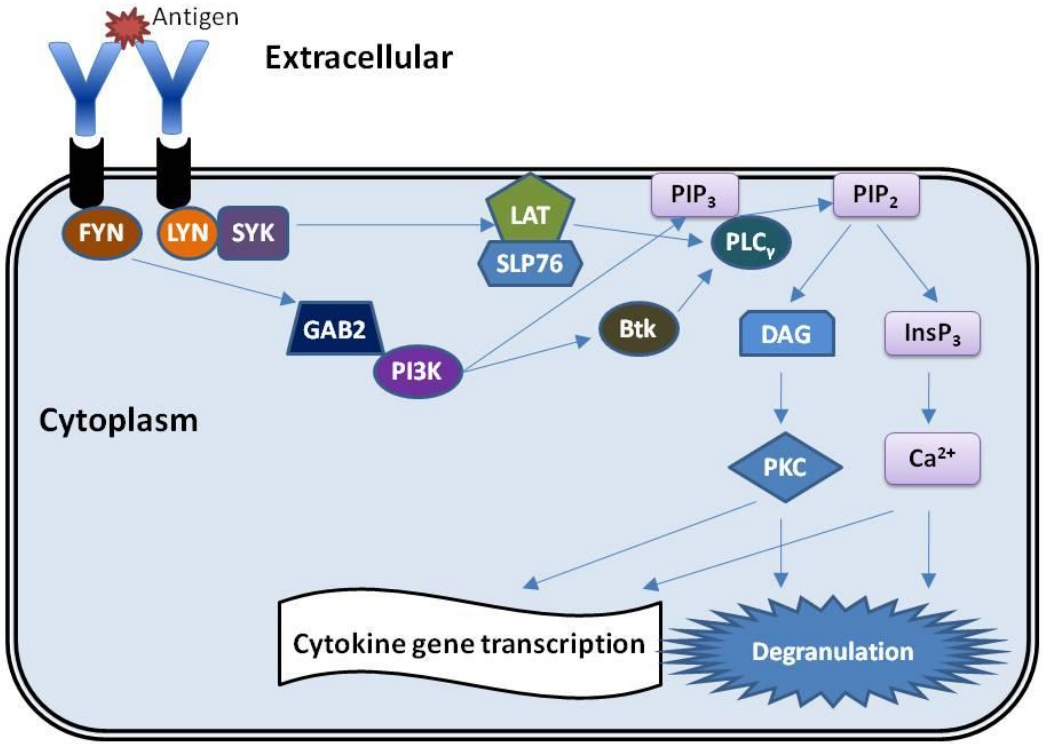

Figure 1-1. Signalling pathways after FcεRI aggregation by antigen. PI3K, phosphatidylinositol 3-kinase; BTK, Bruton's tyrosine kinase.

1.2 CRAC Channel

CRAC channels are expressed in abundance on T lymphocytes, mast cells, and other immune cells but are also found on endothelial cells, glia and hepatocytes (28). Store-operated channels are activated by emptying the intracellular Ca^{2+} store as shown in Fig.1-2*A* (28). Therefore, physiological triggers (for example, receptors that increase $InsP_3$ levels) and pharmacological tools (for example, $InsP_3$ analogues, Ca^{2+} ionophores, and inhibitors of the SERCA pump such as thapsigargin) activate CRAC channels (Table 1-1). CRAC channels are composed of the pore forming Orai1 subunit and STIM1 (29). The Orai family consists of three closely conserved Ca^{2+}-selective ion channels (Orai1–3), each of which contains four transmembrane-spanning domains with intracellular N and C termini as shown in Figure 1-2*B*. STIM is a single-pass ER transmembrane protein, which comprises two EF-hands (ER Ca^{2+} binding domains) and a sterile alpha motif (SAM) domain on the ER luminal side and a coiled-coil region and a polybasic tail on the cytoplasmic side as shown in Figure 1-2*C* (29). The ion-conducting pore of the Orai channel is located on the transmembrane negatively charged glutamate residues (E106 in TM1 and E190 in TM3), which function as putative Ca^{2+} binding sites (Fig. 1-2*B*). By using an RNAi screen in HeLa cells, STIM1 and STIM2 were identified (30). Orai1 has been identified using a combination of two genome-wide approaches: a modified linkage analysis with single-nucleotide polymorphism arrays, and a Drosophila RNA interference screen designed to identify regulators of store-operated Ca^{2+} entry and NFAT nuclear import (31). Mutagenesis has revealed that STIM1 is the Ca^{2+} sensor that detects store Ca^{2+} content and translates this into the opening of Orai1. An earlier study found that the absence of functional CRAC channels in patients with hereditary severe combined immune deficiency (SCID) led to defective store-operated Ca^{2+}

entry (32). Thus, CRAC channels provide the major pathway for T cell receptor (TCR)-activated Ca^{2+} entry in human T cells. The SCID patients are homozygous for a single missense mutation R91W in Orai1 (Fig. 1-2*B*), and expression of wild-type Orai1 in SCID T cells restores store-operated Ca^{2+} influx.

Functional CRAC channels are likely to be a tetramer that consists of four Orai1 subunits. Under resting conditions, Orai1 and STIM1 are widely distributed throughout the plasma membrane and ER, respectively (Fig. 1-3). Following store depletion Ca^{2+} dissociation from the EF hand triggers oligomerization of STIM1 through the SAM domain. This leads to translocation of STIM1 proteins towards the plasma membrane, forming punctae in the vicinity of the plasma membrane (10-25 nm below the plasma membrane) (33). A small highly conserved 107 amino acid CRAC activation domain (CAD) of STIM1 that binds directly to the N and C termini of Orai1 to open the CRAC channel has been identified (34). Hence close location of CAD domain on STIM1 to Orai1 enables CAD to bind to the N and C termini of Orai1, leading to channel opening. Co-expression of STIM1 with Orai1 greatly enhances CRAC currents, two to three orders of magnitude larger than the endogenous CRAC (35). This suggests STIM1 and Orai1 are sufficient to reconstitute I_{CRAC}. STIM1 and calmodulin interact with Orai1 to induce Ca^{2+}-dependent inactivation of CRAC channels (36). A recent study has shown that translocation of STIM1 to ER-PM junctions and subsequent CRAC channel activity is regulated by the dynamin-related mitochondrial protein mitofusin 2 following mitochondrial depolarisation (37).

Table 1-1. ***Biophysical properties of CRAC channels***

Current	Conductance	Selectivity	Permeability Ratio	Activation	Cell Type
I_{CRAC}	0.02pS; 110 Ca^{2+}	$Ba^{2+}>Ca^{2+}\geq Sr^{2+}$	Ca^{2+}: Na^{+}; 10,000:1	Receptor agonist $InsP_3$ Thapsigargin EGTA/BAPTA Ionomycin TPEN	Mast cell RBL-1/2H3 Jurkat T cells Hepatocytes Dendritic cells Megakaryocytes MDCK cells

I_{CRAC}, Ca^{2+} release activated Ca^{2+} current; $InsP_3$, inositol 1, 4, 5-triphosphate.

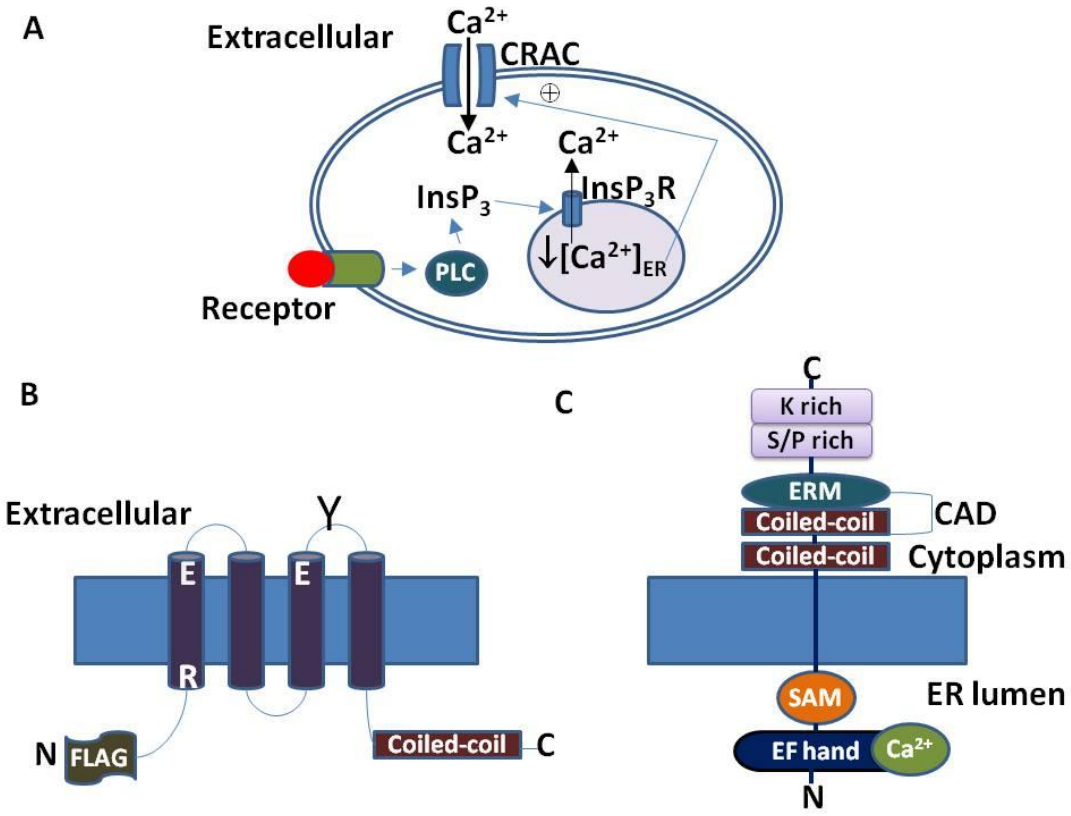

Figure 1-2. Mechanism for CRAC channel activation and structure of CRAC channel subunit, Orai1 and STIM1. a) Depletion of ER Ca^{2+} stores, leading to activation of CRAC channels in the plasma membrane. b) predicted topology of Orai1 and c) STIM1. ERM, ezrin/radixin/moesin; S/P, serine/ proline; K, lysine; E; glutamate; R, Arginine; SAM, sterile alpha motif.

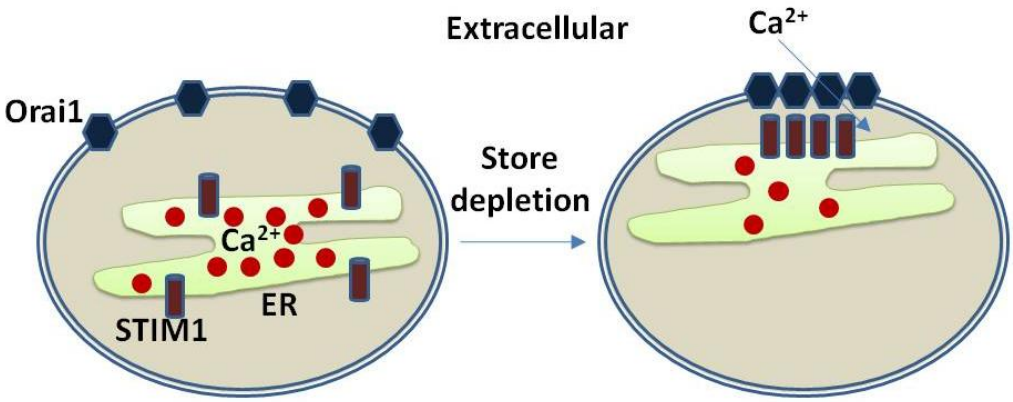

Figure 1-3. Coupling between STIM1 and Orai1 within ER-PM junctions.

1.2.1 CRAC Channels are selective for Ca^{2+}

CRAC channels are highly selective for divalent cations over monovalent ones (Table 1-1). In the presence of external Ca^{2+}, monovalent cations like Na^{+} are almost totally excluded (PCa: PNa is > 10 000, Fig. 1-4). Therefore only a few of these highly Ca^{2+}-selective channels need to be activated for Ca^{2+} entry since almost all incoming ions are Ca^{2+}. For instance, cytoplasmic Ca^{2+} oscillations, which trigger gene expression, are sustained by only small fraction of activated CRAC channels. CRAC channels also distinguish between divalent cations. At negative potentials (negative to -40 mV), Ba^{2+} permeates better than Ca^{2+} whereas Sr^{2+} is very similar to Ca^{2+}.

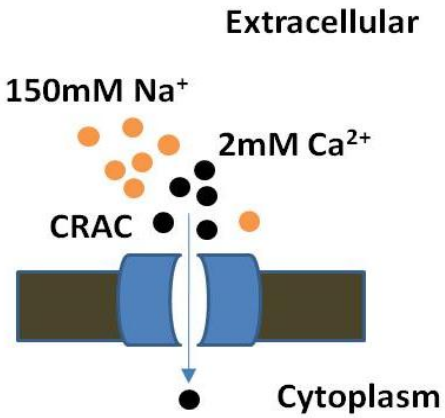

Figure 1-4. CRAC channel has a very high selectivity for Ca^{2+} over Na^{+}.

1.2.2 Pharmacology of CRAC channels

Despite the significance of CRAC channels in cellular physiology, lack of potent and highly specific pharmacological tools has limited the ability to define the function of the CRAC channel and target it from a clinical perspective. Potent inhibitors of CRAC channels are trivalent lanthanide ions like La^{3+} and Gd^{3+}, which work at low concentrations (1 µM) but they obviously are not of any clinical potential (38). Two small molecule blockers, 2-aminoethoxydiphenyl borate (2-APB) and SKF96365, are commonly used to block CRAC channels. Our previous study has shown that pre-treatment with 2-APB (30 µM) blocks the development of I_{CRAC} (39). Another study has demonstrated that 2-APB has differential effects on the three isoforms of Orai (40). Orai1 is completely inhibited by 50 µM 2-APB and Orai2 appears to be significantly less sensitive (50% reduction in I_{CRAC}). Conversely, Orai3 is greatly potentiated by 50 µM 2-APB in a store independent manner. When co-expressed with STIM1 and activated via store depletion, Orai1 and Orai2 are facilitated at low 2-APB concentrations (41). Thus, 2-APB has both agonistic and antagonistic effects on CRAC channels. The inhibition of Orai1 channels by high concentrations of 2-APB

appears to involve a direct block at the channel level as well as an additional uncoupling of STIM1 and Orai1, since the compound reversed the store-dependent multimerization of STIM1. It has also been shown that single-point mutations of the Orai1 pore (E106D and E190A) enable 2-APB to gate Orai1 in a STIM1-independent manner (41), suggesting that 2-APB facilitates CRAC channels by altering the pore architecture. Additionally, another study has shown that 2-APB inhibited STIM1 puncta formation less well in cells co-expressing Orai1, indicating that the inhibitory effects of 2-APB are not solely dependent upon STIM1 reversal (42). SKF-96365 has been shown to block CRAC current reversibly in RBL cells (43). However, these two non selective compounds also interfere with many other ion channels such as Trp channels, limiting their use as CRAC channel-selective probes (28,44,45). One recent development has been the finding of the Synta compound, which will be discussed later in this study.

1.2.3 Single CRAC channel conductance

The single channel conductance of CRAC channels is extremely low (1 pS) (46). Because the conductance is too low to be measured directly, previous studies have relied on noise analysis to estimate the unitary current amplitude. Noise analysis revealed the unitary chord conductance to be 9 femtosiemens (fS) in 2 mM external Ca^{2+} (47). CRAC channel conductance is more than 1000-fold smaller than most Ca^{2+} permeable channels such as L-type voltage-operated Ca^{2+} channels (VOCC). Calculations reveal that immune cells express many CRAC channels, estimated to be >8,000 in T cells and mast cells.

1.2.4 Ca^{2+} microdomains near CRAC channels

The Ca^{2+} influx through an open Ca^{2+} channel in either the plasma membrane or an intracellular organelle evokes a rapid rise in local Ca^{2+} concentration near the open channel, called a Ca^{2+} microdomain (48). The Ca^{2+} concentration within a microdomain can reach tens of microMolar, several-fold higher than the bulk cytoplasmic Ca^{2+} rise, depending on the type of Ca^{2+} channel (49). Ca^{2+} microdomains from activated VOCC drive neurotransmitter release and stimulate excitation-transcription coupling (50). The amplitude of the CRAC channel microdomain in mast cells is estimated to be >3 µM around 10 nm from the open channel pore (49). As CRAC channels cluster into puncta in the plasma membrane after store depletion (51), local Ca^{2+} levels at a cluster will be considerably higher than that achieved by isolated channels. These local Ca^{2+} signals can selectively activate various targets like adenylyl cyclase (52), Ca^{2+} ATPase pumps (53), and Ca^{2+}-dependent phospholipase A_2 ($cPLA_2$) (54), leading to LTC_4 production. Therefore local Ca^{2+} entry is essential for mast cell function.

1.2.5 Mitochondria: a link in the endoplasmic reticulum-CRAC channel axis

Mitochondria are able to take up calcium from the cytosol, a process driven by the large negative potential across the inner mitochondrial membrane (~180 mV) that is set up by proton extrusion along the electron transport chain (55). Ca^{2+} uptake into mitochondria occurs through the ruthenium red-sensitive mitochondrial Ca^{2+} uniporter (MCU), which is located in the organelle's inner membrane (Fig. 1-5) (56). Subsequent electrophysiological studies showed the MCU to be an inward rectifying Ca^{2+} selective channel (55) and a protein essential for Ca^{2+} uptake has recently been discovered (57). Once inside the mitochondrial matrix, Ca^{2+} activates three rate-

limiting enzymes of the Krebs cycle (pyruvate dehydrogenase, NAD^+-isocitrate dehydrogenase, and 2-oxoglutarate dehydrogenase) and thus stimulates ATP production (58). In mast cells, a recent study has shown that cytosolic Ca^{2+} modulates MCU, in a biphasic manner with Ca^{2+} both facilitating and then inhibiting mitochondrial Ca^{2+} uptake (59). Ca^{2+} flux through the uniporter is impaired by calmodulin antagonists, suggesting uptake is a Ca^{2+}/Calmodulin (CaM)-sensitive process (60,61). However, some uniporter activity (approximately 30–40%) was not inhibited in the presence of high concentrations of calmodulin antagonists, suggesting calmodulin-independent uptake too (60). The uniporter has low affinity for Ca^{2+}, with an apparent K_M of approximately 16 μM (60,62). This is around an order of magnitude larger than the peak bulk cytoplasmic Ca^{2+} rise that occurs upon cell stimulation. Even so, several studies have shown Ca^{2+} taken up is rapidly transported into the matrix following agonist-stimulated Ca^{2+} release, when genetically targeted fluorescent proteins or fluorescent dyes are expressed or targeted within the matrix (63). It has been found that Ca^{2+} released through $InsP_3$ receptors on the ER is rapidly propagated into the matrix (62). $InsP_3R$-evoked Ca^{2+} release generates local Ca^{2+} microdomains, which can reach concentrations of tens of μM. This spatially restricted Ca^{2+} signal is sensed by uniporters on the adjacent mitochondria, resulting in rapid mitochondrial Ca^{2+} uptake (64). In some cell types, mitochondrial Ca^{2+} uptake declined despite a sustained elevation of cytosolic Ca^{2+} (65), suggesting the uniporter might desensitize/inactivate. Previous work found that cytosolic Ca^{2+} inactivates the uniporter, with a K_D of approximately 15 μM (60,66). At the same cytoplasmic Ca^{2+} concentration, inactivation occurred approximately two times more slowly (time constant of 16 s) than activation (time constant of 7.9 s). Thus, cytoplasmic Ca^{2+} oscillations (duration of 1–5 s with a frequency of approximately 0.05–1 Hz) can

evoke repetitive mitochondrial Ca^{2+} transients whereas sustained cytoplasmic Ca^{2+} signals do not (67,68).

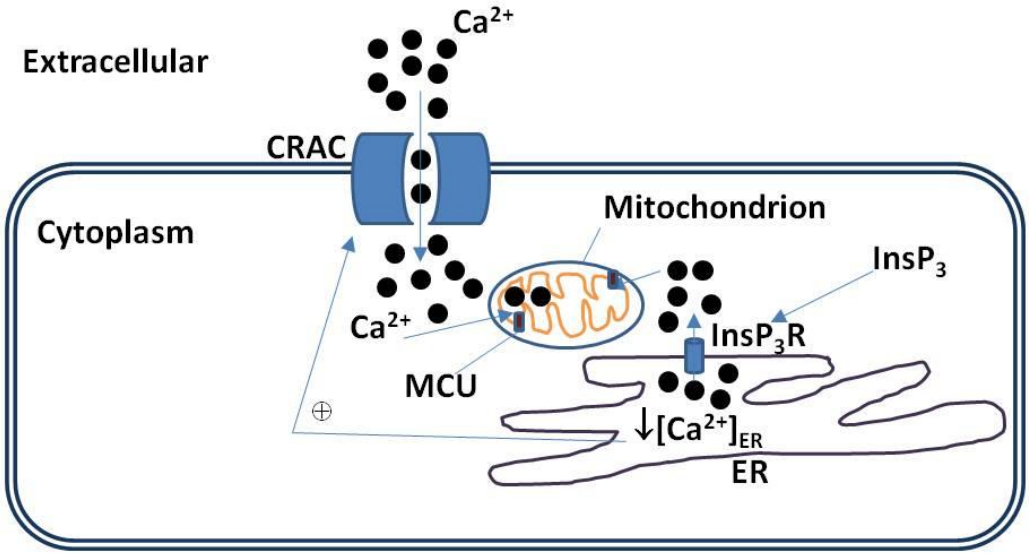

Figure 1-5. Simplified model of regulation of Ca^{2+} by MCU.

The ability of mitochondria to buffer Ca^{2+} that enters the cytosol through Ca^{2+} channels on either the plasma membrane or internal stores indicates that mitochondria influence both activation and inactivation of CRAC channels. Immune cells, like most other cell types, have a low cytoplasmic Ca^{2+} binding ratio (ratio of Ca^{2+} bound to buffer / free Ca^{2+} concentration), in the range of 50–150 (69). In T cells, the Ca^{2+} binding ratio has been reported to be 125 (70), and recent work in mast cells from our laboratory has shown to it be approximately 150 (data not shown). Under physiological conditions, mitochondrial Ca^{2+} uptake therefore plays a fundamental role in cytoplasmic Ca^{2+} buffering. Mitochondrial Ca^{2+} uptake removes Ca^{2+} from the vicinity of the ER following Ca^{2+} release in mast cells (60,63). Therefore, it slows down store refilling by sarco- endoplasmic reticulum Ca^{2+} ATPase (SERCA) pumps. As a result, substantial store emptying occurs and thus leads to robust activation of CRAC channels (71,72). The subsequent rise in bulk cytoplasmic Ca^{2+} due to Ca^{2+}

influx through open CRAC channels feeds back to inactivate the channels slowly, over minutes (73,74). Mitochondria are able to buffer the incoming Ca^{2+} and thus reduce the rate and extent of Ca^{2+}-dependent slow inactivation (71,72,75,76). In T cells, translocation of mitochondria to the plasma membrane was directed by Ca^{2+} entry through CRAC channels and this further sustained Ca^{2+} entry by buffering incoming Ca^{2+} (77). Thus mitochondria facilitate channel opening by promoting more extensive store depletion and then sustain opening by reducing Ca^{2+}-dependent inactivation.

Ca^{2+} uptake by mitochondria stimulates aerobic metabolism and ATP production. Pyruvic acid is produced from glycolysis, an important step in aerobic cell respiration. Previous work from our group has demonstrated that dialysis with pyruvic acid significantly reduced the extent of Ca^{2+}-dependent rapid inactivation of CRAC channels, which develops within milliseconds, over a range of membrane potentials (78). Rapid inactivation is triggered by the build-up of a Ca^{2+} microdomain beneath each open CRAC channel. The mechanism whereby pyruvate reduced rapid inactivation did not involve mitochondrial Ca^{2+} uptake or ATP production and might therefore reflect a direct action on the CRAC channel. Dialysis with different concentrations of pyruvic acid revealed that effects were prominent at concentrations of approximately 1 mM, within the physiological range (78). As glycolytic enzymes exist in a macromolecular complex and are generally attached to the plasma membrane by proteins like anion exchanger 1 (79), local pyruvic acid concentration just below the plasma membrane is likely to be considerably higher than a bulk concentration of 0.5–1 mM. Therefore pyruvic acid regulation of CRAC channel activity is likely to be of considerable physiological relevance. Despite the fact that a type of K^+ channel is regulated by changes in the cytoplasmic ATP ⁄ adenosine

diphosphate (ADP) ratio level (K_{ATP} channels) (80,81), intermediary metabolites have no effects on its channel activity. Hence, CRAC channels are the first ion channel found to be regulated by an intermediary metabolite. CRAC channels might act as a potential plasma membrane nexus, linking energy status of a cell to Ca^{2+} influx.

1.3 CRAC channels in mast cells

CRAC channels play a critical role in IgE-mediated mast cell activation, where they provide the pathway for antigen-evoked Ca^{2+} entry (82,83). Either Orai1- or STIM1-deficient mice evoke weak Ca^{2+} signals in response to agonist (84,85). Importantly, these knockout mice exhibit impaired leukotriene production, histamine release, reduced TNF-α secretion, and fail to mount a subcutaneous anaphylactic response. Therefore, Ca^{2+} entry through CRAC channels is crucial for mast cell function. Previous work from our laboratory has shown that in mast cells, Ca^{2+} influx through CRAC channels activates Ca^{2+}-dependent phopholipase A_2, ERK and 5-lipoxygenase, resulting in LTC_4 secretion (54,86) , as well as gene expression of *c-fos* (25). The proto-oncogene, *c-fos* belongs to the immediate early gene family of transcription factors and it regulates production of cytokines such as TNFα and IL-4 in response to IgE mediated mast cell activation (87).

In mast cells, IgE-mediated activation of FcεRI receptors or stimulation of classical G protein-coupled receptors (adenosine, cysteinyl leukotriene type I) releases Ca^{2+} from internal stores and thus trigger Ca^{2+} entry through CRAC channels (28). Hence, targeting the CRAC channel pharmacologically should be a successful therapy for combating inappropriate mast cell activation in response to a variety of diverse stimuli.

1.3.1 Local Ca^{2+} influx in mast cells: cracking the Ca^{2+} paradox

Ca^{2+} signalling has been implicated in a diverse array of functions including neurotransmitter release, muscle contraction, energy production, cell growth, and proliferation, as well as cell death (88). It has now been established that information is encoded in the amplitude, kinetics, and spatial profile of the intracellular Ca^{2+} signal, thereby generating a specific Ca^{2+}-dependent response (89). The amplitude of a Ca^{2+} microdomain can attain levels of several tens of µM, orders of magnitude larger than the bulk Ca^{2+} rise (48,49). The spatial extent of Ca^{2+} microdomains is in the range of 10-25 nm. An effector located within this range could therefore respond directly to this spatially restricted Ca^{2+} signal, and thus selectively stimulate downstream targets. Ca^{2+} microdomains near open CRAC channels activate responses that underlie both the immediate and late phase responses in mast cells. Local Ca^{2+} influx activates the MEK/ERK pathway, leading to LTC_4 secretion (25). Ca^{2+} microdomains are also relayed to the nucleus, where they activate genes associated with the late response (90).

1.3.2 Ca^{2+} microdomains and the MEK/ ERK pathway in mast cells

Ca^{2+}-dependent cytosolic phospholipase A_2 ($cPLA_2$) hydrolyses phospholipids to form arachidonic acid, a susbstrate for production of leukotrienes. In mast cells, $cPLA_2$ is activated by Ca^{2+} influx through CRAC channels but not by Ca^{2+} release from internal stores (86). Several pieces of evidence support the view that $cPLA_2$ activation is driven by Ca^{2+} microdomains near open CRAC channels and not by a bulk Ca^{2+} rise (25,54,86). First, it has been shown that varying external Ca^{2+} concentration alters ERK activation without changing the bulk Ca^{2+}. Second, reducing the electrical gradient for Ca^{2+} influx by blocking inwardly rectifying K^+ channels has little effect on bulk Ca^{2+} concentration but substantially reduces ERK

activation. Third, the slow Ca^{2+} chelator, EGTA, has no inhibitory effect on ERK activation whereas the fast Ca^{2+} chelator BAPTA abolishes the response when loaded into the cytoplasm. Both chelators have similar affinities for Ca^{2+} and reduce bulk Ca^{2+} to similar extents.

1.3.3 How is local Ca^{2+} detected?

Local Ca^{2+} entry through CRAC channels activates the non receptor tyrosine kinase Syk, which activates ERK via recruitment of PKCα and βI (25). ERK activates $cPLA_2$ by phosphorylation of $cPLA_2$ on Ser-505 (25,91,92). In the presence of Syk inhibition, CRAC channel-driven $cPLA_2$ activation was rescued by stimulation of protein kinase C with phorbol ester (54). Hence, Syk is upstream of PKC and is thought to detect local Ca^{2+} directly or via an intermediate.

1.3.4 Ca^{2+} microdomains and LTC_4 secretion in mast cells

Arachidonic acid is metabolized by 5-lipoxygenase (5-LO) to the unstable intermediate LTA_4, which can be converted to LTB_4 by LTA_4 hydrolase or conjugated with glutathione to LTC_4 by LTC_4 synthase, depending on the enzymes present within the cell (Fig. 1-6) (93). 5-LO is located mainly in the cytosol at rest. Upon stimulation of the cell, it translocates via its amino-terminal C2-like domain to the nuclear membrane where it binds to the protein 5-LO activating protein (FLAP), resulting in enzyme activation (94-96). Our laboratory has previously shown that Ca^{2+} entry through CRAC channels increased association of the 5-LO with the nuclear membrane, whereas Ca^{2+} release from the stores was ineffective. Moreover, ERK, which stimulates $cPLA_2$, was also essential for 5-LO translocation and subsequent activation (25). Hence, ERK acts as a cytoplasmic regulator; by coordinating the activities of both $cPLA_2$ and 5-LO, ERK ensures that arachidonic acid is rapidly

metabolized to LTC_4. This form of metabolic coupling ensures that the levels of the pleiotropic messenger arachidonic acid are tightly regulated. ERK is therefore a key transducer of local Ca^{2+} influx and plays an important role in mast cell activation.

Cysteinyl leukotriene receptors (CysLT1R and CysLT2R) are present on mast cells (97-99). These receptors are 7 transmembrane-spanning receptors which couple to PLCβ via Gα, leading to $InsP_3$ production (100). They are widely expressed, being found in several types of immune cells, epithelial, endothelial and smooth muscle cells. Following activation of 5-LO, the cysteinyl leukotriene, LTC_4 is synthesized de novo from cell membrane phospholipids and then secreted from mast cells. LTC_4 is transported out of the cell by a multi-drug resistance like peptide (101). It can then be converted to LTD_4 and LTE_4. These lipid derived pro-inflammatory mediators were first identified as potent bronchoconstrictors (102) and are now known to be involved in coordinating immune responses, particularly during inflammation (103).

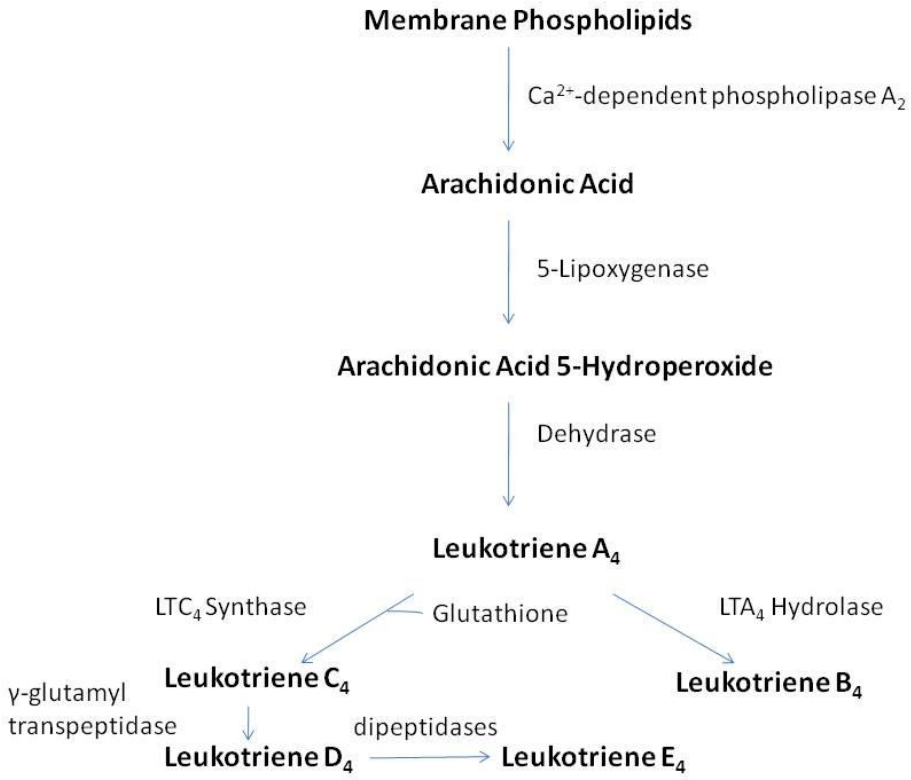

Figure 1-6. The formation of LTA_4 from arachidonic acid via the 5-lipoxygenase pathway and the conversion of LTA_4 to LTC_4 and LTB_4. Arachidonic acid is released from phospholipids in the nuclear and endoplasmic reticulum membranes by Ca^{2+}-dependent phospholipase A_2 ($cPLA_2$). It is then metabolized to generate LTA_4. Next, LTA_4 is converted by the LTC_4 synthase to LTC_4, the parent cysteinyl leukotriene.

1.3.5 Synergy between CRAC channels and protein kinase C generates short-term potentiation in mast cells

Local Ca^{2+} entry through CRAC channels activates the MEK/ ERK pathway via protein kinase C and results in activation of $cPLA_2$, followed by LTC_4 production (25). Stimulation of protein kinase C directly with phorbol ester activates the MEK/ ERK pathway, but this is not sufficient for $cPLA_2$ activation and LTC_4 secretion (25). This is because cytoplasmic Ca^{2+} is not affected by phorbol ester stimulation (25). Thus, activation of ERK in the absence of a Ca^{2+} rise is not sufficient to stimulate $cPLA_2$. Rather, both protein kinase C and a cytoplasmic Ca^{2+} rise are required for stimulating the $cPLA_2$/5-LO pathway. To address whether Ca^{2+} and protein kinase C interact synergistically, a previous study from our laboratory has shown that in low external Ca^{2+} (0.25–0.5 mM), Ca^{2+} influx evoked only modest $cPLA_2$ activation (25). When stimulation of protein kinase C was induced by phorbol ester, these same Ca^{2+} signals were much more effective (25). Protein kinase C thus renders small increases in cytoplasmic Ca^{2+} much more effective in generating arachidonic acid and LTC_4 production. These findings can be fitted into a model for $cPLA_2$ activation that has been developed by Das et al (104). The insertion of the amino-terminal C2 domain of $cPLA_2$ into the nuclear membrane is facilitated by a rise of intracellular Ca^{2+} (105). Simultaneously, phosphorylation of Ser-505 is essential for aliphatic amino acids at

the active site edge to penetrate the membrane, thus forming the catalytic active site. Both the membrane insertion and phosphorylation of Ser-505 were facilitated by Ca^{2+} signals. A small rise in Ca^{2+} promotes insertion of a few $cPLA_2$ molecules into the membrane as well as modest ERK activation. Protein kinase C activation greatly stimulates ERK, and subsequently the small number of $cPLA_2$ molecules embedded in the membrane by Ca^{2+} becomes catalytically more active. Extensive Ca^{2+} entry would stimulate both membrane insertion of $cPLA_2$ and ERK, leading to enormous activation of $cPLA_2$.

1.3.6 Graded versus all-or none responses in mast cells

In mast cells, patch clamp experiments have revealed that CRAC channels activate in an essentially all-or-none manner following receptor stimulation or dialysis with $InsP_3$ (106). All-or-none activation of CRAC channels could reflect either a non-linear step between $InsP_3$ and the store depletion or a mechanism whereby emptying of the store is non-linearly linked to CRAC channel opening. It has been shown that dialysis with the non-metabolizable $InsP_3$ analogue Ins(2,4,5)-P_3 resulted in more graded I_{CRAC}, with a significantly less steep relationship than that seen with $InsP_3$ (106). Hence $InsP_3$ metabolism accounts for the highly non-linear response. $InsP_3$ can be metabolized by the 3-kinase to produce Ins(1,3,4,5)-P_4 or by 5-phosphatase to yield Ins(1,4)-P_2. Dialysis with different concentrations of $InsP_3$-F, an analogue that is broken down by the 5-phosphatase but not metabolized by $InsP_3$-kinase, revealed the same all-or-none pattern was still present (107). Consistent with a major role for 5-phosphatase, inhibition of the 5-phosphatase with 2,3-diphosphoglycerate (2,3-DPG) resulted in a more graded relationship between $InsP_3$ concentration and I_{CRAC} amplitude (108). Recent work on T cells has shown that a non-linear relationship between store Ca^{2+} content and CRAC channel activation, with a Hill coefficient of 4

(109). This is thought to reflect the high affinity of STIM1 for Ca^{2+}, and cooperativity in multimer formation. Only when stores release Ca^{2+} beyond a certain level does STIM1 form multimers and migrate to the plasma membrane to open CRAC channels. These findings support earlier reports that demonstrated significant store depletion was needed for CRAC channels to open (106,110).

Despite all-or-none activation of CRAC channels, mast cells have the ability to produce graded Ca^{2+} signals through mechanisms that either alter the rate of Ca^{2+} entry into, or the rate of Ca^{2+} removal from, the cytoplasm. The rate of Ca^{2+} entry is affected by the prevailing electrical gradient and the availability of CRAC channels. Depolarization of the membrane potential reduces the electrical gradient for Ca^{2+} entry and thus decreases Ca^{2+} entry through CRAC channels. An alteration in the activity of an ion channel would therefore impact upon the Ca^{2+} signal, without necessarily affecting the CRAC channels themselves. Closure of K^+ channels would depolarize the membrane potential, and this would reduce Ca^{2+} entry. CRAC channels in mast cells are subject to numerous inactivation mechanisms that function to limit further influx. These mechanisms include Ca^{2+} itself (39,73,111,112), protein kinase C (113), sphingosine (114), and arachidonic acid (data not shown). The rate of Ca^{2+} removal from the cytoplasm reveals the actions of plasma membrane transporters (Na^+-Ca^{2+} exchange and Ca^{2+} ATPase pump), mitochondrial Ca^{2+} uptake through the uniporter channel, and sequestration into stores by sarco／endoplasmic reticulum Ca^{2+} ATPase (SERCA) pumps and into Golgi by secretory pathway Ca^{2+} ATPase (SPCA). In mast cells, mitochondrial Ca^{2+} uptake, SERCA and plasma membrane Ca^{2+} pumps play the major role in removing Ca^{2+} from the cytoplasm (112). All these mechanisms are regulated by intracellular signals and could thus help

shape the overall Ca^{2+} signal. Thus, a wide range of mechanisms exist that can grade the extent of the Ca^{2+} signal despite all-or-none CRAC channel activation.

Previous work from our laboratory examined whether mast cell responses were graded or all-or-none following CRAC channel activation, by examining the effects of different levels of muscarinic receptor activation on I_{CRAC} activation, cytoplasmic Ca^{2+}, protein kinase C translocation, ERK stimulation, and $cPLA_2$ and 5-LO activities (measured through production of arachidonic acid and LTC_4, respectively) in acutely isolated rat peritoneal mast cells as well as the RBL-1 mast cell line (115). It was shown that increasing agonist concentration increased activation of ERK, $cPLA_2$, and secretion of LTC_4 in a graded manner in cell population measurements. All these responses were abolished by removal of external Ca^{2+} (115). Therefore, Ca^{2+} influx through CRAC channel accounts for the mast cell responses. Despite the graded responses to agonist, I_{CRAC} developed in an all-or-none way in response to muscarinic receptor activation. I_{CRAC} was measured at a single cell level whereas the biochemical studies were carried out on populations of cells. The averaged response from a cell population is based on the assumption that all cells within that population respond to agonist. When PKC translocation in response to agonist was measured at the single cell level, it was found that increasing agonist concentration activated more cells (115). But for any cell that showed PKC translocation regardless of agonist concentration, movement was maximal. The results demonstrated that increasing agonist concentration recruited more cells in the population but each cell responds in an all-or-none manner. Recruiting more cells in an all-or-none manner is an effective approach to generate greater levels of local paracrine signals since at restricted sites of inflammation, where the number of mast cells present may be relatively low.

CRAC channels lead to the synthesis and secretion of LTC_4 and LTC_4 in turn activates CRAC channels. This led to the concept of a positive feedback step between CRAC channels and leukotrienes that would sustain mast cell activation (116). External solution collected from one population of mast cells, in which CRAC channels had been opened evoked large and repetitive Ca^{2+} oscillations in a second resting population of Fura-2-loaded RBL-1 cells, and these signals were totally blocked by the CysLT1 antagonists, montelukast and pranlukast (116). Conversely, pretreatment of the first population (the source of paracrine signal) with zileuton (an inhibitor of 5-LO) prevented the external solution collected from stimulated mast cells from evoking Ca^{2+} signals in the Fura-2 loaded cells (116). External solution taken from the donor cells in which 5-LO had been knocked down was unable to evoke Ca^{2+} signals in the Fura-2-loaded cells (116). Similarly prior knock down of CysLT1 receptor using RNAi in Fura-2 loaded RBL-1 cells rendered the cells insensitive to external solution taken from the stimulated donor cells (116). Hence LTC_4 produced following store depletion was able to stimulate a Ca^{2+} signal in a separate mast cell population. When the cells used to generate LTC_4 were stimulated in the absence of external Ca^{2+}, there was no Ca^{2+} rise in the Fura-2 loaded cells (116). Thus store-operated Ca^{2+} entry drives this form of intercellular signalling. When purified LTC_4 or LTD_4 were applied to RBL-1 cells, oscillatory Ca^{2+} signals were evoked, and these were blocked with montelukast. Collectively, these results demonstrate that leukotrienes play a major role in paracrine activation of mast cells. These results are relevant to primary cells because acutely isolated rat peritoneal mast cells and human nasal mast cells also generated LTC_4 and responded to LTC_4, in a manner that was blocked by CysLT1 antagonists such as montelukast (116,117). These showed the results were in agreement with cultured cells.

It was further shown that Ca^{2+} entry through CRAC channels in a patched cell induced a Ca^{2+} rise in the neighbouring cells, and this rise was prevented by montelukast (116). Therefore activation of CRAC channels in one cell is able to generate sufficient leukotriene for paracrine signalling. This positive feedback model is summarised in Figure 1-7. Mast cell activation results in the opening of CRAC channels. The local Ca^{2+} entry then activates 5-LO, which stimulates the production of LTC_4. Secreted LTC_4 acts on cell surface CysLT1 receptors on adjacent cells, leading to activation of CRAC channels. Ca^{2+} influx into these cells then activates LTC_4 production and the cycle continues. Not only do acutely isolated human mast cells show this type of paracrine signalling in vitro, but staining of mast cells from nasal polyps with the aniline dye toluidine blue indicated mast cells were generally no further than 20–50 μm apart (116). Hence they are close enough to one another to induce paracrine signalling. Moreover, the diffusion coefficient for LTC_4 is quite high, approximately 400 $\mu m^2/s$ (116). This means LTC_4 can readily cross the gap between mast cells in the polyps. Finally, mast cells have high affinity for LTC_4 (about 25% cells responding to 2 pM LTC_4) (116). This would facilitate paracrine signalling by ensuring low concentrations of LTC_4 activate the CysLT1 receptors.

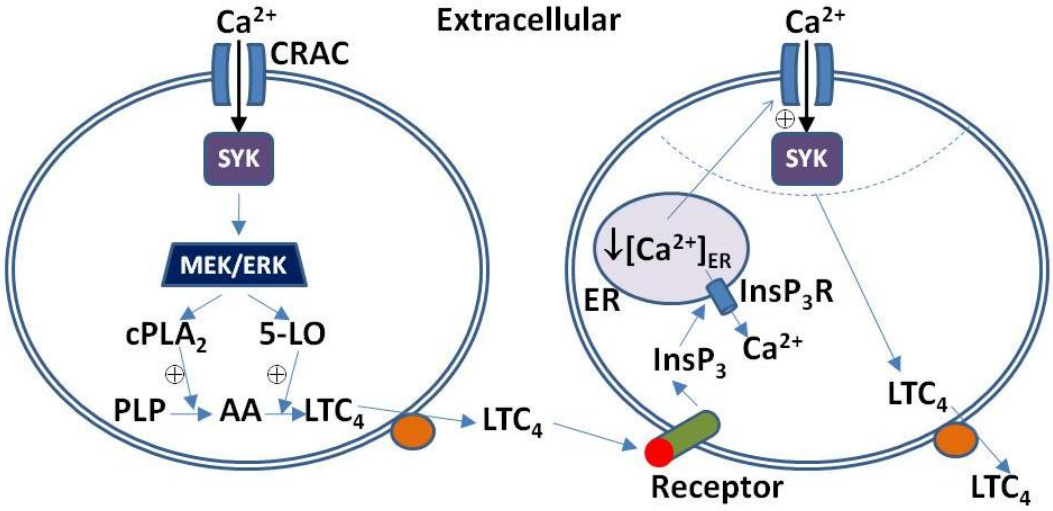

Figure 1-7. Paracrine signalling of LTC_4 in mast cells. PLP, phospholipids.

1.4 Aims of this thesis

Clearly, Ca^{2+} microdomains are essential for mast cell function. Nevertheless, several important questions remain. How is local Ca^{2+} near open CRAC channels sensed? Do Ca^{2+} microdomains contribute to responses evoked by physiological stimuli? How are Ca^{2+} microdomains relayed to the nucleus, an essential process that underlies the second phase of an allergic response? These issues are addressed in this thesis.

- Chapter 3: describes a positive feedback step in mast cell activation where sustained activation of the tyrosine kinase Syk by antigen requires local Ca^{2+} influx through CRAC channels
- Chapter 4: addresses how local Ca^{2+} influx through CRAC channels activate *c-fos* gene expression and identify important roles for Syk and STAT5
- Chapter 5: describes how physiological stimulation of cysteinyl leukotriene type I receptor activates gene expression and reveals the finding that reversible receptor desensitization actually serves to sustain gene expression

Chapter 2 Materials & Methods

2.1 Materials

All chemicals were obtained from Sigma-Aldrich, unless otherwise stated. The CRAC channel blocker used in this study, Synta compound, was kindly provided by Dr. Valerie Morisset at GlaxoSmithKline, UK. The Synta compound is compound 66 from the WO2005/009954 A2 patent (3-fluoropyridine-4-carboxylic acid (2', 5'-dimethoxybiphenyl- 4-yl) amide (Fig. 2-1)). Syk inhibitor was purchased from Calbiochem and thapsigargin was obtained from Merck.

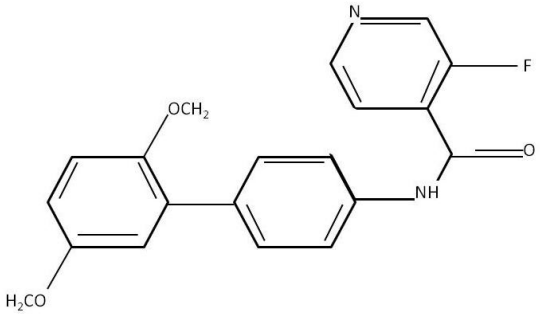

Figure 2-1. Structure of Synta Compound.

2.2 Cell Culture

Rat Basophilic Leukemia (RBL-1) and Human embryonic kidney (HEK293) cells were bought from ATCC. Cells were cultured (37 °C, 5% CO_2) in Dulbecco's modified Eagle's medium (DMEM) with 10% fetal bovine serum and 1% penicillin/streptomycin (final concentration of 100 units/ml penicillin and 100 µg/ml streptomycin, as described previously (106). For Ca^{2+} imaging and patch clamp experiments, cells were passaged using trypsin onto glass coverslips and used 24–48 h after plating. For RT-PCR and western blot, cells were passaged using trypsin onto 6 cm dishes and used at ~80% confluence.

2.3 Cell stimulation

RBL cells were sensitized to antigen (dinitrophenyl-bovine serum albumin, 80 µg/ml, 4 min) by incubation in IgE (2.5 µg/ml) overnight in standard culture medium. Thapsigargin, a SERCA pump inhibitor (2-4 µM, 4 min) was applied to RBL cells for activation of CRAC channels. Cytoplasmic loading with either EGTA or BAPTA was carried out by preincubating cells with EGTA-AM or BAPTA-AM (25 µM, Calbiochem) for 45 min at room temperature.

2.4 Ca^{2+} Imaging

Ca^{2+} imaging experiments were carried out at room temperature using the IMAGO charge-coupled device camera-based system from TILL Photonics, as described previously (25). Cells were alternately excited at 356 and 380 nm (20 ms exposures) using a Polychrome Monochromator. Images were acquired every 2 seconds. Images were then analysed offline using IGOR Pro for Windows. Cells were loaded with Fura-2-AM (4 µM, Invitrogen, UK) for 45 min at room temperature in the dark and then washed in standard external solution of composition 145 mM NaCl, 2.8 mM KCl, 2 mM $CaCl_2$, 2 mM $MgCl_2$, 10 mM D-glucose, 10 mM HEPES, pH 7.4, with NaOH. Ca^{2+}-free solution had the following composition: 145 mM NaCl, 2.8 mM KCl, 2 mM $MgCl_2$, 10 mM D-glucose, 10 mM HEPES, 0.1mM EGTA, pH 7.4, with NaOH. Cells were left for 15 min to allow further deesterification. Ca^{2+} signals are presented as the ratio 356/380.

2.5 Patch Clamp Recordings

Whole cell patch clamp recordings were carried out as described (76). Sylgard-coated, firepolished patch pipettes were filled with a solution that contained 145 mM cesium glutamate, 8 mM NaCl, 1 mM $MgCl_2$, 2 mM Mg-ATP, 10 mM HEPES, 10

mM EGTA, 30 µM $InsP_3$, pH 7.2, with CsOH. Pipette resistance was ~5 megohms when placed in an external solution containing 145 mM NaCl, 2.8 mM KCl, 10 mM CsCl, 10 mM $CaCl_2$, 2 mM $MgCl_2$, 10 mM D-glucose, 10 mM HEPES, pH 7.4, with NaOH. The inwardly rectifying K^+ current was measured with a pipette solution containing 145 mM potassium glutamate, 8 mM NaCl, 1 mM $MgCl_2$, 2 mM Mg-ATP, 10 mM HEPES, 0.1 mM EGTA, pH 7.2, with KOH. Bath solution for measuring the K^+ current contained 108 mM NaCl, 50 mM KCl, 10 mM $CaCl_2$, 2 mM $MgCl_2$, 10 mM D-glucose, 10 mM HEPES, pH 7.4, with NaOH. A correction of +10 mV was applied for the subsequent liquid junction potential that arose from the glutamate-based pipette solutions. Ca^{2+} current through CRAC channels and K^+ current through inwardly rectifying K^+ channels were followed by applying voltage ramps (at 0.5 Hz) spanning -100 to +100 mV in 50 ms from a holding potential of 0 mV. Current amplitudes were measured from the ramps at -80 mV and normalized to cell size by dividing the amplitude by cell capacitance. Currents were filtered using an 8-pole Bessel filter at 2.5 kHz and digitized at 100 µs. Capacitative currents were compensated before each ramp. Leak currents were subtracted by averaging two ramp currents obtained just before I_{CRAC} started to develop from all subsequent recordings. Series resistance was around 8-10 MOhms.

2.6 Preparation of Cell Lysates

Attached cells from 6-cm plastic dishes were washed twice with phosphate-buffered saline (PBS) and lysed with PBS buffer containing 0.5% Triton X-100, 2 mM EGTA, protease inhibitor cocktail (Sigma, UK), 1 mM sodium vanadate and 1 mM PMSF (phenylmethanesulphonyl fluoride), as described (25). Lysates were centrifuged at 8000 g for 5 min, and the supernatants were collected and stored at -80 °C for

subsequent experiments. Protein concentrations were determined by Bio-Rad DC protein assay.

2.7 Western Blotting

Total cell lysates (40–50 µg) were separated by SDS-PAGE on a 10% gel and electrophoretically transferred to nitrocellulose membrane. Membranes were blocked with 5% bovine serum albumin in TBS plus 0.1% Tween 20 (TBST) or 5% nonfat dry milk in PBS plus 0.1% Tween 20 (PBST) buffer for 2 h at room temperature. Membranes were washed with TBST/PBST three times and then incubated with primary antibody overnight at 4 ℃ or for 1 h at room temperature. The membranes were then washed with TBST/PBST again and incubated with a secondary antibody IgG for 1 h at room temperature. After washing with TBST/PBST, the bands were developed for visualization using ECL-plus Western blotting detection system (GE Healthcare, Amersham, UK). Gels were quantified using the UN-SCAN-IT software package (Silk Scientific Inc., Orem, UT, USA). Anti-phospho-Syk antibody, anti-phospho-ERK, anti-phospho-STAT5 and STAT5 were from Cell Signalling *(*Boston, MA, USA) and used at 1:2500 dilution. Total ERK2 antibody was from Santa Cruz Biotechnology (Santa Cruz, CA, USA) and used at a dilution of 1:5000. The membranes were then washed with TBST/PBST again and incubated with a 1:2500–5000 dilution of goat anti-rabbit secondary antibody IgG from Santa Cruz Biotechnology (Santa Cruz, CA, USA) or 1:2000 dilution of peroxidase-linked anti-mouse IgG from Amersham Bioscience (Buckinghamshire, UK) for 1 h at room temperature. Total ERK2 is widely used as a control for gel loading (118-120). The antibody does not discriminate between phosphorylated (and hence active) and non-phosphorylated ERK2 and therefore detects the total amount of this protein, regardless of whether the kinase has been activated. The extent of Syk

phosphorylation and ERK phosphorylation were therefore normalized to the total amount of ERK2 present in each lysate, to correct for differences in amount of cells used for each condition (25). The extent of STAT5 phosphorylation was normalized to the total amount of STAT5 present in each lysate

2.8 Transfection and RNAi

Lipofectamine^{TM}2000 (Invitrogen, Paisley, UK) was used for transfection of HEK293 cells, and Cell line Nucleofector kit V (Lonza, Cologne , Germany) was used for RBL cells (54). Cells were transfected with RNAi directed against Orai1/Syk using the Amaxa system, as previously described (13). Orai siRNA sequence was designed by using Invitrogen block-it software and Syk Stealth^{TM} siRNA duplex oligonucleotide was from Invitrogen, Paisley, UK (Table 2-1). Control cells were transfected under identical conditions with scrambled siRNA (Invitrogen, Paisley, UK) or enhance green fluorescent protein.

Table 2-1. ***siRNA sequences***

Gene	**RNAi Sequence (5'-3')**
Orai1	Sense: GUCCACAACCUCAACUCCTT
Syk	Sense: CCCUCUGGCAGCUAGUGGAACAUUA Antisense: UAAUGUUCCACUAGCUGCCAGAGGG

2.9 Reverse Transcriptase-PCR

Total RNA was extracted from RBL cells by using an RNeasy Mini Kit (Qiagen, West Sussex, UK). RNA was quantitated spectrophotometrically by absorbance at 260 nm. Total RNA (1 µg) was reverse-transcribed using the iScript^{TM} cDNA Synthesis Kit (Bio-Rad, Hemel Hempstead, UK), according to the manufacturer's

instructions. Following cDNA synthesis, PCR amplification was then performed using BIO-X-ACT^{TM} Short DNA Polymerase (Bioline, London, UK) with primers specific for gene of interest. PCR primers (Table 2-2) for the detection of Orai1, β-actin and *c-fos* were synthesized by Invitrogen, UK. The PCR products were electrophoresed through an agarose gel and visualized by ethidium bromide staining.

Table 2-2. ***PCR primer sequences, optimal amplification cycles, and product sizes***

Gene	**Primer Sequence**	**Optimal Conditions**	**Size, bp**
Orai1	Sense: 5'-AGTCCTCACCTTCCCACTGG-3' Antisense: 5'-GCCTCTTCCTTCCACACTCTG-3'	32 cycles	133
β-actin	Sense: 5'-TTGTAACCAACTGGGACGATATG-3' Antisense: 5'-GATCTTGATCTTCATGGTGCTAGG-3'	28 cycles	764
c-fos	Sense: 5'-AGCCGACTCCTTCTCCAGCAT-3' Antisense: 5'-CAGATAGCTGCTCTACTTTGC-3'	32 cycles	298

2.10 Immunofluorescence

Cells were fixed in 4% paraformaldehyde in phosphate buffer for 30 min at room temperature. All the washes used 0.01% PBS (PBS; 137 mM NaCl, 2.7 mM KCl, 8

mM Na_2HPO_4, 1 mM KH_2PO_4). The cells were blocked with 2% BSA and 10% goat serum for 1 h. Anti-Syk or Anti-*c-fos* were used in carrier (0.2% BSA, 1% goat serum) and left overnight at 4°C. Anti-Syk antibody and anti-c-fos antibodies were purchased from Santa Cruz Biotechnology (Santa Cruz, CA, USA) and Cell Signalling *(*Boston, MA, USA) respectively. The secondary anti-rabbit IgG was a HandL chain specific (goat) fluorescein conjugate (Alexa Fluor 568, excitation at 578 nm, emission at 603 nm wavelength) from Invitrogen, Paisley, UK. This was used in PBS for 2 h at room temperature. GFP-transfected cells (excitation at 395/475 nm, emission at 509 nm) acts as control. The cells were mounted in Vectashield mounting medium. Images were obtained using a Leica confocal microscope.

2.11 Statistical Analysis

Results are presented as means ± S.E.M. Statistical significance was assessed using Student's t test for comparison between two groups or analysis of variance (ANOVA) followed by a *post hoc* Newman Keuls multiple comparison test for the difference between groups and considered significant at $p < 0.05$ (*).

Chapter 3 Sustained Activation of the Tyrosine Kinase Syk By Antigen Requires Local Ca^{2+} influx through CRAC channels

3.1 Introduction

The cell surface IgE receptor, FCεRI, recognizes the Fc region of antigen-specific IgE molecules (Fig. 3-1). Cross-linking of FCεRI receptors with antigen is a critical early step in mast cell activation (19,121). FCεRI receptors couple to a cascade of protein kinases, among which the non-receptor tyrosine kinase Syk plays a pivotal role in mast cell stimulation (6,122). Syk binds to tyrosine-phosphorylated residues in the immunoreceptor tyrosine-based activation motif of the FCεRI β and γ chains via its two SH2 domains, increasing enzyme activity (123-125). Syk-null cells fail to degranulate following exposure to antigen and antisense oligonucleotides directed against Syk reduce antigen-driven responses in an *in vivo* rat model of asthma (126). In the RBL mast cell line, inhibition of Syk suppresses degranulation (127) as well as production of the pro-inflammatory cysteinyl leukotrienes (25).

In RBL cells, activated Syk stimulates phospholipase Cγ1 (PLCγ1)(128), which hydrolyzes the phospholipid phosphatidylinositol 4,5-bisphosphate to generate inositol trisphosphate ($InsP_3$) and diacylglycerol (129). $InsP_3$ binds to tetrameric $InsP_3$-gated Ca^{2+} channels in the endoplasmic reticulum, releasing stored Ca^{2+} into the cytosol. The ensuing store depletion then activates store-operated CRAC channels in the plasma membrane (130), which provide a substantial portion of Ca^{2+} needed to activate mast cells. Genome-wide RNAi knockdown strategies have identified two key molecular components of the store-operated Ca^{2+} entry pathway, STIM1 (30,131) and Orai1 (31,132,133). STIM1, a protein that spans the endoplasmic reticulum, is the Ca^{2+} sensor that detects the fall in Ca^{2+} content within the store. It migrates from a relatively homogeneous distribution throughout the endoplasmic reticulum to discrete puncta within 25 nm of the plasma membrane, lining up opposite the plasma membrane protein Orai1 (134). Site-directed mutagenesis has established that Orai1 is

all or part of the CRAC channel pore (135-137). The importance of STIM1 and Orai1 in mast cell function is underscored by the findings that degranulation, secretion of pro-inflammatory cysteinyl leukotrienes and chemokines, as well as the ability to mount an inflammatory response are all severely compromised in mice in which these genes have been ablated (84,85).

Activation of immune cells often requires sustained Ca^{2+} entry through CRAC channels (138). This in turn is dependent on a maintained elevation in $InsP_3$ levels (and thus PLCγ activity), which is needed to ensure the stores are depleted sufficiently for CRAC channels to remain open. Because PLCγ can be activated by Syk, I examined whether the subsequent Ca^{2+} influx can feed back to maintain Syk activation. The findings reveal a novel self-regenerative process whereby local Ca^{2+} influx through CRAC channels increases Syk activity, which in turn sustains CRAC channel activity by preventing store refilling.

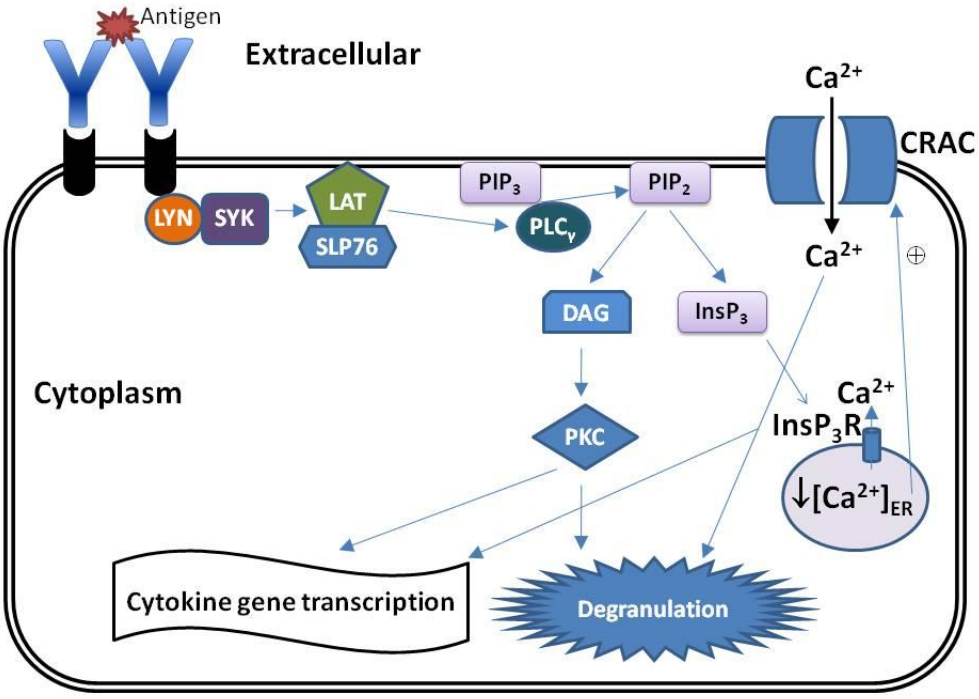

Figure 3-1. IgE-mediated mast cell activation.

3.2 Results

3.2.1 Antigen-evoked responses depend on functional Syk

Phosphorylation and thus activation of Syk is a central early event following FCεRI receptor engagement (122). By regulating PLCγ, Syk drives the generation of cytoplasmic Ca^{2+} signals in response to antigen stimulation. Consistent with this, pre-treatment for 10 min with the Syk inhibitor 3-(1-methyl-1H-indoyl-3-yl-methylene)-2-oxo-2,3-dihydro-1H-indole-5-sulfonamide prevented the generation of the antigen-evoked cytoplasmic Ca^{2+} rise in IgE-sensitized RBL cells (Fig. 3-2*A*). Acute application of the Syk inhibitor after the antigen-activated Ca^{2+} signal had developed also resulted in suppression of the Ca^{2+} signal (Fig. 3-2*B*). Hence Syk activity is critical for both the generation as well as subsequent maintenance of the Ca^{2+} signal following activation of FCεRI receptors.

3.2.2 Ca^{2+} influx enhances Syk activity

The non-receptor tyrosine kinase Syk is activated following phosphorylation of tyrosine residues within the activation loop (139,140). Syk activity was monitored by using a monoclonal antibody that specifically recognized phosphorylated tyrosine residues in this active loop. Stimulation with antigen for 4 min in the presence of external Ca^{2+} resulted in robust Syk phosphorylation (*upper panel* of Fig. 3-2*C*; *lower panel* depicts total (combination of active and non-active) ERK2, which is taken as a control for gel loading; aggregate data from four independent experiments is summarized in Fig. 3-2*D*). However, when cells were stimulated with antigen for the same time but now in the absence of external Ca^{2+}, significantly less (~2-fold) Syk phosphorylation occurred (Fig. 3-2, *C* and *D*). Because Western blotting involves a large population of cells, I was concerned that fewer cells in the population might

respond to antigen in Ca^{2+}-free solution than in the presence of Ca^{2+}, thus accounting for the difference in Syk activation. However, the number of cells responding- to either condition was similar (data not shown; see also Fig. 3-4).

I considered the possibility that Syk phosphorylation induced by antigen in the absence of external Ca^{2+} involved release of Ca^{2+} from internal stores. Cells were exposed to thapsigargin (2 μM) in Ca^{2+}-free solution to deplete the stores and then antigen was applied, still in the absence of external Ca^{2+}. Antigen now failed to trigger a Ca^{2+} response (data not shown). Ca^{2+} release to thapsigargin failed to activate Syk (data not shown and see also Fig. 3-6) but application of antigen after thapsigargin still resulted in Syk phosphorylation and to an extent similar to that seen when cells were stimulated with antigen in Ca^{2+}-free solution but in the absence of thapsigargin (Fig. 3-2*E*). Hence the activation of Syk in the absence of external Ca^{2+} is independent of Ca^{2+} release from the stores.

In mast cells, Ca^{2+} influx can activate protein kinase C α and β II thereby recruiting the MEK/ERK pathway (25). To see whether Syk activation was secondary to this signalling cascade, protein kinase C (PKC) was directly stimulated with the phorbol ester phorbol 12-myristate 13-acetate. No Syk phosphorylation was detected (Fig. 3-2*F*). To confirm specificity for the FCεRI pathway, Syk activation was measured following stimulation of endogenous P_2Y receptors, which couple to PLCβ but not PLCγ to generate $InsP_3$. No Syk phosphorylation was detectable (Fig. 3-2*G*). Finally, Syk activation required the presence of FCεRI receptors, because application of antigen to RBL cells that had not been pre-exposed to IgE failed to evoke Syk phosphorylation (Fig. 3-2*G*). Collectively, these results demonstrate that extracellular Ca^{2+} is required to sustain Syk activity following FCεRI receptor stimulation, and this does not involve PKC or subsequent downstream events.

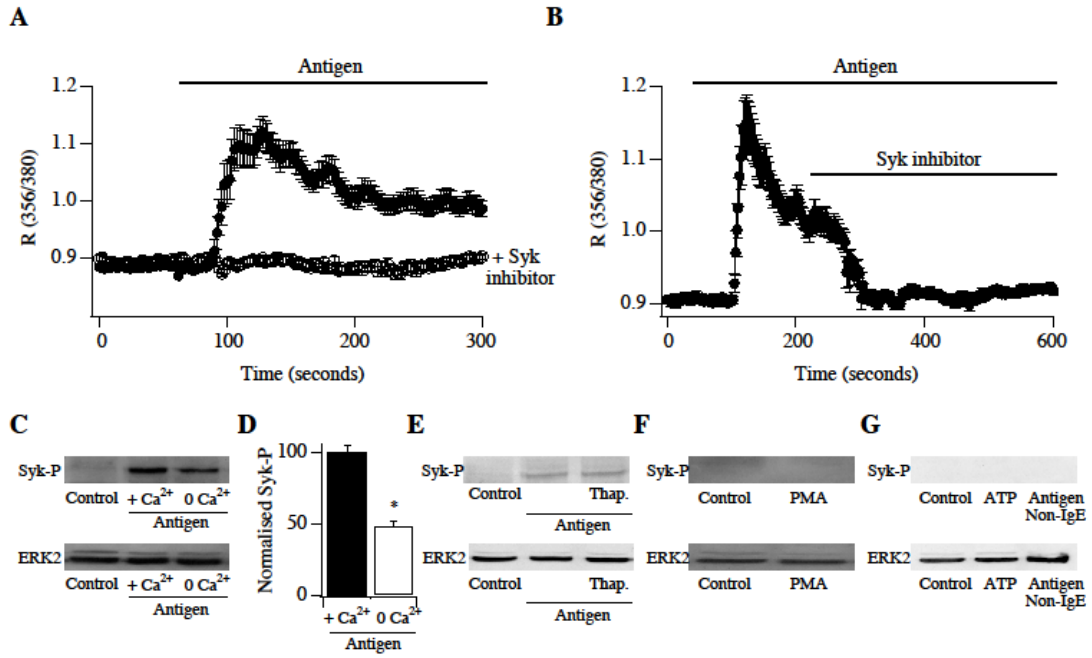

Figure 3-2. Activity of the tyrosine kinase Syk is required for, and sustained by, Ca^{2+} influx in response to FCεRI receptor activation. *A*, stimulation of Fura-2-loaded RBL cells with antigen (80 μg/ml) produced a sustained Ca^{2+} rise, and this was suppressed by pre-treatment with the Syk inhibitor (10 μM for 10 min). *B*, after stimulation with antigen, the Syk inhibitor rapidly abolished the Ca^{2+} signal. *C*, Western blot shows antigen stimulation (4 min) led to robust Syk phosphorylation (denoted Syk-P) in the presence of external Ca^{2+} (+*Ca*$^{2+}$) and this was considerably less when Ca^{2+} was removed (*0Ca*$^{2+}$). *Control* denotes lysate from non-stimulated cells. *Lower panel*, ERK2 blots from the corresponding lysates used in the upper gel. *D*, aggregate data from four independent gels is shown. Gels were quantified as described under Chapter 2. *E*, following store depletion with thapsigargin (2 μM for 10 min in Ca^{2+}-free external solution), antigen (applied in Ca^{2+}-free solution) still triggered Syk phosphorylation. Gels shown are typical of three independent experiments. *F*, direct stimulation of protein kinase C with the phorbol ester phorbol 12-myristate 13-acetate (1 μM for 10 min) failed to evoke Syk phosphorylation. *G*,

neither 100 μM ATP (4 min) nor application of antigen to non-IgE-treated cells led to Syk phosphorylation.

3.2.3 Local Ca^{2+} influx maintains Syk activity

Although the previous results demonstrate a requirement for extracellular Ca^{2+} in sustaining Syk activity, they do not distinguish between a specific role for Ca^{2+} influx or simply the presence of external Ca^{2+} *per se*. To distinguish between these possibilities, the electrical driving force for Ca^{2+} influx was reduced while keeping extracellular Ca^{2+} constant. Cells were depolarized by blocking K^+ channels with the combination of external Cs^+ and TEA^+. Syk activation following antigenic stimulation was significantly reduced (Fig. 3-3*A*, aggregate data from three independent experiments is summarized in Fig. 3-3*B*), demonstrating that Ca^{2+} influx is required for sustaining Syk activity.

I asked whether Ca^{2+} influx activated Syk through a local action or whether it involved a rise in bulk cytoplasm Ca^{2+} concentration. To slow down the rate of rise of bulk cytoplasmic Ca^{2+} and to reduce its extent, cytoplasmic Ca^{2+} buffering was increased by loading cells with the fast Ca^{2+} chelator BAPTA together with Fura-2. With the loading protocol, sufficient BAPTA enters the cytoplasm to substantially blunt the bulk cytoplasmic Ca^{2+} rise following Ca^{2+} influx (54). However, as shown in Fig. 3-3 (*C* and *D*), Syk activation was unaffected. Because BAPTA is a fast Ca^{2+} chelator, this suggests that Ca^{2+} influx acts locally, stimulating Syk phosphorylation within a few nanometers of the Ca^{2+} entry sites.

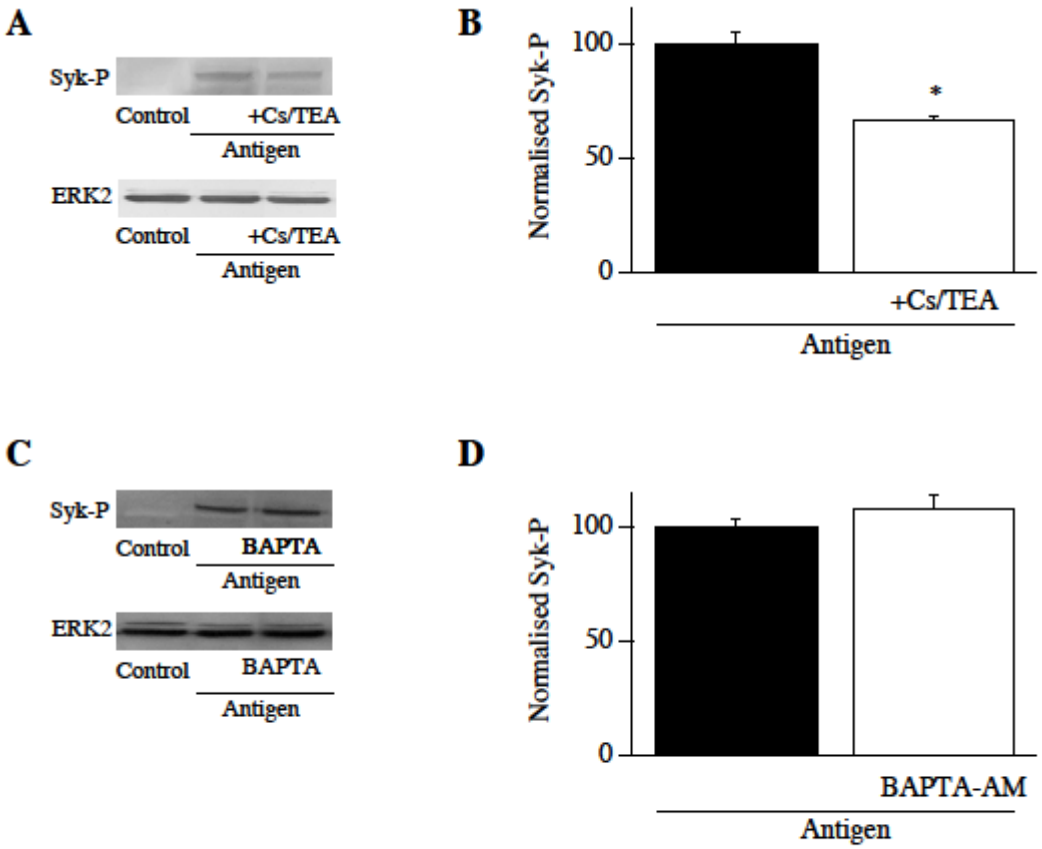

Figure 3-3. Local Ca^{2+} influx activates Syk. *A*, reducing the electrical driving force for Ca^{2+} entry by blocking K^+ channels with Tetraethylammonium (TEA^+) and Cs^+ (applied 4 min before stimulation and both at 10 mM) decreased antigen-evoked Syk phosphorylation. *B*, aggregate data from three independent experiments are summarized. Antigen was applied for 4 min in 2 mM Ca^{2+}. *C*, increased cytoplasmic Ca^{2+} buffering by loading cells with BAPTA (25 µM BAPTA for 45 min) did not prevent Syk phosphorylation by antigen. *D*, aggregate data from four experiments are summarized.

3.2.4 The Ca^{2+} influx pathway sustaining Syk activity is the store-operated CRAC channel

Pharmacological and gene knockdown experiments were carried out to identify the molecular identity of the Ca^{2+} influx pathway activated by antigen. CRAC channels are very sensitive to the trivalent cation Gd^{3+}, with full block occurring in the low micromolar range (38). Our previous work has confirmed that low Gd^{3+} blocks CRAC channels in RBL cells (86). Therefore the extent of Syk phosphorylation to antigen (applied in the presence of 2 mM Ca^{2+}) was compared in the absence and then presence of 2 μM Gd^{3+}. Antigen-triggered Syk phosphorylation was significantly reduced in the presence of Gd^{3+} (Fig. 3-4*A*), and the extent of the remaining Syk phosphorylation was similar to that seen when cells were stimulated with antigen in Ca^{2+}-free solution (Fig. 3-2).

The pharmacological strategy was extended by using a novel CRAC channel blocker, called the Synta compound (see Chapter 2). Store-operated CRAC channels were activated by exposing Fura-2-loaded cells to the sarcoplasmic-endoplasmic reticulum calcium ATPase pump blocker thapsigargin in Ca^{2+}-free solution. By blocking Ca^{2+} reuptake, thapsigargin gradually depletes the stores of Ca^{2+}, thereby opening CRAC channels. Readmission of external Ca^{2+} results in Ca^{2+} entry through the CRAC channels, generating a cytoplasmic Ca^{2+} rise. The rate of rise of cytoplasmic Ca^{2+} was measured following Ca^{2+} readmission, because this is a more reliable indicator of CRAC channel activity than the steady-state amplitude. As shown in Fig. 3-4*B*, 10 μM Synta compound substantially slowed the rate of rise of the cytoplasmic Ca^{2+} signal after readmission of external Ca^{2+}, and this amounted to almost 90% block of the CRAC channels (Fig. 3-4*C*).

To measure CRAC channel activity directly, I carried out whole cell patch clamp recordings in which I activated the CRAC current (I_{CRAC}) by dialyzing cells with $InsP_3$ in 10 mM EGTA. The time course of I_{CRAC} development is shown in Fig. 3-4*D* (*filled circles*) and the current-voltage relationship, taken when I_{CRAC} had reached steady-state, is depicted in Fig. 3-4*E*. Pre-treatment for 5 min with 10 μM Synta compound abolished I_{CRAC} (Fig. 3-4, *D* and *E*). Similarly, after activation of I_{CRAC}, perfusion with the Synta compound resulted in a loss of the current (data not shown). I constructed a dose-inhibition curve for the Synta compound, which is summarized in Fig. 3-4*F*. These data could be fitted with a Hill-type equation, yielding a Hill coefficient of 1.1 and an IC_{50} of 3 μM.

Having established that the Synta compound blocks CRAC channels, I went on to examine the effects of the drug on antigen-evoked Ca^{2+} influx and Syk activation. The Synta compound suppressed Ca^{2+} influx evoked by antigen (Fig. 3-4*G*) and reduced the extent of Syk phosphorylation (Fig. 3-4, *H* and *I*). Strikingly, the fall in Syk activity (~50%, Fig. 3-4*I*) in the presence of Synta compound was similar to that seen when external Ca^{2+} was removed (Fig. 3-2*D*), consistent with suppression of Ca^{2+} influx by Synta compound.

The selectivity of the Synta compound for CRAC channels was tested by examining whether the drug interfered with two other major ion transport mechanisms in the mast cell membrane: inwardly rectifying K^+ channels and the plasma membrane Ca^{2+} ATPase pump. The current-voltage relationship and the amplitude of the inwardly rectifying K^+ current was unaffected by 10 μM Synta compound (Fig. 3-5, *A* and *B*). Similarly, the rate of Ca^{2+} removal from the cytoplasm after stimulation with thapsigargin in Ca^{2+} free solution, which reflects activity of the plasma membrane

Ca^{2+} ATPase pump (112), was similar in the absence and presence of the Synta compound (Fig. 3-5, *C* and *D*).

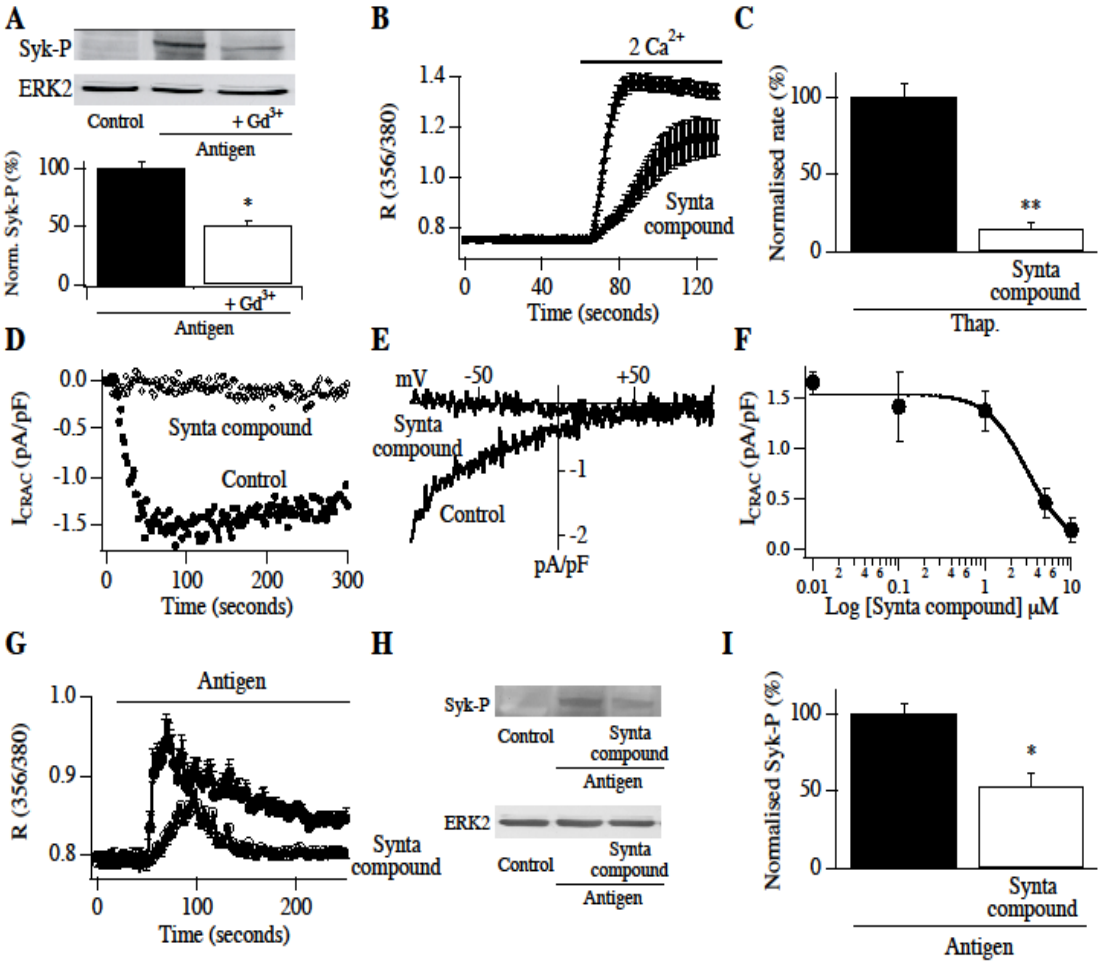

Figure 3-4. Pharmacological block of CRAC channels reduced antigen-evoked Syk phosphorylation. *A*, exposure to antigen in the presence of 2 μM Gd^{3+} prevented Ca^{2+} influx-dependent Syk phosphorylation. The *upper gel* compares the extent of Syk phosphorylation in 2 mM Ca^{2+} and then 2 mM Ca^{2+} and Gd^{3+}; *lower gel*, total ERK2 levels. *B*, the CRAC channel blocker Synta compound (10 μM) inhibited store-operated Ca^{2+} entry. In these experiments, cells were loaded with Fura-2 and pre-treated for 10 min with thapsigargin (2 μM) in Ca^{2+}-free solution. Ca^{2+} was readmitted as indicated. *C*, the rate of rise of the Ca^{2+} signal from experiments as in *panel B* are summarized. Each *bar* represents >80 cells. *D*, pre-treatment with 10 μM

Synta compound suppresses development of I_{CRAC}. *E*, current-voltage relationships from the recordings in *panel D* (~100 s) are shown. *F*, the relation between I_{CRAC} and Synta compound concentration is shown. *G*, 10 μM Synta compound inhibited antigen-evoked Ca^{2+} influx in Fura-2-loaded cells (>60 cells per point). *H*, antigen-triggered phosphorylation of Syk was reduced by 10 μM Synta compound. *I*, aggregate data from four experiments, as in *H*, is summarized. In *H* and *I*, antigen (10 μg/ml) was applied in 2 mM Ca^{2+}.

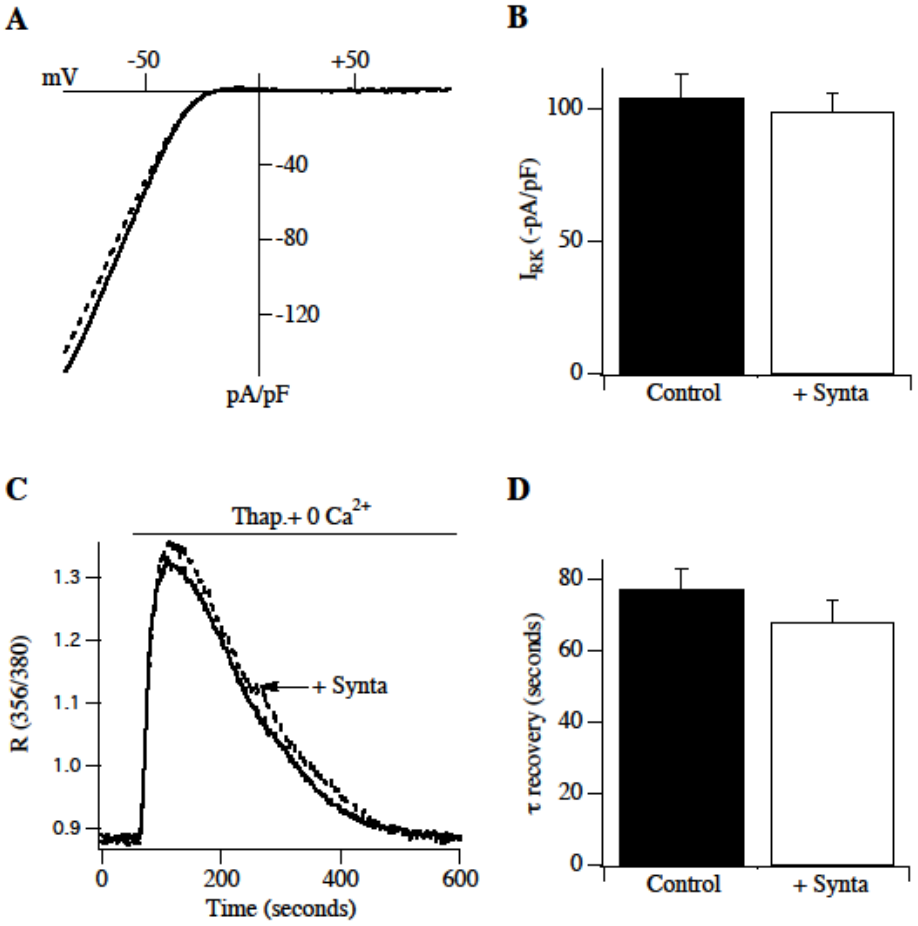

Figure 3-5. The Synta compound does not impair other plasma membrane ion transporters. *A*, current-voltage relationships for inwardly rectifying K^+ current are shown for a control cell and for one exposed to 10 μM Synta compound for 10 min. *B*, aggregate data for control cells (n = 5) and for those exposed to the Synta compound (n = 6) are compared. Current amplitudes were measured from voltage

ramps at –80 mV. *C*, plasma membrane Ca^{2+} ATPase activity was monitored in control cells and in those exposed to the Synta compound by measuring the rate of decline of the cytoplasmic Ca^{2+} signal following stimulation with thapsigargin in Ca^{2+}-free solution (with 0.1 mM EGTA). *D*, aggregate data from experiments as in *panel C* are compared. For both conditions, number of cells was >60.

3.2.5 RNAi knockdown of Orai1 reduces antigen-dependent Syk activation

To strengthen the pharmacological approach, an RNAi knockdown strategy was used to suppress expression of the protein Orai1, which is central to the CRAC channel pathway. Orai1 is a plasma membrane protein that comprises the pore of the CRAC channel (31,132,135-137). Transfection with siRNA to Orai1 resulted in a reduction in Orai1 mRNA levels, measured using reverse transcription-PCR (Fig. 3-6*A*). Knockdown was only partial, because our transfection efficiency was ~60%, judged by expression of eYFP. Co-transfection of Orai1 siRNA with an eYFP construct enabled us to identify transfected cells and thus measure the impact of Orai1 knockdown on store-operated Ca^{2+} entry. Readmission of external Ca^{2+} to cells pre-treated with thapsigargin resulted in robust store-operated Ca^{2+} influx in cells transfected with either eYFP alone or eYFP and scrambled siRNA (Fig. 3-6*B*). However, the rate and extent of Ca^{2+} influx was significantly reduced when cells were transfected with Orai1 siRNA (Fig. 3-6*B*, aggregate data are summarized in Fig. 3-6*C*). Hence knockdown of Orai1 results in significantly less store-operated Ca^{2+} entry. Following Orai1 knockdown, antigen activation of Syk was significantly reduced (Fig. 3-6*D*, aggregate data are summarized in the *lower panel*), demonstrating a role for CRAC channels in Syk activation. The fall in Syk phosphorylation following Orai1 knock down was not as extensive as that seen in Ca^{2+}-free solution (where no Ca^{2+} entry occurs), probably because transfection efficiency was ~60%. Collectively, the pharmacological and RNAi experiments reveal that it is antigen-evoked Ca^{2+} entry through CRAC channels that maintains the activity of Syk.

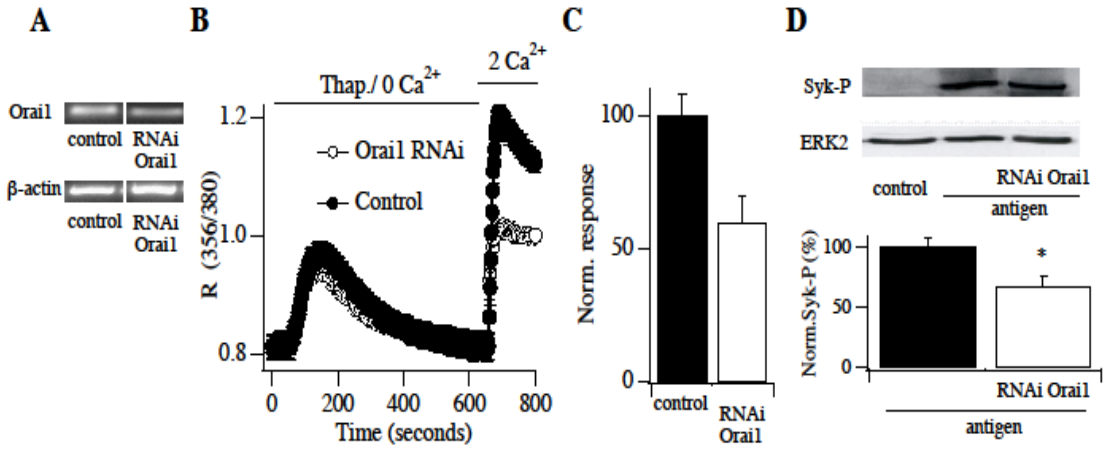

Figure 3-6. Knocking down expression of Orai1 suppressed antigen-evoked Ca^{2+} influx and subsequent Syk phosphorylation. *A*, reverse transcriptase-PCR shows that transfection with siRNA to Orai1 results in reduced Orai1 expression. *Upper panel*, Orai1; *lower panel*, β-actin controls for the samples used in the *upper panel*. *B*, store-operated Ca^{2+} influx is significantly reduced by siRNA to Orai1. Cells were transfected with eYFP alone, eYFP and nonsense siRNA (control), or eYFP and Orai1siRNA. 48–60 h post-transfection, cells were exposed to thapsigargin in Ca^{2+}-free solution and then 2 mM Ca^{2+} was readmitted. The extent of Ca^{2+} release by thapsigargin was similar for the two conditions. *C*, aggregate data from several experiments as in *panel B* are shown. The peak amplitude of the Ca^{2+} signal was measured. Control denotes 77 cells and Orai1 siRNA 61 cells. A similar reduction in the rate of Ca^{2+} influx was also observed. *D*, transfection of cells with RNAi to Orai1 significantly reduced Ca^{2+} influx-dependent activation of Syk in response to antigen stimulation. The *upper gel* compares Syk activation to antigen for control transfected cells and for those in which Orai1 had been knocked down. The *lower gel* is the total ERK2 loading control. The histogram depicts averaged data from four independent experiments.

3.2.6 Synergy between CRAC channels and FcεRI receptors in phosphorylating Syk

Although antigen activates I_{CRAC}, it does so to a submaximal extent even when applied at a supra-maximal concentration (113). The size of the current can be increased by further depletion of stores (113). To see whether antigen activation of Syk could be increased by recruiting more CRAC channels, antigen was applied together with thapsigargin. Thapsigargin depletes stores sufficiently to activate I_{CRAC} maximally (141). The combination of antigen and thapsigargin resulted in substantially more Syk phosphorylation than was observed with antigen alone (Fig. 3-7*A*, aggregate data are depicted in the *lower panel*). By blocking sarcoplasmic-endoplasmic reticulum Ca^{2+} ATPase pumps, thapsigargin not only depletes stores but also reduces Ca^{2+} buffering. This would increase the extent and time course of the Ca^{2+} signal evoked by antigen. To test whether the dramatic potentiating effects of thapsigargin on antigen-evoked Syk phosphorylation were indeed due to the reduction in Ca^{2+} buffering, antigen was applied with thapsigargin but now in Ca^{2+}-free external solution. Under these conditions, the combination of antigen and thapsigargin was only as effective as antigen alone (Fig. 3-7*B*); no potentiation occurred. Reduced cytoplasmic Ca^{2+} clearance therefore cannot explain the significant increase in Syk phosphorylation seen in response to the combination of antigen and thapsigargin. Stimulation with thapsigargin in the presence of external Ca^{2+} failed to evoke any detectable Syk phosphorylation (Fig. 3-7*C*). Hence receptor-independent activation of CRAC channels and subsequent Ca^{2+} entry cannot mimic the effects of antigen stimulation on Syk phosphorylation. Instead, Ca^{2+} entry acts synergistically with an early consequence of FCεRI receptor cross-linking and this interaction sustains Syk activity.

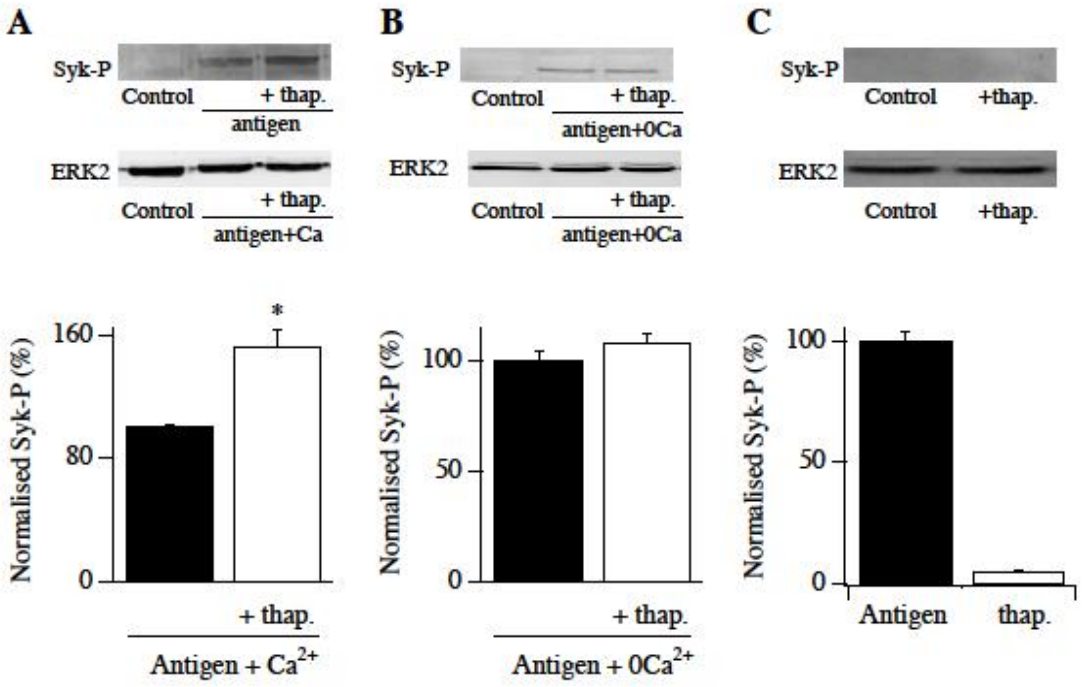

Figure 3-7. Antigen and CRAC channels interact synergistically to sustain Syk phosphorylation. *A, upper panel*; Western blot showing Syk phosphorylation induced by antigen was increased by thapsigargin. Aggregate data from three experiments is summarized in the *lower panel*. *B, upper panel* shows that Syk phosphorylation following stimulation with antigen in Ca^{2+}-free solution was not enhanced by thapsigargin. Aggregate data from two experiments is summarized in the *lower panel*. *C,* activation of CRAC channels by thapsigargin alone did not lead to any detectable Syk phosphorylation (*upper panel*), compared with control (non-stimulated) cells. Averaged data from three experiments are summarized in the *lower panel*, which compares Syk phosphorylation to antigen in 2 mM Ca^{2+} *versus* thapsigargin in 2 mM Ca^{2+}.

3.3 Discussion

My findings reveal a novel positive feedback cascade between Syk activity and Ca^{2+} influx through CRAC channels that sustains mast cell activation. Stimulation of Syk is an early event after antigen stimulation where it contributes to activation of PLCγ and subsequent Ca^{2+} release from intracellular stores (84). This fall in store Ca^{2+} content results in activation of CRAC channels (28). When Syk activity is blocked after the development of a Ca^{2+} plateau (reflecting store-operated Ca^{2+} entry) to antigen, the Ca^{2+} signal falls rapidly. Hence Syk activity is required both to initiate and then sustain Ca^{2+} entry, presumably by maintaining $InsP_3$ at levels sufficient to ensure partial store depletion (138). Syk activity is not independent of CRAC channels, however. Local Ca^{2+} entry through these channels feeds back to sustain Syk activity, providing a mechanism for the prolonged Ca^{2+} influx seen with FCεRI receptor activation and which is needed for appropriate stimulation of mast cells. The finding that Ca^{2+} influx sustains Syk activity provides a molecular mechanism that helps explain how certain G protein-coupled receptors, which themselves fail to trigger degranulation, can potentiate the antigen-driven responses in mast cells (142).

In some other cell types, cytoplasmic Ca^{2+} has been reported to activate Syk. In platelets, Syk was activated by the rise in cytoplasmic Ca^{2+} that accompanied Ca^{2+} ionophore application (143). In a human B cell line, platelet-activating factor stimulated Syk in a Ca^{2+}-dependent manner (144). Finally, in PC12 cells, Ca^{2+} influx led to the rapid activation of the non-receptor tyrosine kinase PYK2 (145). Although the mechanism whereby cytoplasmic Ca^{2+} activated these tyrosine kinases was not resolved, addition of Ca^{2+} to either cell lysates (144) or the isolated kinase (145) did not increase enzyme activity. Hence Ca^{2+} is unlikely to stimulate Syk directly. Consistent with this is my finding that Ca^{2+} influx through CRAC channels following

stimulation with thapsigargin failed to evoke any detectable Syk activation. Instead, an additional signal associated with FCεRI receptors is required. Syk is activated by binding, via SH2 domains, to phosphotyrosine residues in the immunoreceptor tyrosine-based activation motif signalling units on the β and γ chains of the receptor, which are phosphorylated by receptor-associated Src kinases like Lyn (122). It is conceivable that Syk binding to the immunoreceptor tyrosine-based activation motif region is increased by Ca^{2+}, that a phosphorylated immunoreceptor tyrosine-based activation motif region and a Ca^{2+} rise are both needed to increase Syk activity, or that the activity of the upstream tyrosine Lyn, once triggered by receptor cross-linking, is potentiated by Ca^{2+}.

Finally, the fact that Ca^{2+} influx through CRAC channels but not Ca^{2+} release from intracellular stores was able to activate Syk adds to the growing list of examples where the spatial location of the Ca^{2+} rise is important in selectively activating a target (49,62). It is striking that Ca^{2+} entry is able to support Syk activity even in the presence of the fast Ca^{2+} chelator BAPTA in the cytoplasm. BAPTA restricts Ca^{2+} entry to within a few nanometers/tens of nanometers of its point of entry (48), and therefore it is local Ca^{2+} entry through CRAC channels that maintains Syk. Hence FCεRI receptors, Syk, and CRAC channels might be closely apposed, possibly co-localized in a signalling complex. My functional studies lend support to recent observations that FCεRI-dependent signalling occurs in lipid raft domains (146), where store-operated channels can also be found (147).

Chapter 4 Local Ca^{2+} influx through CRAC channels activates *c-fos* gene expression through Syk and STAT5

4.1 Introduction

Ca^{2+} is a universal intracellular messenger, which activates a wide array of important cellular responses, including secretion, mitochondrial metabolism, gene expression, and cell growth and differentiation (89). Because cells can respond to Ca^{2+} by generating more than one type of Ca^{2+}-dependent response, a fundamental question concerns how specificity can occur to such a multifarious signal (49,148). Growing evidence points to a major role for local Ca^{2+} signals in activating specific cellular targets (149). The simplest form of a local Ca^{2+} signal is a Ca^{2+} microdomain, which occurs following the opening of a Ca^{2+}-permeable channel in either the plasma membrane or intracellular organelles (48). Because the volume a microdomain occupies is extremely small, the Ca^{2+} concentration can rise to reach levels that are orders of magnitude greater than the bulk cytoplasmic Ca^{2+} rise (48,49).

Store-operated Ca^{2+} channels are the major route for agonist-evoked Ca^{2+} entry in non-excitable cells and open following stimulation of phospholipase C-coupled receptors (28). These receptors generate inositol 1,4,5-trisphosphate, which releases Ca^{2+} from the ER (129). The fall in Ca^{2+} content within the store is detected by the ER Ca^{2+} sensor STIM1, which migrates to specialized ER-plasma membrane junctions, where it opens the store-operated channels (134). The best characterized store-operated channel is the CRAC channel (28), the pore-forming subunit of which is composed of Orai1 (31,135-137). Ca^{2+} entry through CRAC channels regulates enzyme activity, secretion, gene expression, and cell growth and proliferation (56).

In T cells, NFAT-dependent gene expression requires a global Ca^{2+} rise (150-152). Here, I have examined whether excitation-transcription coupling is driven by global Ca^{2+} signals or Ca^{2+} microdomains arising from open CRAC channels in mast cells. I find that local Ca^{2+} influx signals to the nucleus much more effectively than a robust

bulk Ca^{2+} rise. This leads to the expression of the transcription factor c-*fos*, a regulator of proinflammatory gene expression (87). Furthermore, the non-receptor tyrosine kinase Syk clusters at the cell periphery and couples Ca^{2+} microdomains to c-*fos* expression through recruitment of the cytoplasmic transcription factor STAT5 in a protein kinase C- and MEK/ERK-independent pathway. Ca^{2+} microdomains following CRAC channel activation also activate Ca^{2+}-dependent phospholipase A_2, followed by secretion of cysteinyl leukotrienes (54). However, unlike c-*fos* expression, this is mediated via the MEK/ERK pathway. Parallel processing of the Ca^{2+} microdomain by Syk through two distinct signalling pathways constitutes a novel mechanism to evoke spatially and temporally different cellular responses.

4.2 Results

4.2.1 Local Ca^{2+} influx through CRAC channels induces c-fos mRNA gene expression

Earlier work from our laboratory has demonstrated that activation of store-operated CRAC channels in mast cells triggered expression of the c-*fos* gene (25). To see whether such excitation-transcription coupling was driven by a local or global Ca^{2+} signal, a population of RBL-1 cells (a mast cell line) was stimulated with thapsigargin, a Ca^{2+} ATPase inhibitor on the endoplasmic reticulum, which depletes the Ca^{2+} stores and thereby opens CRAC channels (28). Because the RBL-1 cell culture is a homogenous population and the cells respond to thapsigargin by generating Ca^{2+} signals with very similar kinetics, I was able to relate c-*fos* expression in cell populations to Ca^{2+} signals in individual cells. Stimulation with thapsigargin for 240 s in the absence of external Ca^{2+} produced a transient Ca^{2+} rise in Fura 5F-loaded cells (Fig. 4-1*A*), but the Ca^{2+} signal was not associated with any activation of c-*fos* expression (Fig. 4-1*B*, labeled *0Ca/thap.*; aggregate data are summarized in the *bottom panel*; $p > 0.5$ when compared with control (non-stimulated) cells, ANOVA). On the other hand, stimulation with thapsigargin for the same time in the presence of 2 mM Ca^{2+}, which results in Ca^{2+} influx through CRAC channels, elicited only a slightly larger Ca^{2+} rise (Fig. 4-1*A*), but this nevertheless evoked robust c-*fos* expression (Fig. 4-1*B*; *, $p < 0.01$ when compared with control (non-stimulated) cells, ANOVA). A major mechanism contributing to the decline of the Ca^{2+} signal in Ca^{2+}-free external solution is the plasma membrane Ca^{2+} ATPase pump (112). Block of this pump with La^{3+} increases the size and prolongs the duration of the Ca^{2+} signal in response to thapsigargin (applied in Ca^{2+}-free solution (Fig. 4-1*A*) (54)). Despite this substantial increase in cytoplasmic Ca^{2+} concentration, no c-*fos* expression was induced (Fig. 4-1*B*). These results demonstrate that

excitation-transcription coupling is driven by local Ca^{2+} influx through CRAC channels rather than a bulk Ca^{2+} rise.

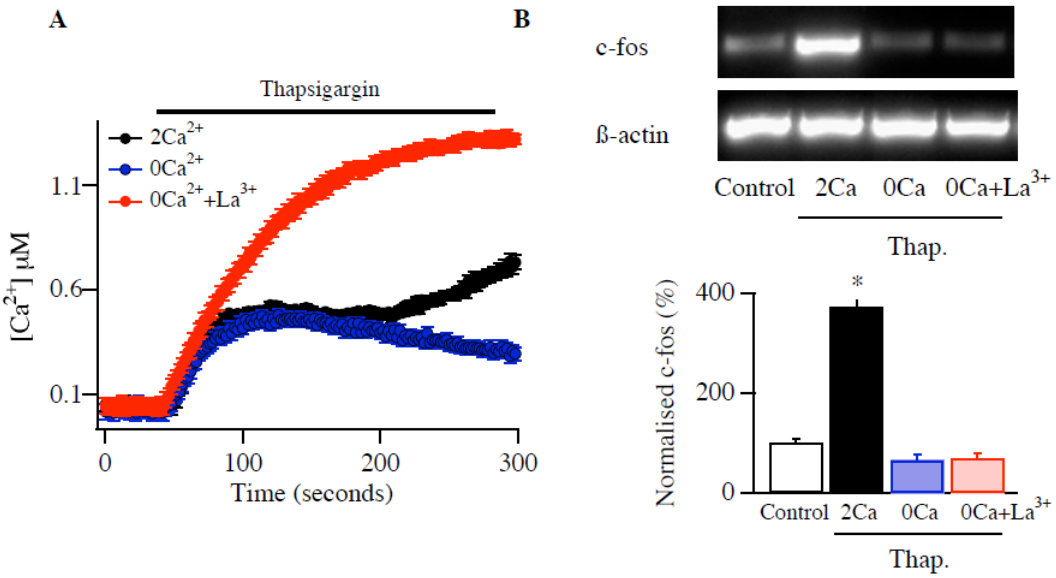

Figure 4-1. Local Ca^{2+} entry activates c-*fos* expression. *A*, Ca^{2+} signals evoked by thapsigargin (2 µM) are shown for the various conditions. *B*, gene expression evoked by thapsigargin (*Thap.*) is compared in 2 Ca^{2+}, 0 Ca^{2+}, and 0 Ca^{2+} plus La^{3+}. *Top panel*, typical gel; *bottom panel*, aggregate data from four experiments. The only stimulation protocol that differed from the control (non-stimulated) state was thapsigargin in 2 mM Ca^{2+} ($p < 0.01$, ANOVA). c-*fos* expression has been normalized to the control level.

4.2.2 Effects of changing the size of the Ca^{2+} microdomain on c-fos expression

A major determinant of the size of a Ca^{2+} microdomain is the single channel current, which depends on the prevailing electrochemical gradient for Ca^{2+} entry (48,49). This gradient was manipulated in two ways: first, the electrical driving force for Ca^{2+} entry was reduced by depolarizing the membrane potential. Second, the concentration gradient for Ca^{2+} influx was altered by varying the external Ca^{2+} concentration. Fig. 4-2*A* summarizes the effects of membrane depolarization on the Ca^{2+} signal following exposure of cells to Cs^+ and TEA^+. These agents fully block the inwardly rectifying K^+ current in RBL-1 cells (153), leading to a membrane depolarization from a resting potential of −80 to −40 mV (154). Over the 4-min exposure to thapsigargin, bulk Ca^{2+} was only slightly lower in depolarized cells (Fig. 4-2*A*). However, c-*fos* expression, following stimulation with thapsigargin for the same time period, was substantially reduced following membrane depolarization (Fig. 4-2*B*; *, $p < 0.01$ when thapsigargin was compared with thapsigargin/Cs^+/TEA^+, ANOVA). Stimulation with thapsigargin in 0.5 mM Ca^{2+} evoked a bulk Ca^{2+} signal that was very similar to that seen in 2 mM Ca^{2+} (Fig. 4-2*C*). However, c-*fos* expression was significantly lower when cells were challenged in 0.5 mM Ca^{2+} (*, $p < 0.01$ for 2 mM *versus* 0.5 mM Ca^{2+}, ANOVA; Fig. 4-2*D*). Stimulation in the presence of a lower Ca^{2+} concentration (0.25 mM) resulted in a smaller bulk Ca^{2+} rise and only modest gene expression (Fig. 4-2, *C* and *D*). Collectively, these results reveal that manoeuvres that alter local Ca^{2+} entry through CRAC channels but have little effect on the bulk Ca^{2+} rise impact strongly on c-*fos* expression.

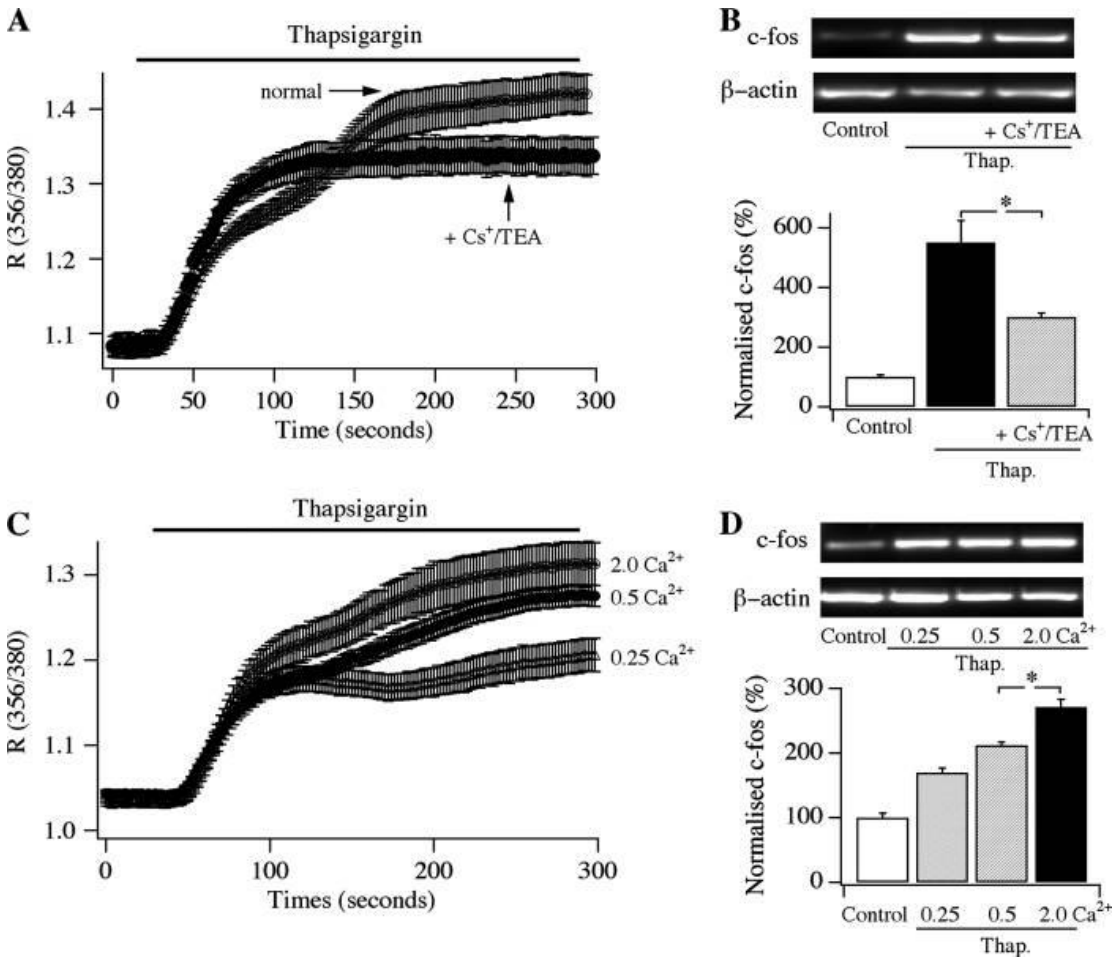

Figure 4-2. Changes in local Ca^{2+} influx impact upon c-*fos* expression. *A*, Ca^{2+} signals in response to 2 μM thapsigargin in 2 mM Ca^{2+} (normal) are compared with those seen in the presence of 10 mM Cs^{+} and 10 mM TEA^{+}, to block inwardly rectifying K^{+} channels. *B*, c-*fos* expression was significantly reduced, compared with thapsigargin (*Thap*.) stimulation, when cells were stimulated with thapsigargin and Cs^{+}/TEA^{+}. Aggregate data from three independent experiments are shown in the *bottom panel*. Both thapsigargin groups were significantly different from the resting group and from each other ($p < 0.01$, ANOVA). *C*, Ca^{2+} signals following stimulation with thapsigargin in different external Ca^{2+} concentrations (0.25, 0.5, and 2 mM) are compared. *D*, c-*fos* expression is compared for the different conditions. Aggregate data from four independent experiments are depicted in the *histogram*. Data have been normalized to control (non-stimulated levels). Differences between each data set

were significant ($p < 0.01$, ANOVA). There was a significant difference between thapsigargin/2 Ca^{2+} and thapsigargin/0.5 Ca^{2+} ($p < 0.01$, ANOVA).

4.2.3 The fast Ca^{2+} chelator BAPTA inhibits thapsigargin-induced c-fos expression

Consistent with the above results, loading cells with the slow Ca^{2+} chelator EGTA failed to reduce gene expression following CRAC channel activation (Fig. 4-3*A*; *, $p < 0.01$ when thapsigargin and thapsigargin/EGTA groups were compared with the control (non-stimulated) group, ANOVA; $p > 0.2$ when thapsigargin was compared with thapsigargin/EGTA, ANOVA), despite substantially slowing the rate of development of the bulk Ca^{2+} signal (Fig. 4-3*B*) (54). Because EGTA is too slow to buffer incoming Ca^{2+} close to the channel pore, it does not impact on local Ca^{2+} signals (49,155). On the other hand, the fast Ca^{2+} chelator BAPTA can reduce the extent of Ca^{2+} microdomains (48,49), and it impaired the ability of CRAC channels to trigger gene expression (Fig. 4-3*A*; $p > 0.3$ for thapsigargin and BAPTA group compared with the control (non-stimulated) group, ANOVA; $p < 0.01$ for thapsigargin/BAPTA *versus* thapsigargin/EGTA, ANOVA), despite reducing bulk Ca^{2+} to a similar extent as that seen in EGTA (Fig. 4-3*B*).

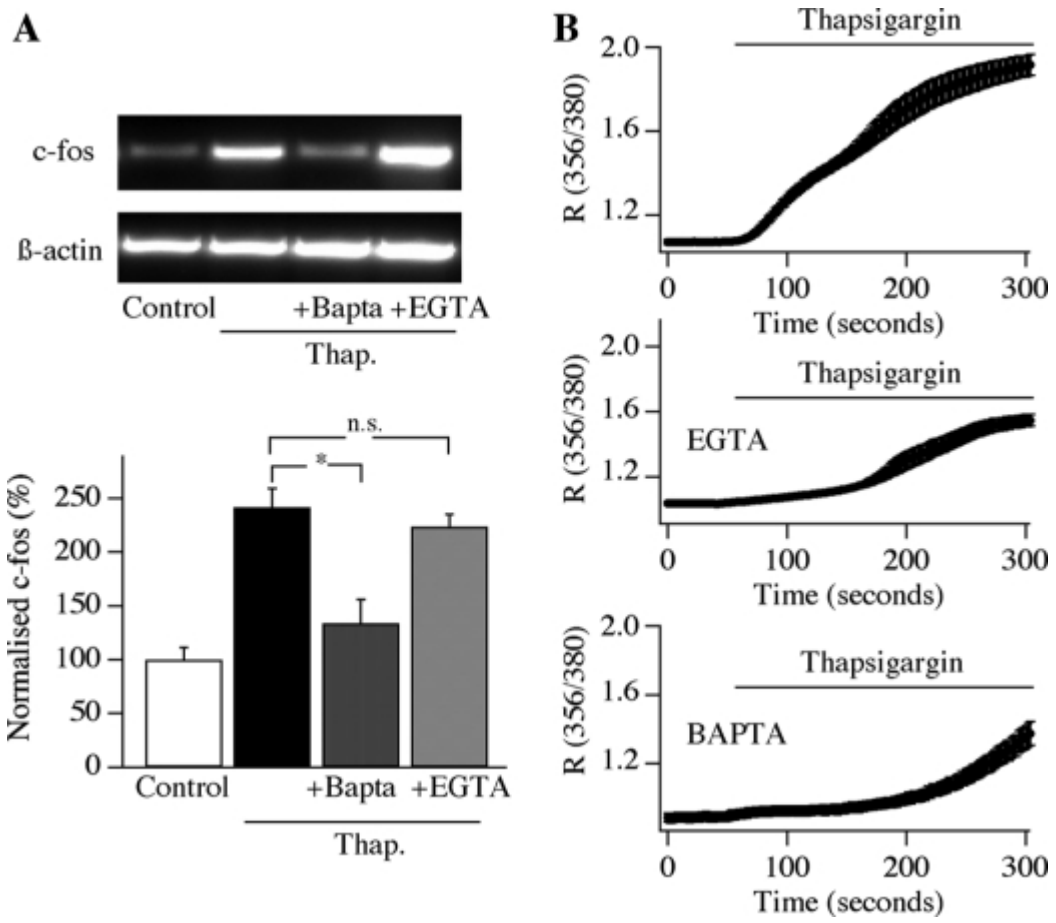

Figure 4-3. Thapsigargin-evoked c-*fos* expression is blocked by cytoplasmic BAPTA but not EGTA. *A*, a typical gel is shown in the *top panel*, and aggregate data from four independent experiments is shown *below*. There was no significant difference between thapsigargin (*Thap*.) and thapsigargin/EGTA groups, but p was <0.01 between thapsigargin and thapsigargin/BAPTA (ANOVA). *B*, thapsigargin-evoked Ca^{2+} signals are compared between control cells, cells loaded with BAPTA, and cells loaded with EGTA (number of cells between 20 and 33). *Error bars* (S.E.) are included in each *graph*.

4.2.4 Syk couples CRAC channel activity to gene expression

Recent work from our laboratory has found that the non-receptor tyrosine kinase Syk can be activated by Ca^{2+} microdomains arising from open CRAC channels (156), prompting us to consider it translates local Ca^{2+} entry into gene expression. This possibility was tested using two different approaches. First, cells were exposed acutely to the Syk inhibitor 3-(1-methyl-1H-indoyl-3-yl-methylene)-2-oxo2,3-dihydro-1H-indole-5-sulfonamide (10 μM for 10 min) and then stimulated with thapsigargin. c-*fos* expression was suppressed (Fig. 4-4*A*; aggregate data from four experiments are summarized in the *bottom panel*). There was no significant difference between the thapsigargin and Syk inhibitor group *versus* the control group (ANOVA), whereas thapsigargin *versus* control was significantly different ($p < 0.01$, ANOVA; the difference between thapsigargin *versus* thapsigargin/Syk was also significant, $p < 0.01$, ANOVA). Importantly, Ca^{2+} flux through CRAC channels was unaffected by the inhibitor (Fig. 4-4, *B* and *C*) as was the membrane potential, measured in current clamp recordings (−78 ± 3 mV control and −74 ± 5 mV after Syk inhibitor; data not shown). Hence, the loss of c-*fos* expression is not due to a change in the CRAC channels themselves nor to the driving force for Ca^{2+} influx. Second, I knocked down expression of Syk using an RNAi approach. Whereas Syk was clearly expressed in control cells (measured in Western blots; Fig. 4-4*D*), transfection with Syk RNAi reduced protein expression by ~60% (Fig. 4-4*D*; *, $p < 0.01$, Student's *t* test). This was associated with a significant reduction in c-*fos* gene activation following stimulation with thapsigargin (Fig. 4-4*E*; aggregate data from four experiments are summarized in the *bottom panel*; *, $p < 0.01$ between control (non-stimulated) and thapsigargin groups, ANOVA; $p < 0.01$ between thapsigargin and thapsigargin/Syk

RNAi groups, ANOVA). Collectively, these results reveal that Syk couples CRAC channel activity to nuclear events.

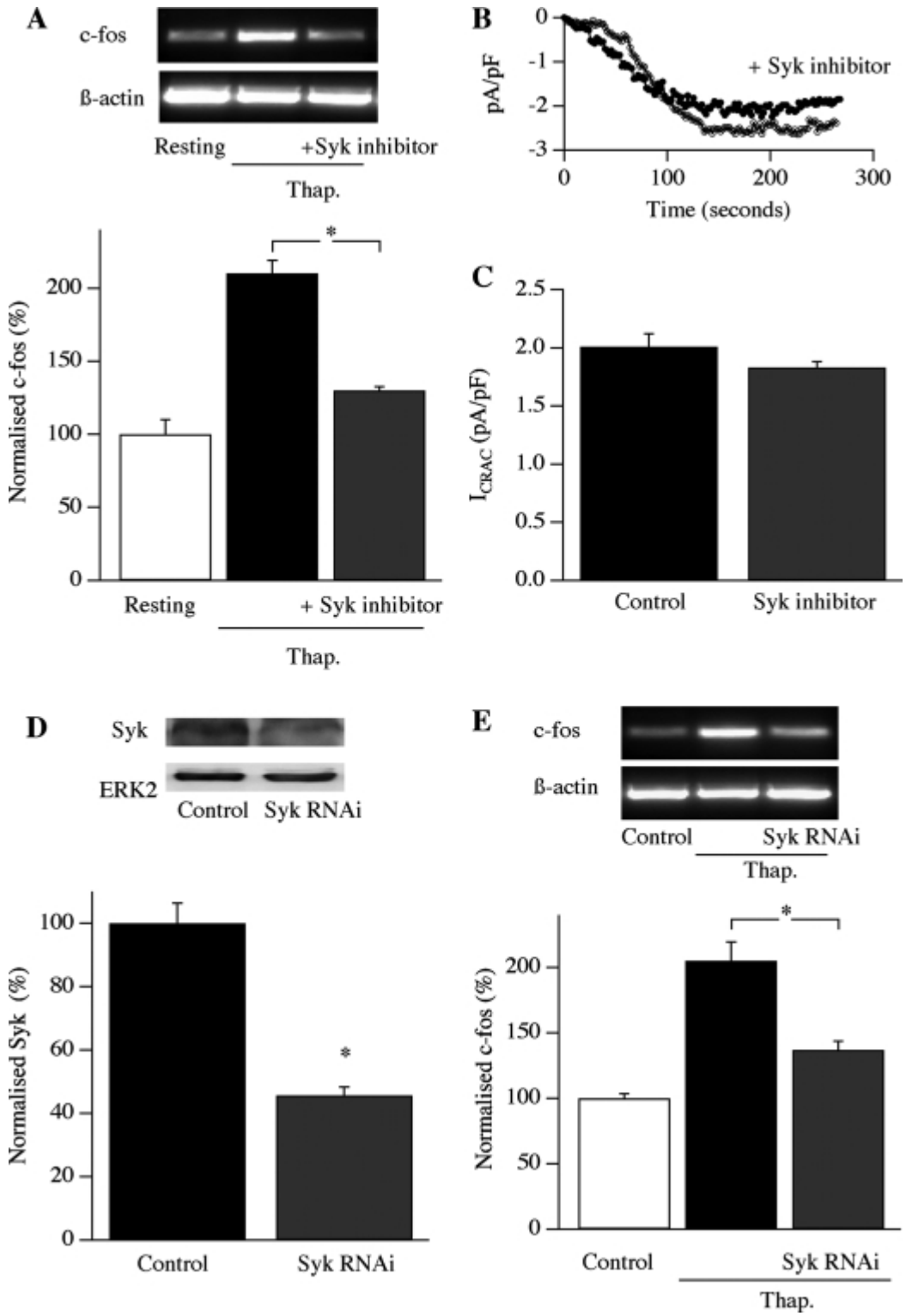

Figure 4-4. Syk is involved in excitation-transcription coupling. *A, top panel,* c-*fos* expression in response to Syk is blocked by the Syk inhibitor. *Bottom panel,* aggregate data from four experiments are shown. $p < 0.01$ between thapsigargin (*Thap*.) and thapsigargin/Syk inhibitor group (ANOVA). *B*, time course of I_{CRAC} in a control cell is compared with one pre-exposed to the Syk inhibitor. The patch pipette contained 10 mM EGTA to deplete the stores. *C*, aggregate data from experiments as in *B* are depicted ($p > 0.3$; number of cells was 7 for control and 8 for the Syk inhibitor). *D, top panel*, Syk expression, measured using Western blotting, is compared between wild type cells transfected with scrambled siRNA and cells transfected with siRNA against Syk. The *bottom panel* depicts aggregate data from three independent experiments for the two conditions; $p < 0.01$, Student's *t* test. *E*, Syk knockdown reduces c-*fos* expression. *Top panel*, a typical gel. *Bottom panel*, aggregate data from four independent experiments are shown. Thapsigargin and thapsigargin/Syk RNAi groups were both significantly different from the control group ($p < 0.01$ and $p < 0.05$, respectively) and significantly different from each other (*, $p < 0.01$, ANOVA). The thapsigargin group had been transfected with scrambled siRNA against Syk.

4.2.5 Syk recruits the transcription factor STAT5

If Syk detects local Ca^{2+} entry, it should be located at the cell periphery. Immunocytochemical studies revealed that this was indeed the case (Fig. 4-5*A*). I plotted the lateral profile of Syk across the cell and found two peaks, corresponding to the two plasma membrane sections, with a substantial dip between them (reflecting bulk cytoplasm; Fig. 4-5*B*). Enhanced green fluorescence protein is widely used to measure the cytoplasmic distribution (157). In marked contrast to Syk, a relatively stable and elevated profile was found when the cytoplasmic profile of enhanced green fluorescence protein was analyzed in the same way (Fig. 4-5*B* and *C*) with no peaks near the plasma membrane. Does Syk migrate to the nucleus after Ca^{2+} influx? To examine this possibility, cells were stimulated with thapsigargin and the spatial profile of Syk was measured. Syk remained at the cell periphery with no detectable translocation into the cytoplasm (Fig. 4-5*D*). An intermediary signal is therefore needed to couple Syk to the nucleus. I tested for the involvement of a range of downstream cascades including PKC, calmodulin, calcineurin, MEK/ERK, and JNK pathways. Inhibition of each of these pathways had no effect on CRAC channel-transcription coupling. Pretreatment for 20–30 min with 1 μM GO-6983 (to block PKC), 10 μM calmidazolium (to block calmodulin), 5 μM cyclosporine (to block calcineurin), and 50 μM AG490 (to block the JNK pathway) all failed to interfere with thapsigargin-evoked c-*fos* expression (data not shown). In agreement with our previous work, block of the MEK/ERK pathway with U0126 (10 μM; 20 min pretreatment) failed to interfere with c-*fos* expression following stimulation with thapsigargin (Fig. 4-5*E*). I also failed to see any phosphorylation of CREB following CRAC channel activation, suggesting this transcription factor likewise is not involved (data not shown). Signal transducers and activators of transcription (STAT), is a

family of cytoplasmic transcription factors (158) that are widely expressed in immune cells. STATs can be activated following tyrosine phosphorylation by non-receptor tyrosine kinases (159). Phosphorylated STATs dimerize and then rapidly translocate to the nucleus, where they bind to enhancer elements and regulate gene expression (159). Using an anti-phospho-specific STAT5 antibody, stimulation with thapsigargin resulted in STAT5 activation within 240 s of stimulation (Fig. 4-5*F*; aggregate data from three independent experiments are summarized in Fig. 4-5*G*), and this was fully prevented by pretreating cells with the Syk inhibitor (Fig. 4-5*G*; *, $p < 0.01$ between control and thapsigargin groups, ANOVA; $p > 0.4$ between control and thapsigargin/Syk inhibitor groups, ANOVA). An anti-phospho-specific STAT3 antibody failed to detect activation of STAT3 following opening of CRAC channels (data not shown). Hence, Syk recruits the transcription factor STAT5.

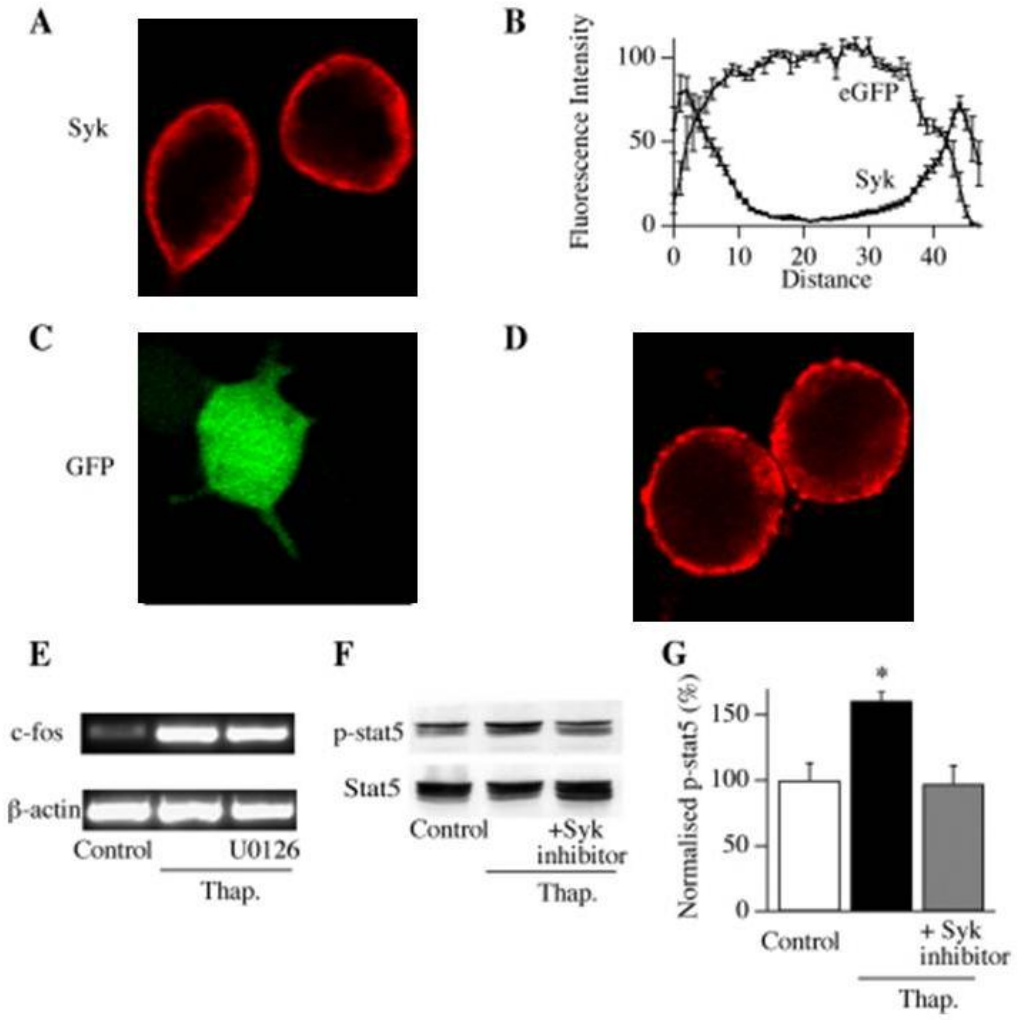

Figure 4-5. Syk recruits the transcription factor STAT5. *A,* distribution of endogenous Syk in resting RBL-1 cells, observed using immunocytochemistry. *B,* aggregate data measuring the intensity of Syk fluorescence across the lateral profile of cells is shown, measured in line scan mode (nine cells for Syk and 11 for green fluorescent protein). *C,* distribution of green fluorescent protein (*GFP*), used as a cytoplasmic marker, in an RBL-1 cell. *D,* Syk remains at the plasma membrane following stimulation with thapsigargin. *E,* thapsigargin (*Thap.*)-evoked c-*fos* expression is unaffected by blocking the MEK/ERK pathway with U0126. *F,* thapsigargin promotes phosphorylation of the transcription factor STAT5, and this is prevented by inhibition of Syk. *G,* aggregate data from three experiments (as in *F*) are shown. The thapsigargin-stimulated group differs significantly from control (non-

stimulated) and thapsigargin/Syk inhibitor groups (*, $p < 0.01$, ANOVA). Thapsigargin/Syk inhibitor group was not significantly different from the control (non-stimulated) one ($p > 0.5$).

4.2.6 RNAi knockdown of Syk reduces ERK phosphorylation

I have recently established that Ca^{2+} microdomains near CRAC channels activate the cytoplasmic enzymes Ca^{2+}-dependent phospholipase A_2 and 5-LO via recruitment of the MEK/ERK pathway (25). This results in the generation of the intracellular messenger arachidonic acid, which is rapidly metabolized by 5-lipoxygenase to the proinflammatory paracrine signal leukotriene C_4 (25,54). Do the Ca^{2+} microdomains couple to gene expression and ERK/$cPLA_2$/leukotrienes by the same mechanism? Pharmacological data implicated Syk in coupling Ca^{2+} microdomains to ERK and $cPLA_2$ activation (54). To strengthen this, ERK activation was measured, before and then after knockdown of Syk. Whereas thapsigargin evoked robust stimulation of ERK in control cells (measured as ERK phosphorylation (54) after 4-min stimulation), the extent of ERK activation was significantly reduced following pretreatment of the cells with siRNA against Syk (Fig. 4-6*A* and *B*). Hence ERK activation and gene expression, which occur over very different time frames, are both triggered by local Ca^{2+} influx-mediated stimulation of Syk. However, the signalling mechanisms then diverge in that Syk activates gene expression independent of the MEK/ERK pathway (Fig. 4-5*E*).

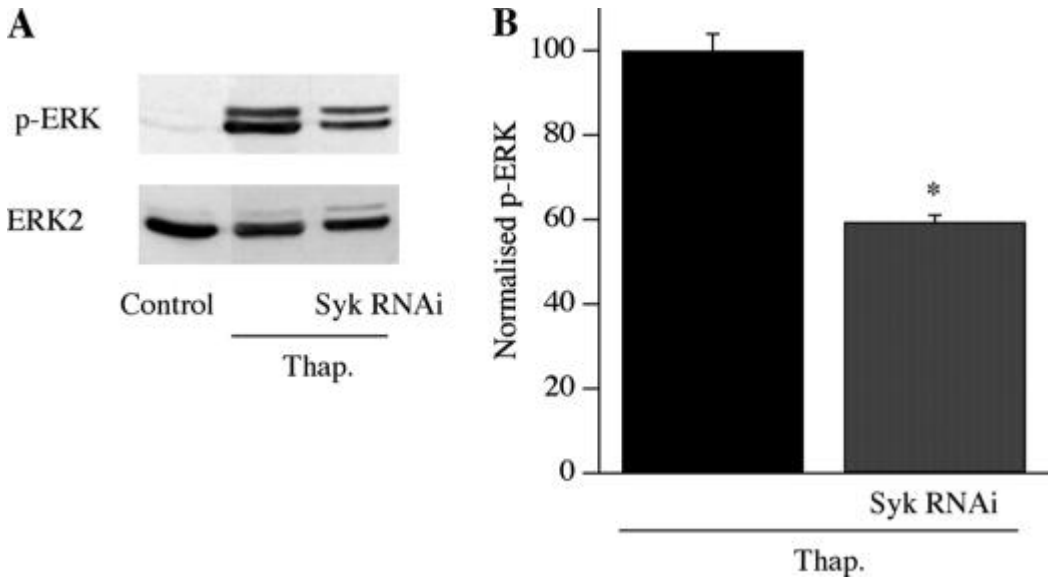

Figure 4-6. Syk knockdown reduces ERK activation. *A*, Western blot showing that ERK phosphorylation evoked by thapsigargin (*Thap.*) (in scrambled siRNA-treated cells) is reduced by siRNA knockdown of Syk. *B*, aggregate data from three independent gels are compared. *, $p < 0.01$, Student's *t* test.

4.3 Discussion

$cPLA_2$ activation and gene expression, which occur over very different time frames, are both triggered by local Ca^{2+} influx-mediated stimulation of Syk (Fig. 4-7). However, the signalling mechanisms then diverge in that Syk activates gene expression independent of the MEK/ERK pathway, whereas the latter is essential for coupling Syk to $cPLA_2$. These findings reveal the versatility of Ca^{2+} microdomains in driving cell responses. Local Ca^{2+} influx can simultanenously activate two spatially and temporally distinct processes by using the same sensor, Syk. My results show that local Ca^{2+} influx can signal to the nucleus, several micrometres away, to activate gene expression. This arises because CRAC channels have a privileged access to Syk, which then activates the cytoplasmic transcription factor STAT5. Syk might detect the local Ca^{2+} signal directly, or a Ca^{2+}-dependent tyrosine kinase like Pyk-2 (145) could act as an intermediary, linking the Ca^{2+} microdomain to Syk. Such an intimate interaction between the Ca^{2+} channel and signal transduction to the nucleus would greatly increase the fidelity, speed, and selectivity of excitation-transcription coupling.

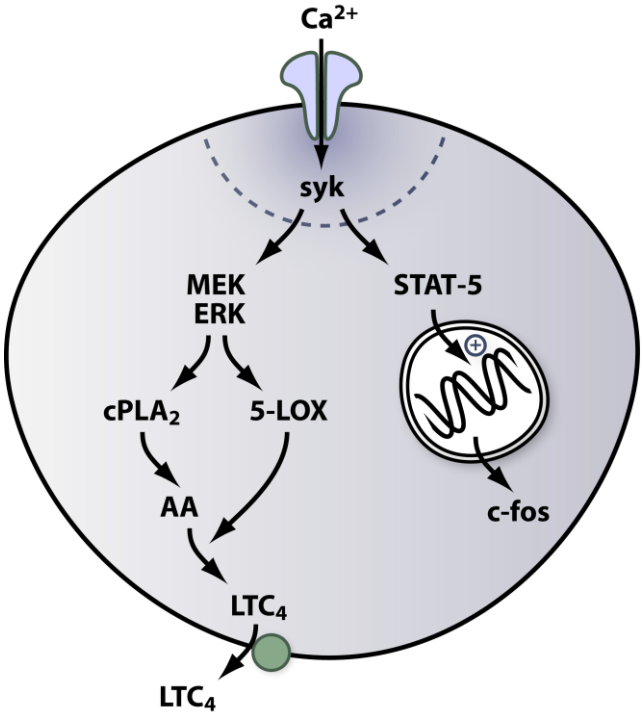

Figure 4-7. Parallel processing of the Ca^{2+} microdomain by Syk. Local Ca^{2+} entry is detected by Syk, which then activates two distinct signalling pathways. Syk recruits PKC and the MEK/ERK cascade, resulting in activation of $cPLA_2$ and 5-lipoxygenase. This generates the intracellular messenger arachidonic acid (AA) and the proinflammatory paracrine signal LTC_4 (54). At the same time, Syk phosphorylates the transcription factor STAT5, which then migrates to the nucleus, where it increases c-*fos* expression. The Ca^{2+} microdomain can therefore be processed by Syk through two parallel pathways into the activation of temporally distinct cellular responses.

Chapter 5 Cysteinyl leukotriene type I receptor desensitization sustains Ca^{2+}-dependent gene expression

5.1 Introduction

The G protein-coupled receptor (GPCR) family contains more than 800 members, and accounts for ~4% of the entire protein coding human genome (160). GPCRs activate a plethora of cellular activities (161), ranging from rapid effects such as exocytosis and enhanced metabolism to slowly developing, protracted responses involving gene expression and cell growth and differentiation. Manipulating GPCR activity is an effective therapeutic strategy for a range of diseases (162) and almost 40% of all prescription drugs target GPCRs. A characteristic trait of most GPCRs is their ability to develop homologous desensitization (161), where sustained exposure to the agonist uncouples the receptor from the underlying second messenger pathway, leading to termination of the cellular response. Receptor desensitization poses a paradox: how can long-term responses be evoked if the receptor inactivates? This is a particularly acute problem in immune cells, where cell differentiation and clonal selection develops over hours in the continued presence of external cues. I have addressed this paradox by activating cysteinyl leukotriene type I (CysLT1) receptors with the endogenous pro-inflammatory agonist leukotriene C_4 (LTC_4) to evoke gene expression in mast cells, important components of both the innate and adaptive immune system. CysLT1 receptors couple to phospholipase C, to generate inositol 1,4,5-trisphosphate ($InsP_3$) and diacylglycerol (DAG). $InsP_3$ releases Ca^{2+} from the ER, and this leads to the opening of CRAC channels in the plasma membrane. DAG, together with cytoplasmic Ca^{2+}, activates protein kinase C. Ca^{2+} signals following activation of CysLT1 receptors with LTC_4 are oscillatory in nature (116). These arise from regenerative Ca^{2+} release, which is sustained by Ca^{2+} entry (163). Local Ca^{2+} entry through CRAC channels and not the Ca^{2+} oscillations *per se* drive gene expression (163). Desensitization of CysLT1 receptors is well-defined and is

principally mediated by protein kinase C-mediated phosphorylation of three serine residues (S313, S315, S316) in the carboxy terminal of the receptor (164). Phosphorylation uncouples the receptor from phospholipase C and then leads to receptor internalization. There is no involvement of other protein kinases or β-arrestins (165). CysLT1 receptors are therefore an excellent model to study the impact of receptor desensitization on slowly developing responses.

5.2 Results

5.2.1 CysLT1 receptor activation and thapsigargin induce similar c-fos expression despite different extents of I_{CRAC} activation

Stimulation of CysLT1 receptors with LTC_4 (160 nM for 8 minutes) led to robust expression of the immediate early gene *c-fos* (Fig. 5-1*Ai* and *Aii*), which dimerises with *c-jun* to form the AP-1 complex that regulates expression of numerous genes important to cell growth and development. Maximal activation of CRAC channels with thapsigargin (2 μM, 8 minutes stimulation) led to a similar increase in *c-fos* expression (Fig. 5-1*Ai* and *Aii*). Both LTC_4 and thapsigargin induce *c-fos* expression through the build-up of Ca^{2+} microdomains near open store-operated CRAC channels because the responses to both stimuli are i) abolished by loading the cytoplasm with the fast Ca^{2+} chelator BAPTA but not the slow chelator EGTA (90,163), ii) are suppressed by removal of external Ca^{2+} (90,163) and iii) are inhibited by CRAC channel blockers (90,163). The similar increase in *c-fos* expression to LTC_4 and thapsigargin was therefore surprising, because thapsigargin activated significantly more Ca^{2+} influx than LTC_4. Cytoplasmic Ca^{2+} measurements revealed that thapsigargin led to a large, relatively sustained Ca^{2+} increase whereas LTC_4 produced oscillatory responses (Fig. 5-1*Bi*, see also refs.(90,163)) and the rate of Ca^{2+} entry, seen following readmission of Ca^{2+} to cells stimulated with thapsigargin or LTC_4 in Ca^{2+}-free solution, was ~ 2-fold less for LTC_4 than thapsigargin (Fig. 5-1*Bii*). This is consistent with patch clamp recordings that showed CysLT1 receptor activation evoked a CRAC current that was ~ 40% that elicited by thapsigargin in these cells (116).

Various explanations were considered for why Ca^{2+}-dependent expression of *c-fos* was similar for LTC_4 and thapsigargin, despite agonist evoking significantly less

CRAC channel activation. One possibility was that *c-fos* detection with RT-PCR could have had a relatively narrow range, such that measurements had already saturated with LTC_4 and thus a potential further increase by thapsigargin was masked. Alternatively, *c-fos* was measured on cell populations whereas Ca^{2+} was monitored in single cells, and there could be variations in gene expression between the stimuli at the single cell level. To address these issues, *c-fos* induction was measured at the single cell level, using confocal microscopy to detect protein expression within the nucleus. Cells were co-stained with the nuclear marker DAPI and a *c-fos* antibody (Fig. 5-1*C*). Nuclear accumulation of *c-fos* following stimulation with LTC_4 or thapsigargin was similar (Fig. 5-1*C*), demonstrating that both evoked comparable levels of *c-fos* protein expression, when measured at a single cell level. Another possible explanation for the similar increase in *c-fos* to LTC_4 and thapsigargin despite differences in Ca^{2+} influx was that the CysLT1R tapped into a different signalling mechanism linking CRAC channel microdomains to *c-fos* to that utilised by thapsigargin. CRAC channel activation following stimulation with thapsigargin signals to the nucleus via recruitment of the non-receptor tyrosine kinase Syk and the cytoplasmic transcription factor STAT5 (90). CysLT1 receptors link into the same pathway because i) pharmacological block of Syk abolished LTC_4-driven *c-fos* expression (Fig. 5-1*Di* and *ii*) without altering the development of the cytoplasmic Ca^{2+} signal (Fig. 5-1*E*) and ii) knockdown of Syk using an siRNA approach abolished the ability of LTC_4 to activate c-fos (Fig. 5-1*Fi* and *ii*). Hence both thapsigargin and CysLT1 receptors couple to c-fos induction via Syk. Furthermore, the results reveal that a G protein-coupled receptor recruits non-receptor tyrosine kinases to drive cellular responses.

Because local Ca^{2+} entry through CRAC channels drives c-fos expression (163), any manoeuvre that increases the size of the Ca^{2+} microdomain should enhance excitation-transcription coupling. I considered the possibility that local Ca^{2+} entry through CRAC channels was larger following CysLT1 receptor activation than thapsigargin, because the former might hyperpolarize the membrane potential and thereby increase the driving force for Ca^{2+} entry. Three findings argue against this. First, application of LTC_4 to cells already stimulated with thapsigargin in 2 mM Ca^{2+} (for 5 minutes) failed to increase the Ca^{2+} signal, which would have been expected had agonist hyperpolarised the membrane potential (ΔF was < 0.1 unit, following LTC_4 after thapsigargin). Second, patch clamp recordings showed that the inwardly rectifying K^+ current, which sets the resting membrane potential in RBL-1 cells (153), was unaffected by LTC_4 (data not shown). Third, current clamp recordings showed no difference in membrane potential between thapsigargin- and LTC_4-stimulated cells (-76 ± 5 mV; -80 ± 4 mV).

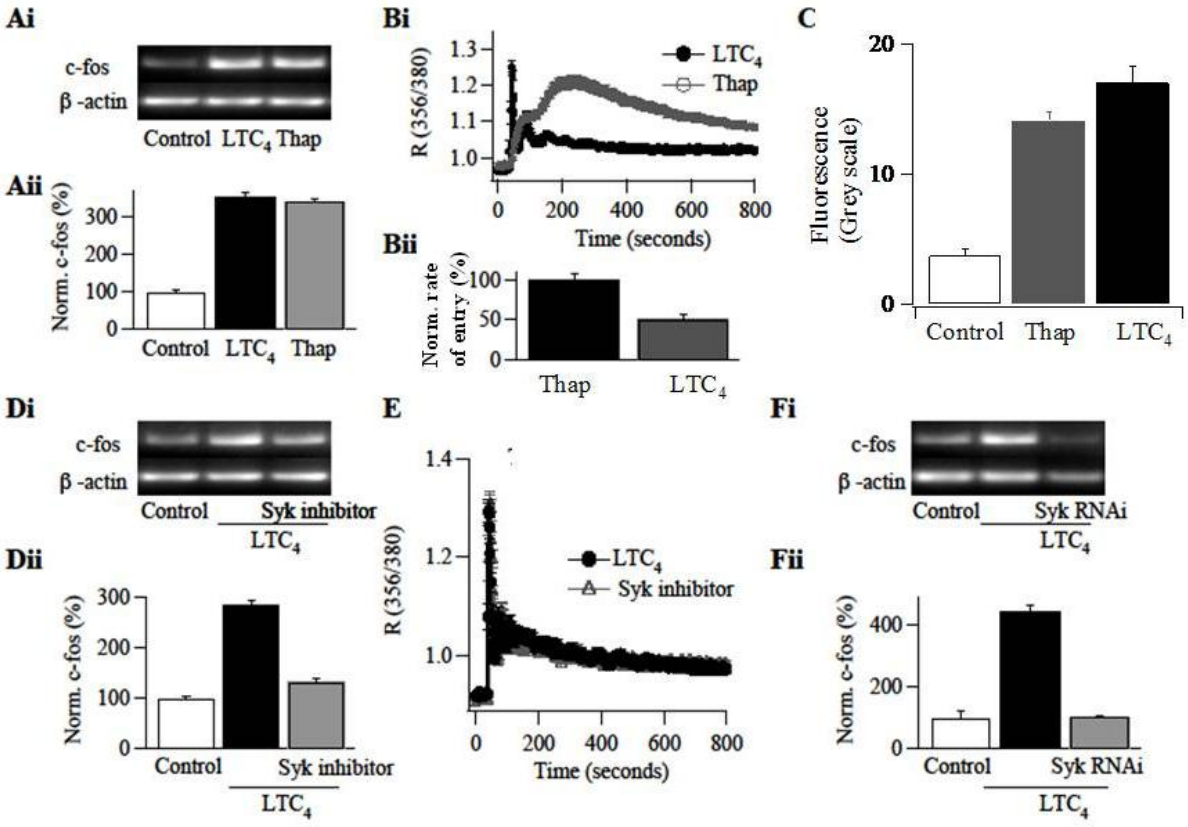

Figure 5-1. CysLT1 receptor activation and thapsigargin induce similar c-fos expression despite different extents of I_{CRAC} activation. *Ai*, *c-fos* mRNA expression is compared between control (non-stimulated), LTC_4- and thapsigargin-stimulated cells. *Aii*, aggregate data from three independent experiments as in *Ai* are compared. *Bi*, Ca^{2+} signals evoked by LTC_4 and thapsigargin are shown (average of >50 cells per graph). *Bii*, the rate of Ca^{2+} entry is compared for the conditions shown. *C*, *c-fos* protein expression for the three conditions (from > 20 cells each) is compared. *Di*, agonist-driven *c-fos* expression are suppressed by the Syk inhibitor (1 μM, 10 mins pre-treatment). *Dii*, aggregate data are summarised. *E*, the Syk inhibitor does not alter agonist-evoked Ca^{2+} signals. *Fi*, knockdown of Syk inhibits agonist-driven gene expression. *Fii*, aggregate data from three independent experiments are summarised.

5.2.2 There is no synergistic effect between cytoplasmic Ca^{2+} and protein kinase C

The dual signalling hypothesis of Berridge proposes that cytoplasmic Ca^{2+} and protein kinase C act synergistically to drive a cellular response (166). I therefore considered that CysLT1 receptor activation of *c-fos* expression might involve both Ca^{2+} and protein kinase C, with the latter increasing the sensitivity of gene expression to the former. To test this, I stimulated cells with thapsigargin but in the presence of lowered external Ca^{2+} (0.5 mM; resulting in submaximal induction of c-fos (90)) and compared these responses with those where I simultaneously activated protein kinase C with the phorbol ester PMA. No synergistic effect was seen (Fig. 5-2*A* and *B*). In case another receptor-dependent protein kinase might be involved, I repeated these experiments but used LTC_4 instead of PMA. Again, no increase in *c-fos* expression was found (Fig. 5-2*C* and *D*). Hence the results do not support a synergistic interaction between cytoplasmic Ca^{2+} and protein kinase C.

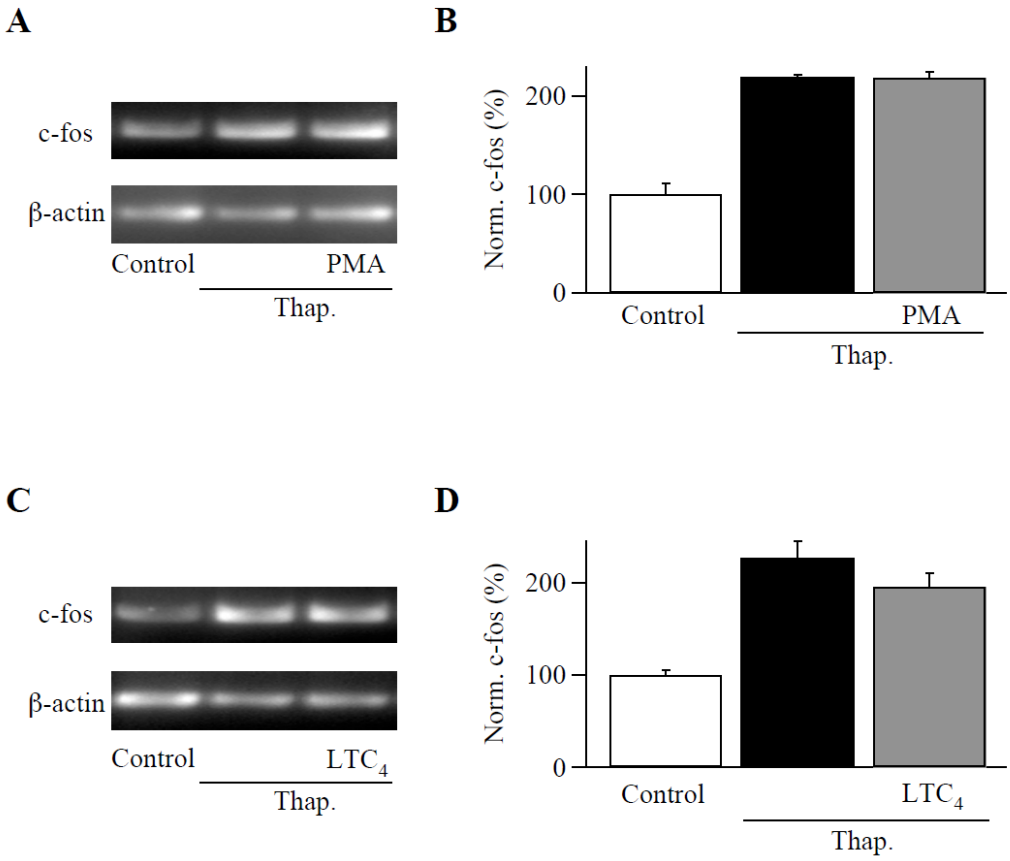

Figure 5-2. No synergistic effect between cytoplasmic Ca^{2+} and protein kinase C occurs. *A*, gel comparing *c-fos* induction to thapsigargin (in 0.5 mM Ca^{2+}) with thapsigargin plus PMA (1 µM). *B*, aggregate data from four gels as in *A* are summarised. *C*, c-fos induction is compared between cells stimulated with thapsigargin (in 0.5 mM Ca^{2+}) and thapsigargin plus LTC_4. *D*, aggregate data from three gels are compared.

5.2.3 Interference with protein kinase C activity impairs agonist-but not thapsigargin-evoked c-fos expression

Experiments described in Figure 5-3 revealed an important role for protein kinase C in agonist-evoked gene expression. Pre-treatment with the structurally distinct protein kinase C blockers G06983 or calphostin C (both at 1 μM) abolished CysLT1 receptor-driven *c-fos* expression (Fig. 5-3*A* and *B*). Protein kinase C block also had a dramatic effect on the Ca^{2+} signal evoked by LTC_4. Whereas cytoplasmic Ca^{2+} oscillations were routinely observed with LTC_4 (Fig. 5-3*C*), the response was converted into a large, single, slowly decaying Ca^{2+} spike after protein kinase C inhibition (Fig. 5-3*C* and *D*). The involvement of protein kinase C was specific to CysLT1 receptors because thapsigargin-evoked c-fos expression (Fig. 5-3*D* and *E*) and cytoplasmic Ca^{2+} signals (Fig. 5-3*F*) were unaffected by either G06983 or calphostin C.

In mast cells, overnight exposure to phorbol ester downregulates the Ca^{2+}-dependent protein kinase C isozymes α and β. Using this protocol, c-fos expression was substantially reduced in response to CysLT1 receptor stimulation (Fig. 5-3*G* and *H*), whereas no significant reduction was seen when the inactive 4α-phorbol was used instead. The Ca^{2+} signal to LTC_4 was strongly altered by protein kinase C downregulation (Fig. 5-3*I*), and in a manner similar to that seen with the protein kinase C blockers. Downregulation of protein kinase C had little effect on thapsigargin-evoked c-fos expression (Fig. 5-3*H*).

Because agonist-evoked and not thapsigargin-driven gene expression was suppressed by protein kinase C inhibition, I reasoned that the target for protein kinase C was upstream of CRAC channel activation. I noticed that the agonist-evoked initial Ca^{2+}

signal was dramatically prolonged either by protein kinase C inhibition (Fig. 5-3*C* and *D*) or following enzyme downregulation (Fig. 5-3*I*). Such prolongation of a Ca^{2+} transient is characteristic of loss of receptor desensitization, particularly for CysLT1 receptors where desensitization is mediated exclusively by protein kinase C (164) and prevention of desensitization leads to broader Ca^{2+} signals (167).

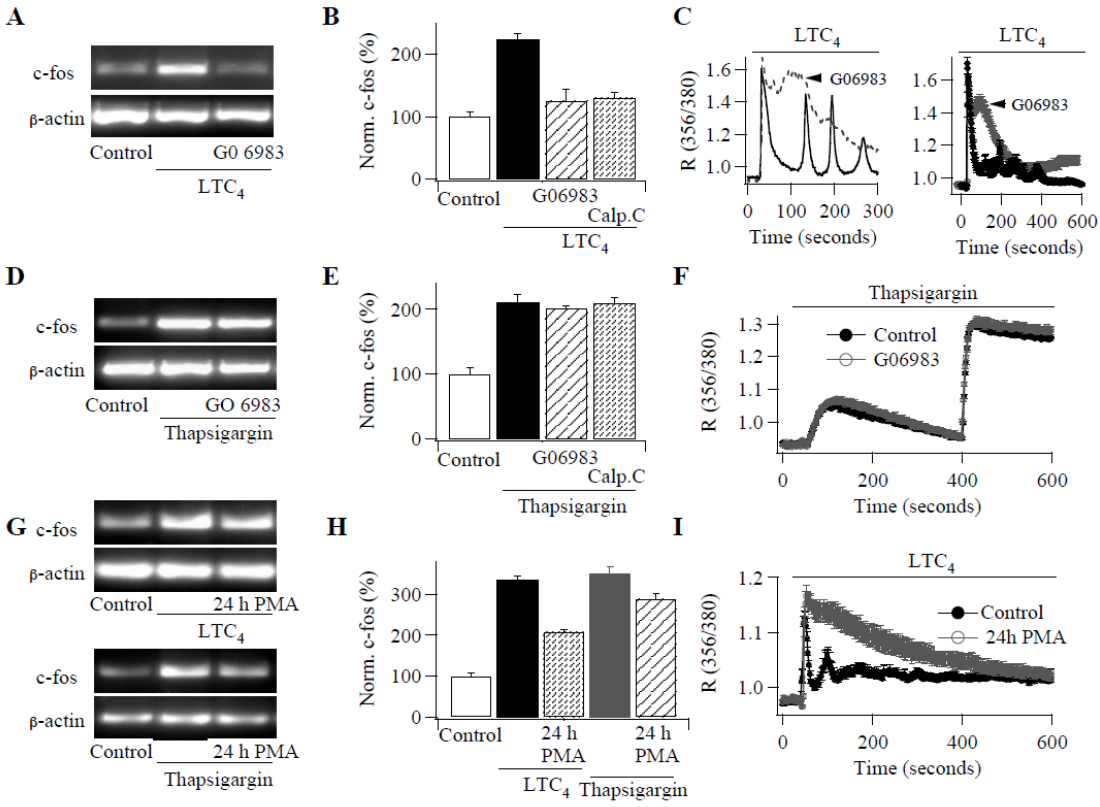

Figure 5-3. Interference with protein kinase C activity impairs agonist-but not thapsigargin-evoked c-fos expression. *A*, block of protein kinase C with G06983 (1 μM; 10 minutes pre-treatment) suppresses LTC_4-induced *c-fos* expression. *B*, aggregate data from three independent experiments summarizes the effects of G06983 and calphostin C (1 μM; 10 minutes pre-treatment). *C*, the Ca^{2+} signal evoked by CysLT1 receptors is altered by protein kinase C block. The left hand panel compares two single cells. The right hand panel is the average of > 45 cells for each condition. *D*, G06983 fails to alter *c-fos* expression to thapsigargin. *E*, aggregate data from four

experiments are summarized. *F*, Ca^{2+} signals to thapsigargin are unaffected by protein kinase C block. *G*, downregulation of protein kinase C following chronic exposure to PMA (1 μM, 24 hours) reduces LTC_4-driven gene expression (upper panel) but not thapsigargin-induced *c-fos* induction. *H*, aggregate data from four independent experiments are shown. *I*, protein kinase C downregulation alters the LTC_4-driven Ca^{2+} signal.

5.2.4 CysLT1 receptor-driven gene expression can be rescued by preventing a bulk cytoplasmic Ca^{2+} rise

Inhibition of cysLT1 receptor desensitization is predicted to lead to greater $InsP_3$ production and hence more extensive Ca^{2+} store emptying. To test this, the extent of Ca^{2+} release was compared in the absence and then presence of protein kinase C block. Stimulation with LTC_4 in Ca^{2+}-free external solution evoked an initial Ca^{2+} transient that decayed back rapidly to pre-stimulation levels within 30 seconds (Fig. 5-4*A*, control), and this was then followed by one or two further Ca^{2+} oscillations of similar duration. Although the initial Ca^{2+} spike was well-synchronised between cells, the subsequent Ca^{2+} oscillations were out of phase and hence are not readily apparent in the averaged Ca^{2+} signal from the whole population (Fig. 5-4*A*). Stimulation with LTC_4 in the presence of protein kinase C block led to a much more sustained Ca^{2+} release event, which lasted ~ 5 times longer than the control (Fig. 5-4*A*). The amount of Ca^{2+} remaining in the stores after LTC_4 stimulation was estimated by applying the Ca^{2+} ionophore ionomycin, also in Ca^{2+}-free solution. Ionomycin rapidly releases stored Ca^{2+} and is widely used to measure store Ca^{2+} content (168). Substantially less Ca^{2+} was mobilised by ionomycin in cells that had been exposed to LTC_4 in the presence of protein kinase C block than in corresponding control cells (Fig. 5-4*A*). $InsP_3$ production following CysLT1 receptor activation was measured using the GFP-PH construct (169), which is displaced from the plasma membrane following hydrolysis of PIP_2. Whereas very little GFP-PH movement was detected in cells stimulated with low levels of LTC_4 (presumably reflecting the small increase in $InsP_3$ that is associated with oscillatory Ca^{2+} signals), I observed a significant increase in GFP-PH movement to the cytosol after stimulation in the presence of protein kinase C blockers (Fig. 5-4*B*). Collectively, these results would be entirely consistent with

the view that less receptor desensitization has taken place following inhibition of protein kinase C and this leads to more extensive $InsP_3$ production and Ca^{2+} release. Cytoplasmic Ca^{2+} inhibits CRAC channels through three independent mechanisms (28): i) fast inactivation, which occurs with time constants of ~ 10 and ~ 100 milliseconds, and arises from the build-up of Ca^{2+} microdomains in the vicinity of open channels; ii) slow inactivation, which develops over several tens of seconds and requires a rise in bulk Ca^{2+} and iii) Ca^{2+}-dependent store refilling, which develops over several seconds and also requires a rise in bulk Ca^{2+}. The sustained Ca^{2+} release signal evoked by LTC_4 in the presence of non-desensitizing receptors should therefore inactivate CRAC channels, and thus suppress agonist-evoked gene expression. If this is indeed the case, then loading cells with a Ca^{2+} chelator will prevent the loss of gene expression. Loading the cytoplasm with the slow Ca^{2+} chelator EGTA rescued gene expression to cysLT1 receptor activation in the presence of either G06983 (Fig. 5-4 *Ci* and *Cii*) or calphostin C (Fig. 5-4*Di* and *Dii*).

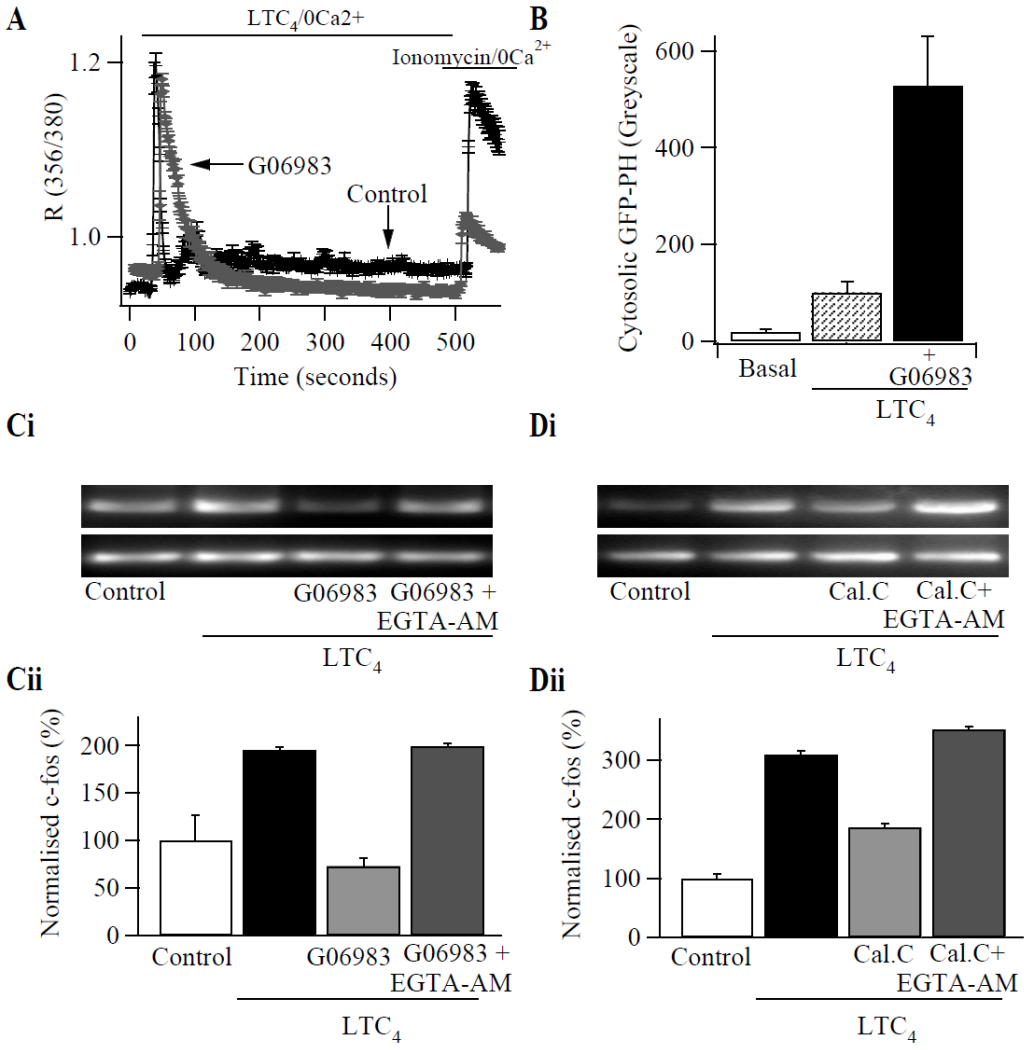

Figure 5-4. CysLT1 receptor-driven gene expression can be rescued by preventing a bulk cytoplasmic Ca^{2+} rise. *A*, Stimulation with LTC_4 in the presence of G06983 evokes a more sustained Ca^{2+} release response, and this leads to more extensive store depletion (measured through the Ca^{2+} response evoked by 1 µM ionomycin). Both LTC_4 and ionomycin were applied in Ca^{2+}-free external solution. *B*, Cytosolic GFP-PHD levels, a measure of ambient $InsP_3$ levels, rise when CysLT1 receptors are stimulated in the presence of G06983 indicating a loss of receptor desensitization. *Ci*, Loading cells with the Ca^{2+} chelator EGTA prevents loss of gene expression to agonist when protein kinase C is blocked. *Cii*, Aggregate data from 5

independent gels are summarised. *Di*, as in *Ci*, but calphostin C was used to block protein kinase C instead. *Dii*, aggregate data from 3 independent gels are summarised.

5.2.5 Ca^{2+}-dependent slow inactivation underlies the suppression of c-fos expression to non-desensitizing cysLT1 receptors

Because Ca^{2+} mobilisation following CysLT1 receptor activation was increased by protein kinase C block and store content was reduced (Fig. 5-4*A*), the inhibitory effects of cytoplasmic Ca^{2+} are not mediated through enhanced Ca^{2+}-dependent store refilling. Similarly, Ca^{2+}-dependent fast inactivation of CRAC channels is unlikely to contribute because i) it is unaffected by the slow chelator EGTA (111,170), which reversed the inhibitory effects of protein kinase C block and ii) the rate and extent of fast inactivation was unaffected by cysLT1 receptor activation in the presence of protein kinase C down regulation (Fig. 5-5*A*). Instead, Ca^{2+}-dependent slow inactivation is likely to be the dominant mechanism for several reasons: i) it is suppressed by EGTA (73,74) and c-fos expression is rescued by loading the cytoplasm with EGTA; ii) the Ca^{2+}-dependence of slow inactivation has a K_D of ~0.5 μM and full block occurs at ~ 1 μM (Fig. 5-5*B*), which is similar to the peak Ca^{2+} rise evoked by LTC_4 in the presence of protein kinase C inhibitors or following downregulation of protein kinase C (0.87 ± 01 μM); iii) Ca^{2+}-dependent slow inactivation develops with a time course similar to the duration of the prolonged Ca^{2+} rise seen to LTC_4 following loss of protein kinase C activity (73,74). Although Ca^{2+} release to LTC_4 in the absence of protein kinase C blockers reaches a similar extent, it is the prolonged duration of the Ca^{2+} release signal in the presence of protein kinase C block that enables slow inactivation of CRAC channels to develop. Patch clamp experiments described in Figure 5-5*D* provide further evidence for the recruitment of the Ca^{2+}-dependent slow inactivation mechanism by sustained CysLT1 receptor-evoked Ca^{2+} release. The development of I_{CRAC} to thapsigargin (in the presence of weak Ca^{2+} buffer in the patch pipette solution) was compared between cells

stimulated with LTC_4 immediately prior to break in with those exposed to LTC_4 in the presence of impaired protein kinase C activity. If the sustained Ca^{2+} release evoked by non-desensitizing receptors that occurs in the absence of active protein kinase C inhibits CRAC channels, then a smaller current should be evoked by thapsigargin. This was indeed the case (Fig. 5-5*D*), although there was some variability in the kinetics of I_{CRAC} development and overall extent of the current. This may reflect the time of LTC_4 exposure prior to the onset of whole cell recording and that some thapsigargin leaked into the cell during cell-attached state. However no inhibitory effect was seen when this protocol was repeated on cells dialysed with a strongly buffered Ca^{2+}-containing pipette solution (140 nM free Ca^{2+}, 10 mM total EGTA, Fig. 5-5*E*), which suppresses Ca^{2+}-dependent slow inactivation of CRAC channels (73). Another protocol was designed to test further for an involvement of Ca^{2+}-dependent slow inactivation in inhibiting gene expression to non-desensitizing receptors. I reasoned that an increase in the time between the termination of Ca^{2+} release and subsequent store-operated Ca^{2+} entry should enable some recovery of Ca^{2+}-dependent slow inactivation to take place and this should partially rescue gene expression. I therefore stimulated cells with LTC_4 in Ca^{2+}-free solution and then readmitted external Ca^{2+} 5 minutes after the Ca^{2+} signal had returned to resting levels. Robust *c-fos* expression was induced (Fig. 5-5*F*). Strikingly, significant gene expression also occurred in cells stimulated with LTC_4 in the presence of either calphostin C or after downregulation of protein kinase C (Fig. 5-5*F*). Hence allowing CRAC channels time to recover from Ca^{2+}-dependent inactivation results in rescue of agonist-driven gene expression.

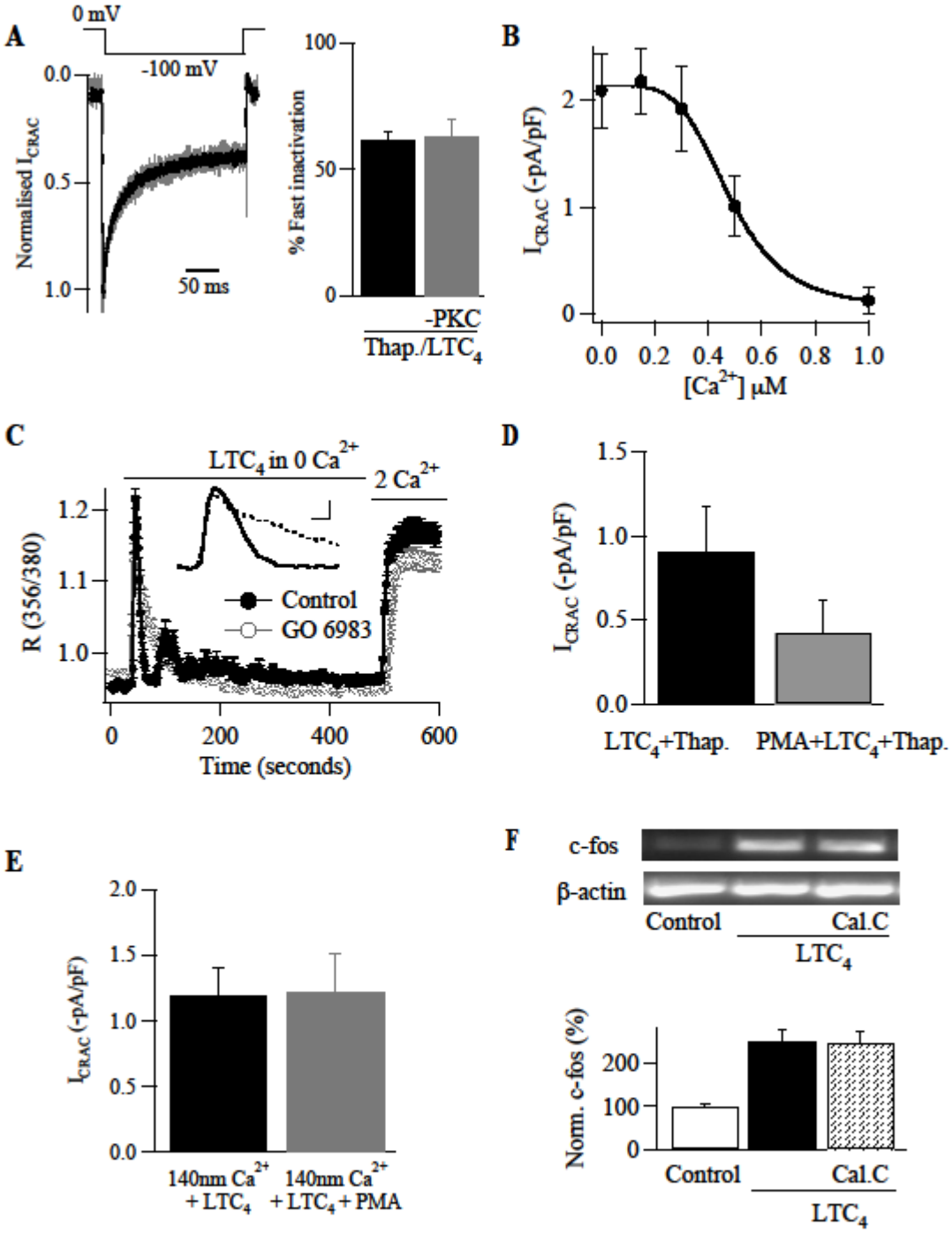
A
0 mV
-100 mV
0.0
0.5
1.0
Normalised I_{CRAC}
50 ms
100
50
0
% Fast inactivation
-PKC
Thap./LTC_4
B
2
1
0
I_{CRAC} (-pA/pF)
0.0 0.2 0.4 0.6 0.8 1.0
$[Ca^{2+}]$ μM
C
LTC_4 in 0 Ca^{2+}
2 Ca^{2+}
1.2
1.1
1.0
R (356/380)
Control
GO 6983
0 200 400 600
Time (seconds)
D
1.5
1.0
0.5
0.0
I_{CRAC} (-pA/pF)
LTC_4+Thap.
PMA+LTC_4+Thap.
E
2.0
1.5
1.0
0.5
0.0
I_{CRAC} (-pA/pF)
140nm Ca^{2+} + LTC_4
140nm Ca^{2+} + LTC_4 + PMA
F
c-fos
β-actin
Control
Cal.C
LTC_4
200
100
0
Norm. c-fos (%)
Control
Cal.C
LTC_4

Figure 5-5. Ca^{2+}-dependent slow inactivation underlies the suppression of *c-fos* expression to non-desensitizing CysLT1 receptors. *A*, Ca^{2+}-dependent fast inactivation was unaffected by CysLT1 receptor activation in the presence of downregulation of protein kinase C. *B*, the dependence of Ca^{2+}-dependent slow inactivation on pipette Ca^{2+} concentration is shown. The K_D for 50% inactivation was ~ 0.5 mM. *C*, Increasing the time interval between Ca^{2+} release and subsequent Ca^{2+} entry results in partial recovery of store-operated Ca^{2+} entry. The inset shows the prolongation of Ca^{2+} release under these conditions. *D*, Patch clamp experiments revealed that stimulation of non-desensitizing receptors with LTC_4 prior to break-in significantly reduced the size of I_{CRAC} that developed in response to dialysis with thapsigargin in weak buffer (0.2 mM EGTA). CysLT1 receptor stimulation had no inhibitory effects when applied to cells in which protein kinase C had not been downregulated. *E*, as in *C*, but now cells were dialysed with a pipette solution containing strong Ca^{2+} buffer (10 mM EGTA, 140 nM Ca^{2+}). Under these conditions, non-desensitizing receptors failed to impair activation of I_{CRAC} to thapsigargin. *F*, *c-fos* expression occurs to agonist, despite protein kinase C block, when Ca^{2+} entry is initiated several minutes after Ca^{2+} release has reached completion. In these experiments, cells were stimulated with LTC_4 in Ca^{2+}-free solution, and then external Ca^{2+} was readmitted 5 minutes after the Ca^{2+} signal has returned to resting levels. Gene expression was measured after 5 minutes of continuous Ca^{2+} entry (followed by 30 minutes in Ca^{2+}-free solution).

5.2.6 c-fos expression has high sensitivity to Ca^{2+} influx and is a high gain system

Despite evoking a smaller CRAC current, LTC_4 is as effective as thapsigargin in activating c-fos. This is because gene expression has high sensitivity to local Ca^{2+} entry. Stimulation with concentrations of thapsigargin that caused submaximal Ca^{2+} entry (Fig. 5-6*A*) led to prominent *c-fos* expression (Fig. 5-6*B*). 100 nM thapsigargin was ~ half as effective as 2 μM thapsigargin in activating CRAC channels but evoked as much c-fos expression as the higher concentration (Fig. 5-6*A* and *B*). This high sensitivity to Ca^{2+} entry can be seen in Figure 5-6*C*, which shows *c-fos* expression in response to LTC_4 or 0.1 μM thapsigargin is as high as that evoked by 2 μM thapsigargin, despite considerably smaller Ca^{2+} signals (amplitude and duration; measured as the integrated area under the curve). Another important finding was that *c-fos* expression occurred in response to brief Ca^{2+} entry: transient stimulation for just 2 minutes was sufficient for subsequent gene expression. Both thapsigargin and LTC_4 activated c-fos with time-constants of ~ 2.5 minutes and with initial slopes of ~35% of maximal gene expression per minute (Fig. 5-6*D* and *E*). A final principle to emerge is that gene expression to agonist has high gain. The relationship between *c-fos* expression and I_{CRAC} amplitude was very steep (Fig. 5-6*F*), with an increase in gene expression of ~5% of maximum per 1% increase in the size of I_{CRAC}. Ca^{2+} microdomains near CRAC channels therefore impart high fidelity (due to the high sensitivity), rapidity and amplification, ensuring efficient gene expression to bursts of CRAC channel activity following physiological levels of receptor stimulation. These features enable long-term gene expression to occur despite reversible receptor desensitization.

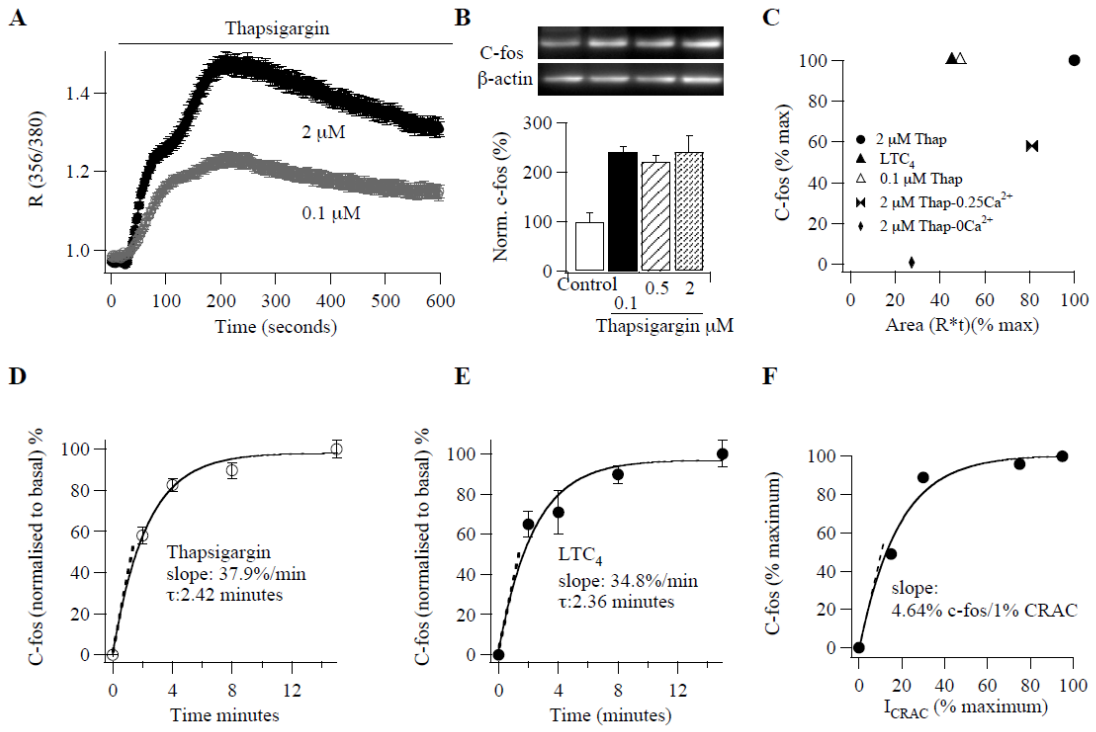

Figure 5-6. c-fos expression has high sensitivity to Ca^{2+} influx and is a high gain system. *A*, comparison of Ca^{2+} signals to 0.1 and 2 μM thapsigargin. *B*. effects of different concentrations of thapsigargin on c-fos expression. Note 0.1 and 2 μM thapsigargin give similar gene expression despite substantially different Ca^{2+} signals. *C*, the graph plots the extent of *c-fos* expression (normalised to the response in thapsigargin in 2 mM external Ca^{2+}, which is taken as the maximal response) versus the Ca^{2+} signal, integrated over 8 minutes. *D*, kinetics of *c-fos* expression following stimulation with thapsigargin for different times. *E*, kinetics of *c-fos* expression following stimulation with LTC_4 for different times. In *D* and *E*, cells were exposed to stimulus in 2 mM Ca^{2+} solution for the times indicated, and then perfused in the absence of stimulus in Ca^{2+}-free solution for 30 minutes prior to RNA extraction. *F*, relationship between *c-fos* expression and I_{CRAC} activity. *c-fos* expression to LTC_4 was measured in different external Ca^{2+} concentrations and this was plotted against I_{CRAC} amplitude, measured in the different Ca^{2+} concentrations. Gene expression in 2

mM external Ca^{2+} and the size of I_{CRAC} in 10 mM Ca^{2+} were taken as the respective maxima. Gene expression did not increase further in 5 mM Ca^{2+}. The initial slope showed a gain of ~ 5.

5.3 Discussion

Collectively, my findings reveal a novel and counter-intuitive function for receptor desensitization. Rather than terminating a response, homologous receptor desensitization is essential for maintaining excitation-transcription coupling. Desensitization of CysLT1 receptors is mediated principally by protein kinase C-dependent phosphorylation of a series of seine residues in the carboxy terminus (164). Prevention of receptor desensitization through either acute block or degradation of protein kinase C led to a loss of Ca^{2+}-dependent gene expression, despite potentiation of Ca^{2+} release. Mechanistically, the prolonged Ca^{2+} release phase accelerated Ca^{2+}-dependent slow inactivation of CRAC channels, resulting in loss of Ca^{2+} entry. Because Ca^{2+} microdomains near open CRAC channels drive c-fos expression through recruitment of Syk and the STAT transcription factors, the decline in CRAC channel activity abolishes excitation-transcription coupling. The interval between Ca^{2+} oscillations following CysLT1 receptor activation is ~ 25 seconds (163). Because $InsP_3$ has a short half-life in the cytoplasm (~ 1 second) (171), store refilling will occur quickly and CRAC channel activity will be transient following cysLT1 receptor stimulation. The short duration of Ca^{2+} entry, determined by receptor desensitization, will ensure Ca^{2+}-dependent slow inactivation does not develop, since this inhibitory mechanism requires a sustained Ca^{2+} rise for several seconds. It is therefore the kinetics of receptor desensitization and recovery from desensitization that ensures bursts of store-operated Ca^{2+} entry occur that are sufficient for the activation of c-fos expression, without the build-up of the Ca^{2+}-dependent slow inactivation pathway that would abolish the response. Thapsigargin evokes much smaller and more sluggish Ca^{2+} release, which is not sufficient to trigger Ca^{2+}-dependent slow inactivation of the CRAC channels.

Chapter 6 General Discussion

6.1 General discussion

CRAC channels play an important, and in some cell types including T lymphocytes and mast cells, a non-redundant role in driving fundamental cellular responses. Patients with a single point mutation in Orai1 (R91W) exhibited a range of clinical phenotypes including severe combined deficiency, skeletal muscle myopathy, and ectodermal dysplasia (31,32). The patients died within a few years of birth due to a high susceptibility to infections. The R91W mutant trafficks normally and is expressed in the plasma membrane, but is not functional. It acts as a dominant negative subunit.

The Orai1 channel knockout mouse has been made by two groups, and the mouse showed several characteristics including defective immune cell development, growth retardation, insensitivity to subcutaneous anaphylactic response (indicating an inability to develop mast cell-triggered allergy), hair loss and eyelid irritation (85,172). A limitation with animal knockout studies is that other proteins might compensate for the loss of Orai1, at least partially. Interestingly, in fibroblasts taken from the SCID patients, transient transfection with either Orai2 or Orai3 failed to rescue store-operated Ca^{2+} entry (172). Hence in some cell types, Orai1 appears to have a non-redundant role. An interesting paradox nevertheless arises. As Orai1 is widely distributed, why are the phenotypes in both the SCID patients and knockout mice so restricted? One possibility is that other, presumably non-store-operated channels are upregulated. These could include VOCCs and TRPCs. Interestingly, knock down of STIM1 abolishes store-operated entry but increases activity of VOCCs (173,174). This is because STIM1 simultaneously activates Orai1 whilst inhibiting VOCCs. Hence loss of Orai1 could upregulate other non-store-operated Ca^{2+} permeable pathways.

A complimentary approach to animal knockout mice is to knockdown transiently Orai1 expression using an RNAi approach. Such studies shown CRAC channels directly regulate a range of cellular responses from exocytosis to gene regulation (175). CRAC channels are particularly important in mast cells, where they drive both rapid responses (including secretion of histamine and ATP, synthesis and secretion of pro-inflammatory leukotriene C_4) and slower ones (developing over hours) that involve expression of genes that help coordinate and sustain the inflammatory response (176). These genes include chemokines such as TNF-α and cytokines including IL-2, IL-4, and IL-13.

The results in this thesis add to our understanding of CRAC channel function in mast cells, using the well established RBL-1 cell line as a model system. In Chapter 3, I show that stimulation of RBL cells with a physiological trigger (antigen) generates a positive feedback cycle that sustains mast cells activation. Engagement of FCεRI receptors leads to receptor phosphorylation by the tyrosine kinase Lyn, and the phosphorylated tyrosine recruits and activates the non-receptor tyrosine kinase Syk. Syk activation stimulates PLCγ1, leading to $InsP_3$ production, store depletion and subsequent CRAC channel opening. Unexpectedly, I found that sustained Syk activity required Ca^{2+} entry through CRAC channels. Following stimulation of antigen receptors, Syk activity was reduced significantly following removal of external Ca^{2+}, block of CRAC channels with Synta or by knockdown of Orai1. Ca^{2+} regulation of Syk was local, because it was unaffected by the fast Ca^{2+} chelator BAPTA. Since receptors and TRPC channels can cluster together, it seems likely that FCεRI-associated Syk and Orai1 co-localize. Indeed, immunocytochemical studies reveal that Syk is located at the plasma membrane and might form puncta analogous to Orai1/STIM1 after store depletion. Future work attempting co-immunoprecipitation

(co-IP) of Orai1 and Syk or FRET analysis between the two proteins would test this idea more directly. Ca^{2+} microdomains near open CRAC channels fail to activate Syk unless antigen receptors have been stimulated. Either the Ca^{2+}-dependence of Syk is imparted by prior binding to FCεRI receptors or an additional signal from the receptors is needed for the Ca^{2+} dependence of Syk. Regardless, had I only used thapsigargin as a stimulus then I would have missed this form of Syk regulation. My results reinforce the importance of carrying out receptor-driven activation rather than simpler stimulation protocols. My findings reveal a novel positive feedback step that sustains activation on an individual cell basis. Antigen receptors activate PLCγ1 and generate $InsP_3$ via Syk. This leads to store depletion and subsequent activation of CRAC channels. Local Ca^{2+} entry near the open CRAC channels maintains activation of Syk, thus sustaining $InsP_3$ production, store depletion and open probability of the CRAC channels. The physiological importance of this mechanism is that it enables CRAC channels to maintain their own activity. Although antigen receptors produce $InsP_3$, the elevation is small in comparison with G-protein coupled receptors. Hence boosting $InsP_3$ production by CRAC channels would ensure $InsP_3$ levels are sustained, and at a level sufficient to support CRAC channel opening.

An important consequence of CRAC channel opening is activation of gene expression. Chapter 4 describes how Ca^{2+} microdomains near CRAC channels signal to the nucleus to upregulate that immediate early gene c-fos, an important component of the AP-1 complex that regulates many immune cell genes. Local Ca^{2+} entry was relayed to the nucleus via the non-receptor tyrosine kinase Syk and then STAT5. Activation of $cPLA_2$ and 5-LO were also driven by local Ca^{2+} signals and a central early step in this pathway involves Syk. Hence, Syk senses Ca^{2+} microdomains and relays the signal down parallel routes. One involves the PKC, MEK/ERK pathway,

leading to leukotriene production and the other signals to the nucleus via STAT5. Hence Ca^{2+} microdomains can activate spatially and temporally distinct responses via Syk. It will be interesting in future work to design experiment to see if the same microdomain activates both pathways simultaneously or whether different microdomains tap into different pathway. It is tempting to speculate that different STIM1/Orai1 puncta, each of which contains numerous CRAC channels, might recruit different Ca^{2+} sensors, thereby having different functional effects.

Stimulation of endogenous cell surface CysLT1 receptors with low levels of LTC_4 that evoke Ca^{2+} oscillations also leads to expression of *c-fos* and through a mechanism involving Ca^{2+} microdomains near CRAC channels and Syk, as described in Chapter 5. Despite evoking less Ca^{2+} entry, agonist was as effective as thapsigargin in driving gene expression. This was found to reflect a high sensitivity of gene expression to local Ca^{2+} entry. Submaximal CRAC channel activation evoked robust gene expression. A major role for PKC was revealed using both pharmacology and protein downregulation. The involvement of PKC was specific to the agonist pathway and did not involve an increase in sensitivity of gene expression to Ca^{2+}. Rather, the effect was pinpointed to receptor desensitization. It has been well established that CysLT1 receptors desensitize following PKC mediated phosphorylation of three serine residues in the receptor carboxy tail (164). Phosphorylation initially uncouples the receptor from PLC and then, after several minutes, results in endocytosis of the receptor (164). Consistent with this, I found that loss of PKC activity increases CysLT1R-dependent $InsP_3$ production, Ca^{2+} release and store depletion. Paradoxically, this leads to less gene expression. The molecular mechanism underlying this reflects Ca^{2+}-dependent slow inactivation of the CRAC channel, due to the prolonged Ca^{2+} release by $InsP_3$. The findings suggest receptor desensitization

might actually serve to sustain gene expression rather than terminate it. CysLT1 activation produces a series of repetitive Ca^{2+} oscillations. Each oscillation lasts around 10s-15s and the interspike interval is approximately 30s. The transient duration of the spike and the relatively large interval between oscillations may help ensure what little Ca^{2+}-dependent inactivation that occurs during the spike reverses within the interpulse period. Loss of this pattern results in sustained Ca^{2+} release and subsequent inactivation of the CRAC channels. Future works should address the specific identity of the PKC isoforms involved in receptor desensitization, whether other CysLT1R-dependent responses in mast cell are also affected in this way and if the principle developed in Chapter 5 is applicable to other receptors.

Chapter 7 References

7.1 References

1. Ehrlich, P. 1877. Beiträge zur kenntnis der anilinfärbungen und ihrer verwendung in der mikroskopischen technik. *Archiv fuer mikroskopische Anatomie* 13:263-277.

2. Kitamura, Y., S. Go, and K. Hatanaka. 1978. Decrease of mast cells in W/Wv mice and their increase by bone marrow transplantation. *Blood* 52:447-452.

3. Kitamura, Y., M. Yokoyama, H. Matsuda, T. Ohno, and K. J. Mori. 1981. Spleen colony-forming cell as common precursor for tissue mast cells and granulocytes. *Nature* 291:159-160.

4. Sonoda, T., Y. Kitamura, Y. Haku, H. Hara, and K. J. Mori. 1983. Mast-cell precursors in various haematopoietic colonies of mice produced in vivo and in vitro. *Br.J.Haematol.* 53:611-620.

5. Kitamura, Y. 1989. Heterogeneity of mast cells and phenotypic change between subpopulations. *Annu.Rev.Immunol.* 7:59-76.

6. Metcalfe, D. D., D. Baram, and Y. A. Mekori. 1997. Mast cells. *Physiol.Rev.* 77:1033-1079.

7. Bischoff, S. C. 2007. Role of mast cells in allergic and non-allergic immune responses: comparison of human and murine data. *Nat.Rev.Immunol.* 7:93-104.

8. Lee, D. M., D. S. Friend, M. F. Gurish, C. Benoist, D. Mathis, and M. B. Brenner. 2002. Mast cells: a cellular link between autoantibodies and inflammatory arthritis. *Science* 297:1689-1692.

9. Lu, L. F., E. F. Lind, D. C. Gondek, K. A. Bennett, M. W. Gleeson, K. Pino-Lagos, Z. A. Scott, A. J. Coyle, J. L. Reed, J. Van Snick, T. B. Strom, X. X. Zheng, and R. J. Noelle. 2006. Mast cells are essential intermediaries in regulatory T-cell tolerance. *Nature* 442:997-1002.

10. Galli, S. J., S. Nakae, and M. Tsai. 2005. Mast cells in the development of adaptive immune responses. *Nat.Immunol.* 6:135-142.

11. Vliagoftis, H. and A. D. Befus. 2005. Mast cells at mucosal frontiers. *Curr.Mol.Med.* 5:573-589.

12. Marshall, J. S. 2004. Mast-cell responses to pathogens. *Nat.Rev.Immunol.* 4:787-799.

13. Malaviya, R. and A. Georges. 2002. Regulation of mast cell-mediated innate immunity during early response to bacterial infection. *Clin.Rev.Allergy Immunol.* 22:189-204.

14. Barbara, G., V. Stanghellini, R. De Giorgio, C. Cremon, G. S. Cottrell, D. Santini, G. Pasquinelli, A. M. Morselli-Labate, E. F. Grady, N. W. Bunnett, S. M. Collins, and R. Corinaldesi. 2004. Activated mast cells in proximity to

colonic nerves correlate with abdominal pain in irritable bowel syndrome. *Gastroenterology* 126:693-702.

15. Theoharides, T. C. and D. E. Cochrane. 2004. Critical role of mast cells in inflammatory diseases and the effect of acute stress. *J.Neuroimmunol.* 146:1-12.

16. Theoharides, T. C., D. Kempuraj, M. Tagen, P. Conti, and D. Kalogeromitros. 2007. Differential release of mast cell mediators and the pathogenesis of inflammation. *Immunol.Rev.* 217:65-78.

17. Mekori, Y. A. and D. D. Metcalfe. 2000. Mast cells in innate immunity. *Immunol.Rev.* 173:131-140.

18. Hansen, I., L. Klimek, R. Mosges, and K. Hormann. 2004. Mediators of inflammation in the early and the late phase of allergic rhinitis. *Curr.Opin.Allergy Clin.Immunol.* 4:159-163.

19. Metzger, H. 1992. The receptor with high-affinity for IgE. *Immunol.Rev.* 125:37-48.

20. Sommers, C. L., L. E. Samelson, and P. E. Love. 2004. LAT: a T lymphocyte adapter protein that couples the antigen receptor to downstream signaling pathways. *Bioessays* 26:61-67.

21. Saitoh, S., R. Arudchandran, T. S. Manetz, W. Zhang, C. L. Sommers, P. E. Love, J. Rivera, and L. E. Samelson. 2000. LAT is essential for FcεRI-mediated mast cell activation. *Immunity* 12:525-535.

22. Gu, H., K. Saito, L. D. Klaman, J. Shen, T. Fleming, Y. Wang, J. C. Pratt, G. Lin, B. Lim, J. P. Kinet, and B. G. Neel. 2001. Essential role for Gab2 in the allergic response. *Nature* 412:186-190.

23. Nishizumi, H. and T. Yamamoto. 1997. Impaired tyrosine phosphorylation and Ca^{2+} mobilization, but not degranulation, in lyn-deficient bone marrow-derived mast cells. *J.Immunol.* 158:2350-2355.

24. Parravicini, V., M. Gadina, M. Kovarova, S. Odom, C. Gonzalez-Espinosa, Y. Furumoto, S. Saitoh, L. E. Samelson, J. J. O'Shea, and J. Rivera. 2002. Fyn kinase initiates complementary signals required for IgE-dependent mast cell degranulation. *Nat.Immunol.* 3:741-748.

25. Chang, W. C., C. Nelson, and A. B. Parekh. 2006. Ca^{2+} influx through CRAC channels activates cytosolic phospholipase A_2, leukotriene C_4 secretion, and expression of c-fos through ERK-dependent and -independent pathways in mast cells. *Faseb J.* 20:2381-2383.

26. Hoth, M. and R. Penner. 1992. Depletion of intracellular calcium stores activates a calcium current in mast cells. *Nature* 355:353-356.

27. Feske, S. 2010. CRAC channelopathies. *Pflugers Arch.* 460:417-435.

28. Parekh, A. B. and J. W. Putney. 2005. Store-operated calcium channels. *Physiol.Rev.* 85:757-810.

29. Feske, S. 2007. Calcium signalling in lymphocyte activation and disease. *Nat.Rev.Immunol.* 7:690-702.

30. Liou, J., M. L. Kim, W. D. Heo, J. T. Jones, J. W. Myers, J. E. Ferrell, and T. Meyer. 2005. STIM is a Ca^{2+} sensor essential for Ca^{2+}-store-depletion-triggered Ca^{2+} influx. *Curr.Biol.* 15:1235-1241.

31. Feske, S., Y. Gwack, M. Prakriya, S. Srikanth, S. H. Puppel, B. Tanasa, P. G. Hogan, R. S. Lewis, M. Daly, and A. Rao. 2006. A mutation in Orai1 causes immune deficiency by abrogating CRAC channel function. *Nature* 441:179-185.

32. Feske, S., M. Prakriya, A. Rao, and R. S. Lewis. 2005. A severe defect in CRAC Ca^{2+} channel activation and altered K^+ channel gating in T cells from immunodeficient patients. *J.Exp.Med.* 202:651-662.

33. Wu, M. M., J. Buchanan, R. M. Luik, and R. S. Lewis. 2006. Ca^{2+} store depletion causes STIM1 to accumulate in ER regions closely associated with the plasma membrane. *J.Cell Biol.* 174:803-813.

34. Park, C. Y., P. J. Hoover, F. M. Mullins, P. Bachhawat, E. D. Covington, S. Raunser, T. Walz, K. C. Garcia, R. E. Dolmetsch, and R. S. Lewis. 2009.

STIM1 clusters and activates CRAC channels via direct binding of a cytosolic domain to Orai1. *Cell* 136:876-890.

35. Peinelt, C., M. Vig, D. L. Koomoa, A. Beck, M. J. Nadler, M. Koblan-Huberson, A. Lis, A. Fleig, R. Penner, and J. P. Kinet. 2006. Amplification of CRAC current by STIM1 and CRACM1 (Orai1). *Nat.Cell Biol.* 8:771-773.

36. Mullins, F. M., C. Y. Park, R. E. Dolmetsch, and R. S. Lewis. 2009. STIM1 and calmodulin interact with Orai1 to induce Ca^{2+}-dependent inactivation of CRAC channels. *Proc.Natl.Acad.Sci.U.S.A.* 106:15495-15500.

37. Singaravelu, K., C. Nelson, D. Bakowski, d. B. Martins, S. W. Ng, J. Di Capite, T. Powell, L. Scorrano, and A. B. Parekh. 2011. Mitofusin 2 regulates STIM1 migration from the Ca^{2+} store to the plasma membrane in cells with depolarised mitochondria. *J.Biol.Chem. Epub*

38. Putney, J. W., Jr. 2001. Pharmacology of capacitative calcium entry. *Mol.Interv.* 1:84-94.

39. Bakowski, D., M. D. Glitsch, and A. B. Parekh. 2001. An examination of the secretion-like coupling model for the activation of the Ca^{2+} release-activated Ca^{2+} current I_{CRAC} in RBL-1 cells. *J.Physiol.* 532:55-71.

40. Lis, A., C. Peinelt, A. Beck, S. Parvez, M. Monteilh-Zoller, A. Fleig, and R. Penner. 2007. CRACM1, CRACM2, and CRACM3 are store-operated Ca^{2+} channels with distinct functional properties. *Curr.Biol.* 17:794-800.

41. Peinelt, C., A. Lis, A. Beck, A. Fleig, and R. Penner. 2008. 2-aminoethoxydiphenyl borate directly facilitates and indirectly inhibits STIM1-dependent gating of CRAC channels. *J.Physiol.* 586:3061-3073.

42. DeHaven, W. I., J. T. Smyth, R. R. Boyles, G. S. Bird, and J. W. Putney, Jr. 2008. Complex actions of 2-aminoethyldiphenyl borate on store-operated calcium entry. *J.Biol.Chem.* 283:19265-19273.

43. Kozak, J. A., H. H. Kerschbaum, and M. D. Cahalan. 2002. Distinct properties of CRAC and MIC channels in RBL cells. *J.Gen.Physiol* 120:221-235.

44. Xu, S. Z., F. Zeng, G. Boulay, C. Grimm, C. Harteneck, and D. J. Beech. 2005. Block of TRPC5 channels by 2-aminoethoxydiphenyl borate: a differential, extracellular and voltage-dependent effect. *Br.J.Pharmacol.* 145:405-414.

45. Zhu, X., M. Jiang, and L. Birnbaumer. 1998. Receptor-activated Ca^{2+} influx via human Trp3 stably expressed in human embryonic kidney HEK293 cells. Evidence for a non-capacitative Ca^{2+} entry. *J.Biol.Chem.* 273:133-142.

46. Prakriya, M. and R. S. Lewis. 2003. CRAC channels: activation, permeation, and the search for a molecular identity. *Cell Calcium* 33:311-321.

47. Zweifach, A. and R. S. Lewis. 1993. Mitogen-regulated Ca^{2+} current of T lymphocytes is activated by depletion of intracellular Ca^{2+} stores. *Proc.Natl.Acad.Sci.U.S.A.* 90:6295-6299.

48. Neher, E. 1998. Vesicle pools and Ca^{2+} microdomains: New tools for understanding their roles in neurotransmitter release. *Neuron* 20:389-399.

49. Parekh, A. B. 2008. Ca^{2+} microdomains near plasma membrane Ca^{2+} channels: impact on cell function. *J.Physiol.* 586:3043-3054.

50. Urbano, F. J., R. S. Depetris, and O. D. Uchitel. 2001. Coupling of L-type calcium channels to neurotransmitter release at mouse motor nerve terminals. *Pflugers Arch.* 441:824-831.

51. Luik, R. M., M. M. Wu, J. Buchanan, and R. S. Lewis. 2006. The elementary unit of store-operated Ca^{2+} entry: local activation of CRAC channels by STIM1 at ER-plasma membrane junctions. *J.Cell Biol.* 174:815-825.

52. Willoughby, D. and D. M. Cooper. 2007. Organization and Ca^{2+} regulation of adenylyl cyclases in cAMP microdomains. *Physiol.Rev.* 87:965-1010.

53. Bautista, D. M. and R. S. Lewis. 2004. Modulation of plasma membrane calcium-ATPase activity by local calcium microdomains near CRAC channels in human T cells. *J.Physiol.* 556:805-817.

54. Chang, W. C., J. Di Capite, K. Singaravelu, C. Nelson, V. Halse, and A. B. Parekh. 2008. Local Ca^{2+} influx through Ca^{2+} release-activated Ca^{2+} (CRAC) channels stimulates production of an intracellular messenger and an intercellular pro-inflammatory signal. *J.Biol.Chem.*283:4622-4631.

55. Rizzuto, R., P. Bernardi, and T. Pozzan. 2000. Mitochondria as all-round players of the calcium game. *J.Physiol.* 529 Pt 1:37-47.

56. Parekh, A. B. 2007. Functional consequences of activating store-operated CRAC channels. *Cell Calcium* 42:111-121.

57. Perocchi, F., V. M. Gohil, H. S. Girgis, X. R. Bao, J. E. McCombs, A. E. Palmer, and V. K. Mootha. 2010. MICU1 encodes a mitochondrial EF hand protein required for Ca^{2+} uptake. *Nature* 467:291-296.

58. McCormack, J. G., A. P. Halestrap, and R. M. Denton. 1990. Role of calcium ions in regulation of mammalian intramitochondrial metabolism. *Physiol.Rev.* 70:391-425.

59. Parekh, A. B. 2003. Store-operated Ca^{2+} entry: dynamic interplay between endoplasmic reticulum, mitochondria and plasma membrane. *J.Physiol.* 547:333-348.

60. Moreau, B., C. Nelson, and A. B. Parekh. 2006. Biphasic regulation of mitochondrial Ca^{2+} uptake by cytosolic Ca^{2+} concentration. *Curr.Biol.* 16:1672-1677.

61. Csordas, G. and G. Hajnoczky. 2003. Plasticity of mitochondrial calcium signaling. *J.Biol.Chem.* 278:42273-42282.

62. Rizzuto, R. and T. Pozzan. 2006. Microdomains of intracellular Ca^{2+}: Molecular determinants and functional consequences. *Physiol.Rev.* 86:369-408.

63. Rizzuto, R., M. Brini, M. Murgia, and T. Pozzan. 1993. Microdomains with high Ca^{2+} close to IP_3-sensitive channels that are sensed by neighboring mitochondria. *Science* 262:744-747.

64. Filippin, L., P. J. Magalhaes, G. Di Benedetto, M. Colella, and T. Pozzan. 2003. Stable interactions between mitochondria and endoplasmic reticulum allow rapid accumulation of calcium in a subpopulation of mitochondria. *J.Biol.Chem.* 278:39224-39234.

65. Collins, T. J., P. Lipp, M. J. Berridge, and M. D. Bootman. 2001. Mitochondrial Ca^{2+} uptake depends on the spatial and temporal profile of cytosolic Ca^{2+} signals. *J.Biol.Chem.* 276:26411-26420.

66. Moreau, B. and A. B. Parekh. 2008. Ca^{2+}-dependent inactivation of the mitochondrial Ca^{2+} uniporter involves proton flux through the ATP synthase. *Curr.Biol.* 18:855-859.

67. Hajnoczky, G., L. D. Robb-Gaspers, M. B. Seitz, and A. P. Thomas. 1995. Decoding of cytosolic calcium oscillations in the mitochondria. *Cell* 82:415-424.

68. Robert, V., P. Gurlini, V. Tosello, T. Nagai, A. Miyawaki, F. Di Lisa, and T. Pozzan. 2001. Beat-to-beat oscillations of mitochondrial [Ca^{2+}] in cardiac cells. *EMBO J.* 20:4998-5007.

69. Neher, E. 1995. The use of fura-2 for estimating Ca buffers and Ca fluxes. *Neuropharmacology* 34:1423-1442.

70. Bautista, D. M., M. Hoth, and R. S. Lewis. 2002. Enhancement of calcium signalling dynamics and stability by delayed modulation of the plasma-membrane calcium-ATPase in human T cells. *J.Physiol.* 541:877-894.

71. Gilabert, J. A. and A. B. Parekh. 2000. Respiring mitochondria determine the pattern of activation and inactivation of the store-operated Ca^{2+} current ICRAC. *EMBO J.* 19:6401-6407.

72. Gilabert, J. A., D. Bakowski, and A. B. Parekh. 2001. Energized mitochondria increase the dynamic range over which inositol 1,4,5-trisphosphate activates store-operated calcium influx. *EMBO J.* 20:2672-2679.

73. Parekh, A. B. 1998. Slow feedback inhibition of calcium release-activated calcium current by calcium entry. *J.Biol.Chem.* 273:14925-14932.

74. Zweifach, A. and R. S. Lewis. 1995. Slow calcium-dependent inactivation of depletion-activated calcium current. Store-dependent and -independent mechanisms. *J.Biol.Chem.* 270:14445-14451.

75. Hoth, M., D. C. Button, and R. S. Lewis. 2000. Mitochondrial control of calcium-channel gating: a mechanism for sustained signaling and transcriptional activation in T lymphocytes. *Proc.Natl.Acad.Sci.U.S.A.* 97:10607-10612.

76. Glitsch, M. D., D. Bakowski, and A. B. Parekh. 2002. Store-operated Ca^{2+} entry depends on mitochondrial Ca^{2+} uptake. *Embo J.* 21:6744-6754.

77. Quintana, A., C. Schwindling, A. S. Wenning, U. Becherer, J. Rettig, E. C. Schwarz, and M. Hoth. 2007. T cell activation requires mitochondrial translocation to the immunological synapse. *Proc.Natl.Acad.Sci.U.S.A.* 104:14418-14423.

78. Bakowski, D. and A. B. Parekh. 2007. Regulation of store-operated calcium channels by the intermediary metabolite pyruvic acid. *Curr.Biol.* 17:1076-1081.

79. Chu, H. and P. S. Low. 2006. Mapping of glycolytic enzyme-binding sites on human erythrocyte band 3. *Biochem.J.* 400:143-151.

80. Burdakov, D. 2007. K^+ channels stimulated by glucose: a new energy-sensing pathway. *Pflugers Arch.* 454:19-27.

81. Ashcroft, F. M. 2006. K_{ATP} channels and insulin secretion: a key role in health and disease. *Biochem.Soc.Trans.* 34:243-246.

82. Ali, H., K. Maeyama, R. Sagi-Eisenberg, and M. A. Beaven. 1994. Antigen and thapsigargin promote influx of Ca^{2+} in rat basophilic RBL-2H3 cells by ostensibly similar mechanisms that allow filling of inositol 1,4,5-trisphosphate-sensitive and mitochondrial Ca^{2+} stores. *Biochem.J.* 304 (Pt 2):431-440.

83. Zhang, L. and M. A. McCloskey. 1995. Immunoglobulin E receptor-activated calcium conductance in rat mast cells. *J.Physiol.* 483 (Pt 1):59-66.

84. Baba, Y., K. Nishida, Y. Fujii, T. Hirano, M. Hikida, and T. Kurosaki. 2008. Essential function for the calcium sensor STIM1 in mast cell activation and anaphylactic responses. *Nat.Immunol.* 9:81-88.

85. Vig, M., W. I. DeHaven, G. S. Bird, J. M. Billingsley, H. Wang, P. E. Rao, A. B. Hutchings, M. H. Jouvin, J. W. Putney, and J. P. Kinet. 2008. Defective mast cell effector functions in mice lacking the CRACM1 pore subunit of store-operated calcium release-activated calcium channels. *Nat.Immunol.* 9:89-96.

86. Chang, W. C. and A. B. Parekh. 2004. Close functional coupling between Ca^{2+} release-activated Ca^{2+} channels, arachidonic acid release, and leukotriene C_4 secretion. *J.Biol.Chem.* 279:29994-29999.

87. Lee, Y. N., J. Tuckerman, H. Nechushtan, G. Schutz, E. Razin, and P. Angel. 2004. c-fos as a regulator of degranulation and cytokine production in FcεRI-activated mast cells. *J.Immunol.* 173:2571-2577.

88. Carafoli, E. 2002. Calcium signaling: a tale for all seasons. *Proc.Natl.Acad.Sci.U.S.A.* 99:1115-1122.

89. Berridge, M. J., M. D. Bootman, and H. L. Roderick. 2003. Calcium signalling: dynamics, homeostasis and remodelling. *Nat.Rev.Mol.Cell Biol.* 4:517-529.

90. Ng, S. W., C. Nelson, and A. B. Parekh. 2009. Coupling of Ca^{2+} microdomains to spatially and temporally distinct cellular responses by the tyrosine kinase Syk. *J.Biol.Chem.* 284:24767-24772.

91. Lin, L. L., M. Wartmann, A. Y. Lin, J. L. Knopf, A. Seth, and R. J. Davis. 1993. $cPLA_2$ is phosphorylated and activated by MAP kinase. *Cell* 72:269-278.

92. Qiu, Z. H. and C. C. Leslie. 1994. Protein kinase C-dependent and -independent pathways of mitogen-activated protein kinase activation in macrophages by stimuli that activate phospholipase A_2. *J.Biol.Chem.* 269:19480-19487.

93. Boyce, J. A. 2005. Eicosanoid mediators of mast cells: receptors, regulation of synthesis, and pathobiologic implications. *Chem.Immunol.Allergy* 87:59-79.

94. Chen, X. S. and C. D. Funk. 2001. The N-terminal "beta-barrel" domain of 5-lipoxygenase is essential for nuclear membrane translocation. *J.Biol.Chem.* 276:811-818.

95. Brock, T. G., R. W. McNish, and M. Peters-Golden. 1995. Translocation and leukotriene synthetic capacity of nuclear 5-lipoxygenase in rat basophilic leukemia cells and alveolar macrophages. *J.Biol.Chem.* 270:21652-21658.

96. Hammarberg, T., P. Provost, B. Persson, and O. Radmark. 2000. The N-terminal domain of 5-lipoxygenase binds calcium and mediates calcium stimulation of enzyme activity. *J.Biol.Chem.* 275:38787-38793.

97. Funk, C. D. 2001. Prostaglandins and leukotrienes: advances in eicosanoid biology. *Science* 294:1871-1875.

98. Mellor, E. A., A. Maekawa, K. F. Austen, and J. A. Boyce. 2001. Cysteinyl leukotriene receptor 1 is also a pyrimidinergic receptor and is expressed by human mast cells. *Proc.Natl.Acad.Sci.U.S.A.* 98:7964-7969.

99. Sjostrom, M., P. J. Jakobsson, M. Juremalm, A. Ahmed, G. Nilsson, L. Macchia, and J. Z. Haeggstrom. 2002. Human mast cells express two leukotriene C4 synthase isoenzymes and the CysLT1 receptor. *Biochim.Biophys.Acta* 1583:53-62.

100. Lynch, K. R., G. P. O'Neill, Q. Liu, D. S. Im, N. Sawyer, K. M. Metters, N. Coulombe, M. Abramovitz, D. J. Figueroa, Z. Zeng, B. M. Connolly, C. Bai, C. P. Austin, A. Chateauneuf, R. Stocco, G. M. Greig, S. Kargman, S. B. Hooks, E. Hosfield, D. L. Williams, Jr., A. W. Ford-Hutchinson, C. T. Caskey, and J. F. Evans. 1999. Characterization of the human cysteinyl leukotriene CysLT1 receptor. *Nature* 399:789-793.

101. Rius, M., J. Hummel-Eisenbeiss, and D. Keppler. 2008. ATP-dependent transport of leukotrienes B_4 and C_4 by the multidrug resistance protein ABCC4 (MRP4). *J.Pharmacol.Exp.Ther.* 324:86-94.

102. Dahlen, S. E., P. Hedqvist, P. Westlund, E. Granstrom, S. Hammarstrom, J. A. Lindgren, and O. Radmark. 1983. Mechanisms of leukotriene-induced contractions of guinea pig airways: leukotriene C_4 has a potent direct action whereas leukotriene B_4 acts indirectly. *Acta Physiol.Scand.* 118:393-403.

103. Kanaoka, Y. and J. A. Boyce. 2004. Cysteinyl leukotrienes and their receptors: cellular distribution and function in immune and inflammatory responses. *J.Immunol.* 173:1503-1510.

104. Das, S., J. D. Rafter, K. P. Kim, S. P. Gygi, and W. Cho. 2003. Mechanism of group IVA cytosolic phospholipase A_2 activation by phosphorylation. *J.Biol.Chem.* 278:41431-41442.

105. Schievella, A. R., M. K. Regier, W. L. Smith, and L. L. Lin. 1995. Calcium-mediated translocation of cytosolic phospholipase A_2 to the nuclear envelope and endoplasmic reticulum. *J.Biol.Chem.* 270:30749-30754.

106. Parekh, A. B., A. Fleig, and R. Penner. 1997. The store-operated calcium current I_{CRAC}: Nonlinear activation by $InsP_3$ and dissociation from calcium release. *Cell* 89:973-980.

107. Glitsch, M. D. and A. B. Parekh. 2000. Ca^{2+} store dynamics determines the pattern of activation of the store-operated Ca^{2+} current I_{CRAC} in response to $InsP_3$ in rat basophilic leukaemia cells. *J.Physiol.* 523 Pt 2:283-290.

108. Hermosura, M. C., H. Takeuchi, A. Fleig, A. M. Riley, B. V. Potter, M. Hirata, and R. Penner. 2000. $InsP_4$ facilitates store-operated calcium influx by inhibition of InsP3 5-phosphatase. *Nature* 408:735-740.

109. Luik, R. M., B. Wang, M. Prakriya, M. M. Wu, and R. S. Lewis. 2008. Oligomerization of STIM1 couples ER calcium depletion to CRAC channel activation. *Nature* 454:538-542.

110. Toescu, E. C., T. Moller, H. Kettenmann, and A. Verkhratsky. 1998. Long-term activation of capacitative Ca^{2+} entry in mouse microglial cells. *Neuroscience* 86:925-935.

111. Fierro, L. and A. B. Parekh. 1999. Fast calcium-dependent inactivation of calcium release-activated calcium current (CRAC) in RBL-1 cells. *J.Membr.Biol.* 168:9-17.

112. Moreau, B., S. Straube, R. J. Fisher, J. W. Putney, and A. B. Parekh. 2005. Ca^{2+}-calmodulin-dependent facilitation and Ca^{2+} inactivation of Ca^{2+} release-activated Ca^{2+} channel. *J.Biol.Chem.* 280:8776-8783.

113. Parekh, A. B. and R. Penner. 1995. Depletion-activated calcium current is inhibited by protein kinase in RBL-2H3 Cells. *Proc.Natl.Acad.Sci.U.S.A.* 92:7907-7911.

114. Mathes, C., A. Fleig, and R. Penner. 1998. Calcium release-activated calcium current (I_{CRAC}) is a direct target for sphingosine. *J.Biol.Chem.* 273:25020-25030.

115. Chang, W. C., J. Di Capite, C. Nelson, and A. B. Parekh. 2007. All-or-none activation of CRAC channels by agonist elicits graded responses in populations of mast cells. *J.Immunol.* 179:5255-5263.

116. Di Capite, J., A. Shirley, C. Nelson, G. Bates, and A. B. Parekh. 2009. Intercellular Ca^{2+} wave propagation involving positive feedback between CRAC channels and cysteinyl leukotrienes. *FASEB J.* 23:894-905.

117. Di Capite, J., C. Nelson, G. Bates, and A. B. Parekh. 2009. Targeting Ca^{2+} release-activated Ca^{2+} channel channels and leukotriene receptors provides a novel combination strategy for treating nasal polyposis. *J.Allergy Clin.Immunol.* 124:1014-1021.

118. Vega, S., A. V. Morales, O. H. Ocana, F. Valdes, I. Fabregat, and M. A. Nieto. 2004. Snail blocks the cell cycle and confers resistance to cell death. *Genes & Development* 18:1131-1143.

119. Obara, Y., K. Labudda, T. J. Dillon, and P. J. Stork. 2004. PKA phosphorylation of Src mediates Rap1 activation in NGF and cAMP signaling in PC12 cells. *J.Cell Sci.* 117:6085-6094.

120. Xu, D. Z., R. D. Patten, T. Force, and J. M. Kyriakis. 2006. Gene 33/RALT is induced by hypoxia in cardiomyocytes, where it promotes cell death by suppressing phosphatidylinositol 3-kinase and extracellular signal-regulated kinase survival signaling. *Mol.Cell.Biol.* 26:5043-5054.

121. Segal, D. M., J. D. Taurog, and H. Metzger. 1977. Dimeric immunoglobulin-E serves as a unit signal for mast-cell degranulation. *Proc.Natl.Acad.Sci.U.S.A.* 74:2993-2997.

122. Turner, H. and J. P. Kinet. 1999. Signalling through the high-affinity IgE receptor FcεRI. *Nature* 402:B24-B30.

123. Kihara, H. and R. P. Siraganian. 1994. Src homology-2 domains of Syk and Lyn bind to tyrosine phosphorylated subunits of the high-affinity IgE receptor. *J.Biol.Chem.* 269:22427-22432.

124. Minoguchi, K., M. Benhamou, W. D. Swaim, Y. Kawakami, T. Kawakami, and R. P. Siraganian. 1994. Activation of protein-tyrosine kinase p72syk by FcεRI aggregation in rat basophilic leukemia cells p72syk is a minor component but the major protein-tyrosine kinase of Pp72. *J.Biol.Chem.* 269:16902-16908.

125. Jouvin, M. H. E., M. Adamczewski, R. Numerof, O. Letourneur, A. Valle, and J. P. Kinet. 1994. Differential control of the tyrosine kinases Lyn and Syk by the 2 signaling chains of the high-affinity immunoglobulin-E receptor. *J.Biol.Chem.* 269:5918-5925.

126. Stenton, G. R., M. Ulanova, R. E. Dery, S. Merani, M. K. Kim, M. Gilchrist, L. Puttagunta, S. Musat-Marcu, D. James, A. D. Schreiber, and A. D. Befus. 2002. Inhibition of allergic inflammation in the airways using aerosolized antisense to Syk kinase. *J.Immunol.* 169:1028-1036.

127. Dauvillier, S., P. Merida, M. Visintin, A. Cattaneo, C. Bonnerot, and P. Dariavach. 2002. Intracellular single-chain variable fragments directed to the src homology 2 domains of Syk partially inhibit FcεRI signaling in the RBL-2H3 cell line. *J.Immunol.* 169:2274-2283.

128. Yoon, E., S. Beom, H. Cheong, S. Kim, M. Oak, D. Cho, and K. M. Kim. 2004. Differential regulation of phospholipase C gamma subtypes through FcεRI, high affinity IgE receptor. *Biochem.Biophy.Res.Commun.* 325:117-123.

129. Berridge, M. J. 1993. Inositol Trisphosphate and Calcium Signaling. *Nature* 361:315-325.

130. Parekh, A. B. and R. Penner. 1997. Store depletion and calcium influx. *Physiol.Rev.* 77:901-930.

131. Roos, J., P. J. DiGregorio, A. V. Yeromin, K. Ohlsen, M. Lioudyno, S. Y. Zhang, O. Safrina, J. A. Kozak, S. L. Wagner, M. D. Cahalan, G. Velicelebi, and K. A. Stauderman. 2005. STIM1, an essential and conserved component of store-operated Ca^{2+} channel function. *J.Cell Biol.* 169:435-445.

132. Vig, M., C. Peinelt, A. Beck, D. L. Koomoa, D. Rabah, M. Koblan-Huberson, S. Kraft, H. Turner, A. Fleig, R. Penner, and J. P. Kinet. 2006. CRACM1 is a plasma membrane protein essential for store-operated Ca^{2+} entry. *Science* 312:1220-1223.

133. Zhang, S. L., A. V. Yeromin, X. H. F. Zhang, Y. Yu, O. Safrina, A. Penna, J. Roos, K. A. Stauderman, and M. D. Cahalan. 2006. Genome-wide RNAi screen of Ca^{2+} influx identifies genes that regulate Ca^{2+} release-activated Ca^{2+} channel activity. *Proc.Natl.Acad. Sci.U.S.A.* 103:9357-9362.

134. Lewis, R. S. 2007. The molecular choreography of a store-operated calcium channel. *Nature* 446:284-287.

135. Vig, M., A. Beck, J. M. Billingsley, A. Lis, S. Parvez, C. Peinelt, D. L. Koomoa, J. Soboloff, D. L. Gill, A. Fleig, J. P. Kinet, and R. Penner. 2006. CRACM1 multimers form the ion-selective pore of the CRAC channel. *Curr.Biol.* 16:2073-2079.

136. Prakriya, M., S. Feske, Y. Gwack, S. Srikanth, A. Rao, and P. G. Hogan. 2006. Orai1 is an essential pore subunit of the CRAC channel. *Nature* 443:230-233.

137. Yeromin, A. V., S. Y. L. Zhang, W. H. Jiang, Y. Yu, O. Safrina, and M. D. Cahalan. 2006. Molecular identification of the CRAC channel by altered ion selectivity in a mutant of Orai. *Nature* 443:226-229.

138. Scharenberg, A. M. and J. P. Kinet. 1998. Ptdlns-3,4,5-P_3: A regulatory nexus between tyrosine kinases and sustained calcium signals. *Cell* 94:5-8.

139. Zhang, J., M. L. Billingsley, R. L. Kincaid, and R. P. Siraganian. 2000. Phosphorylation of Syk activation loop tyrosines is essential for Syk function - An in vivo study using a specific anti-Syk activation loop phosphotyrosine antibody. *J.Biol.Chem.* 275:35442-35447.

140. Zhang, J., E. Berenstein, and R. P. Siraganian. 2002. Phosphorylation of Tyr342 in the linker region of Syk is critical for FcεRI signaling in mast cells. *Mol.Cell.Biol.* 22:8144-8154.

141. Fierro, L. and A. B. Parekh. 1999. On the characterisation of the mechanism underlying passive activation of the Ca^{2+} release-activated Ca^{2+} current ICRAC in rat basophilic leukaemia cells. *J.Physiol.* 520:407-416.

142. Kuehn, H. S. and A. M. Gilfillan. 2007. G protein-coupled receptors and the modification of FcepsilonRI-mediated mast cell activation. *Immunol.Lett.* 113:59-69.

143. Wang, X. Y., K. Sada, S. Yanagi, C. Yang, K. Rezaul, and H. Yamamura. 1994. Intracellular Calcium-Dependent Activation of p72syk in Platelets. *J.Biochem.* 116:858-861.

144. Rezaul, K., K. Sada, T. Inazu, and H. Yamamura. 1997. Platelet-activating factor stimulates calcium-dependent activation of protein-tyrosine kinase Syk in a human B cell line. *Biochem.Biophy.Res.Commun.* 239:23-27.

145. Lev, S., H. Moreno, R. Martinez, P. Canoll, E. Peles, J. M. Musacchio, G. D. Plowman, B. Rudy, and J. Schlessinger. 1995. Protein-tyrosine kinase Pyk2 involved in Ca^{2+}-induced regulation of ion channel and Map kinase functions. *Nature* 376:737-745.

146. Sheets, E. D., D. Holowka, and B. Baird. 1999. Critical role for cholesterol in Lyn-mediated tyrosine phosphorylation of FcεRI and their association with detergent-resistant membranes. *J.Cell Biol.* 145:877-887.

147. Lockwich, T. P., X. B. Liu, B. B. Singh, J. Jadlowiec, S. Weiland, and I. S. Ambudkar. 2000. Assembly of Trp1 in a signaling complex associated with caveolin-scaffolding lipid raft domains. *J.Biol.Chem.* 275:11934-11942.

148. Clapham, D. E. 2007. Calcium signaling. *Cell* 131:1047-1058.

149. Berridge, M. J. 2006. Calcium microdomains: organization and function. *Cell Calcium* 40:405-412.

150. Dolmetsch, R. E., K. Xu, and R. S. Lewis. 1998. Calcium oscillations increase the efficiency and specificity of gene expression. *Nature* 392:933-936.

151. Gallo, E. M., K. Cante-Barrett, and G. R. Crabtree. 2006. Lymphocyte calcium signaling from membrane to nucleus. *Nat.Immunol.* 7:25-32.

152. Li, W., J. Llopis, M. Whitney, G. Zlokarnik, and R. Y. Tsien. 1998. Cell-permeant caged $InsP_3$ ester shows that Ca^{2+} spike frequency can optimize gene expression. *Nature* 392:936-941.

153. Straube, S. and A. B. Parekh. 2002. Inwardly rectifying potassium currents in rat basophilic leukaemia (RBL-1) cells: regulation by spermine and implications for store-operated calcium influx. *Pflugers Arch.* 444:389-396.

154. Bakowski, D. and A. B. Parekh. 2007. Voltage-dependent Ba^{2+} permeation through store-operated CRAC channels: implications for channel selectivity. *Cell Calcium* 42:333-339.

155. Neher, E. 1998. Usefulness and limitations of linear approximations to the understanding of Ca^{2+} signals. *Cell Calcium* 24:345-357.

156. Ng, S. W., J. Di Capite, K. Singaravelu, and A. B. Parekh. 2008. Sustained activation of the tyrosine kinase Syk by antigen in mast cells requires local Ca^{2+} influx through Ca^{2+} release-activated Ca^{2+} channels. *J.Biol.Chem.* 283:31348-31355.

157. Frieden, M., D. James, C. Castelbou, A. Danckaert, J. C. Martinou, and N. Demaurex. 2004. Ca^{2+} homeostasis during mitochondrial fragmentation and perinuclear clustering induced by hFis1. *J.Biol.Chem.* 279:22704-22714.

158. Darnell, J. E., Jr. 1997. STATs and gene regulation. *Science* 277:1630-1635.

159. Bromberg, J. F. 2001. Activation of STAT proteins and growth control. *Bioessays* 23:161-169.

160. Lagerstrom, M. C. and H. B. Schioth. 2008. Structural diversity of G protein-coupled receptors and significance for drug discovery. *Nat.Rev.Drug Discov.* 7:339-357.

161. Pierce, K. L., R. T. Premont, and R. J. Lefkowitz. 2002. Seven-transmembrane receptors. *Nat.Rev.Mol.Cell Biol.* 3:639-650.

162. Ma, P. and R. Zemmel. 2002. Value of novelty? *Nat.Rev.Drug Discov.* 1:571-572.

163. Di Capite, J., S. W. Ng, and A. B. Parekh. 2009. Decoding of cytoplasmic Ca^{2+} oscillations through the spatial signature drives gene expression. *Curr.Biol.*

164. Naik, S., C. K. Billington, R. M. Pascual, D. A. Deshpande, F. P. Stefano, T. A. Kohout, D. M. Eckman, J. L. Benovic, and R. B. Penn. 2005. Regulation of

cysteinyl leukotriene type 1 receptor internalization and signaling. *J.Biol.Chem.* 280:8722-8732.

165. Beck, A., M. Kolisek, L. A. Bagley, A. Fleig, and R. Penner. 2006. Nicotinic acid adenine dinucleotide phosphate and cyclic ADP-ribose regulate TRPM2 channels in T lymphocytes. *FASEB J.* 20:962-964.

166. Berridge, M. J. 1987. Inositol trisphosphate and diacylglycerol: two interacting second messengers. *Annu.Rev.Biochem.* 56:159-193.

167. Deshpande, D. A., R. M. Pascual, S. W. Wang, D. M. Eckman, E. C. Riemer, C. D. Funk, and R. B. Penn. 2007. PKC-dependent regulation of the receptor locus dominates functional consequences of cysteinyl leukotriene type 1 receptor activation. *FASEB J.* 21:2335-2342.

168. Bird, G. S. and J. W. Putney, Jr. 2005. Capacitative calcium entry supports calcium oscillations in human embryonic kidney cells. *J.Physiol* 562:697-706.

169. Stauffer, T. P., S. Ahn, and T. Meyer. 1998. Receptor-induced transient reduction in plasma membrane PtdIns(4,5)P_2 concentration monitored in living cells. *Curr.Biol.* 8:343-346.

170. Zweifach, A. and R. S. Lewis. 1995. Rapid inactivation of depletion-activated calcium current ($I_{CRAC)}$ due to local calcium feedback. *J.Gen.Physiol* 105:209-226.

171. Kasai, H. and O. H. Petersen. 1994. Spatial dynamics of second messengers: IP_3 and cAMP as long-range and associative messengers. *Trends Neurosci.* 17:95-101.

172. Gwack, Y., S. Srikanth, M. Oh-Hora, P. G. Hogan, E. D. Lamperti, M. Yamashita, C. Gelinas, D. S. Neems, Y. Sasaki, S. Feske, M. Prakriya, K. Rajewsky, and A. Rao. 2008. Hair loss and defective T- and B-cell function in mice lacking ORAI1. *Mol.Cell Biol.* 28:5209-5222.

173. Park, C. Y., A. Shcheglovitov, and R. Dolmetsch. 2010. The CRAC channel activator STIM1 binds and inhibits L-type voltage-gated calcium channels. *Science* 330:101-105.

174. Wang, Y., X. Deng, S. Mancarella, E. Hendron, S. Eguchi, J. Soboloff, X. D. Tang, and D. L. Gill. 2010. The calcium store sensor, STIM1, reciprocally controls Orai and CaV1.2 channels. *Science* 330:105-109.

175. Parekh, A. B. 2010. Store-operated CRAC channels: function in health and disease. *Nat.Rev.Drug Discov.* 9:399-410.

176. Di Capite, J. and A. B. Parekh. 2009. CRAC channels and Ca^{2+} signaling in mast cells. *Immunol.Rev.* 231:45-58.